DETECTORS FOR COSMIC MICROWAVE BACKGROUND RESEARCH

Silvia Masi and Paolo de Bernardis

Dipartimento di Fisica

Universita' La Sapienza, Roma – Italy

9th Topical Seminar

Innovative Particle and Radiation Detectors

Siena, 23 May 2004

Preliminary:

- I am a CMB detectors **user**.
- I'll try to give you the feeling of:
  - The status of this research
  - The ultimate cosmology and fundamental physics goals involving these detectors
  - The experimental challanges demanded by these applications
- I'll limit myself to bolometers becouse are the ones I know better and are linked to microcalorimeters

What is the CMB

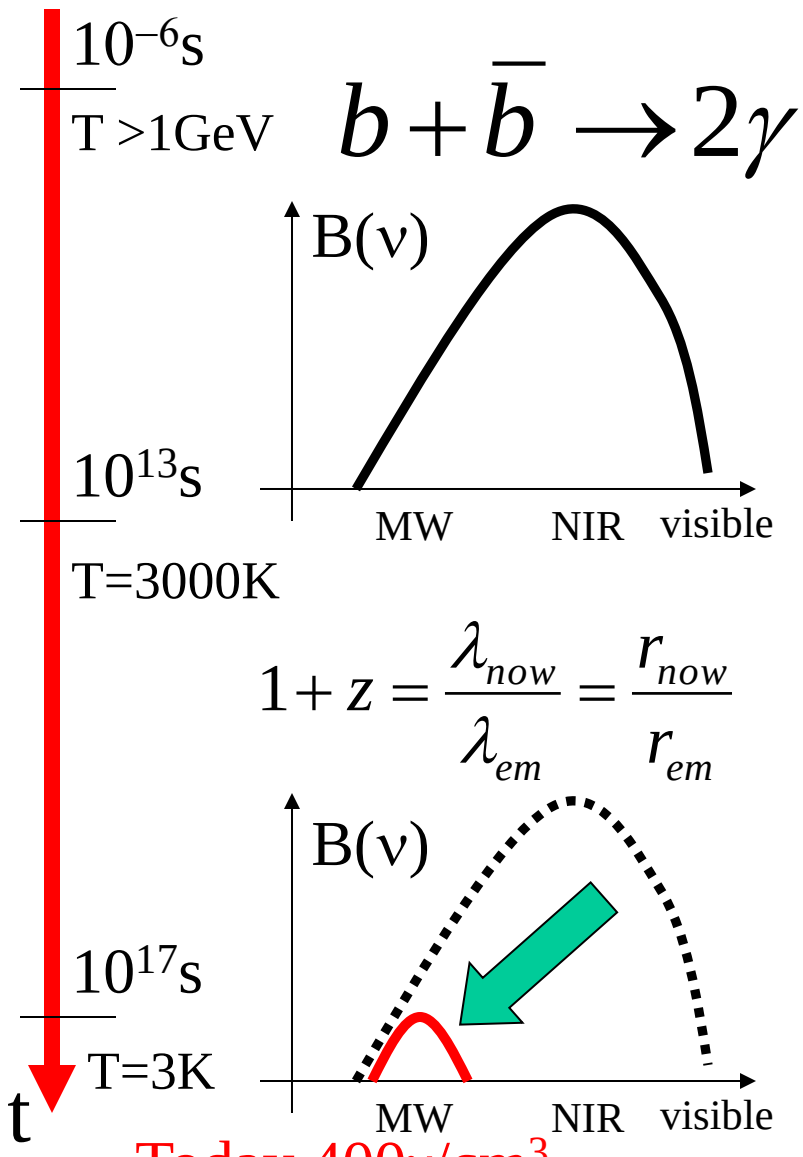

According to modern cosmology:

An abundant background of photons filling the Universe.

- **Generated** in the very early universe, less than 4 μs after the Big Bang ($10^9\gamma$ for each baryon)
- **Thermalized** in the primeval fireball (in the first 380000 years after the big bang) by repeated scattering against free electrons
- **Redshifted** to microwave frequencies **and diluted** in the subsequent 14 Gyrs of expansion of the Universe

Why is the CMB important

- **Is the most ancient fossil remnant of the early Universe.**
- **Its characteristics tell us a lot about the physical processes happening in the early Universe.**
- **Modern cosmology is heavily based on observations of the CMB.**

CMB and cosmology

- 1992: COBE-FIRAS measures the spectrum of the CMB with incredible precision (1/10000)
- The thermal spectrum at 2.725K and the high photons to barions ratio together with the measured primordial abundances of light elements is evidence for a hot initial phase of the Universe.

J. Mather et al. 1992

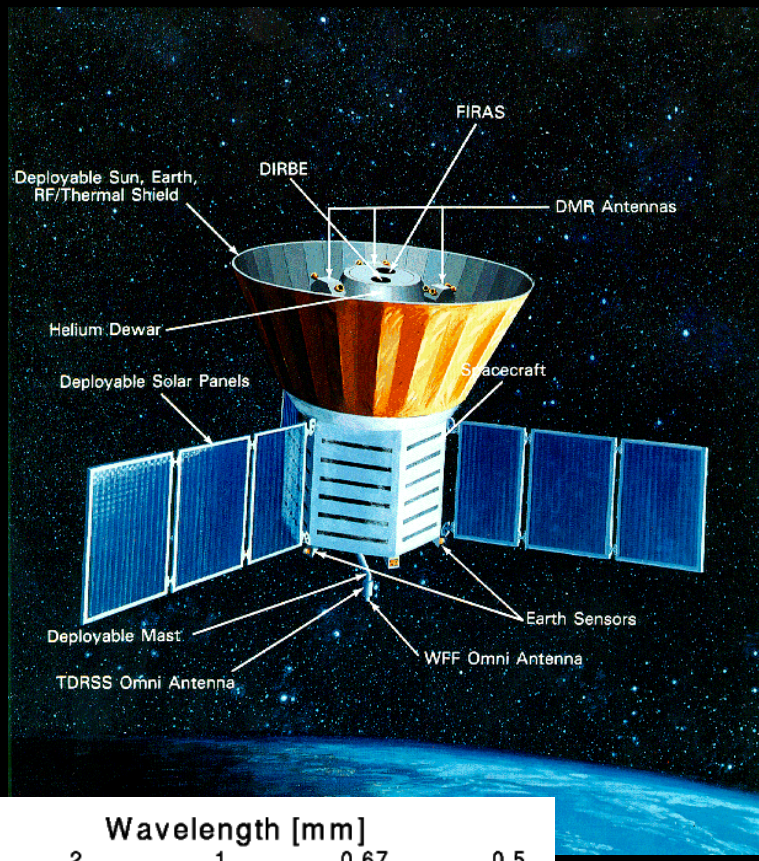

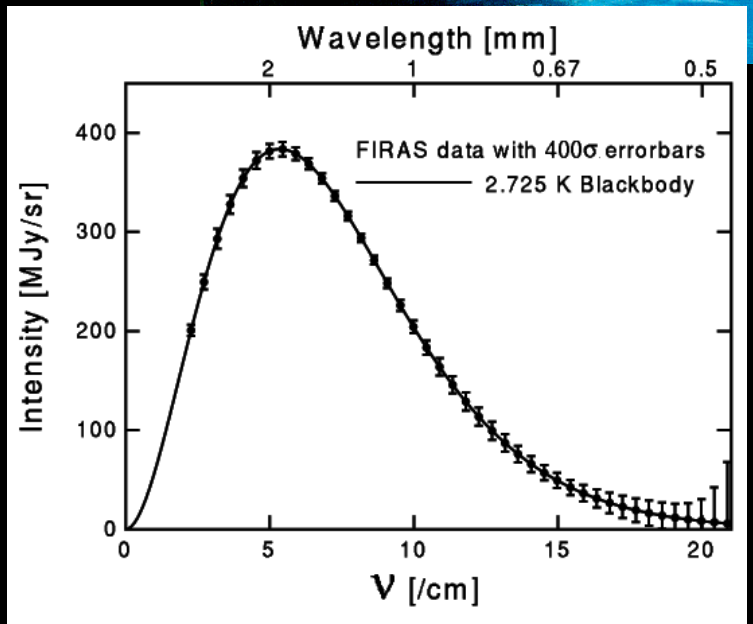

CMB observables

- **The spectrum**

$$B(\nu,T)=\frac{2h}{c^2}\frac{\nu^3}{e^x-1} \qquad x=\frac{h\nu}{kT}$$

- **The angular distribution**

$$\Delta B(\nu,T)=\frac{xe^x}{e^x-1}B(\nu,T)\frac{\Delta T}{T}$$

- **The polarization state**

$$\Delta B_P(\nu,T)=\frac{xe^x}{e^x-1}B(\nu,T)\frac{\Delta T_P}{T}$$

- **The noise**

$$\sqrt{\left\langle \Delta W^2(\nu,T)\right\rangle}=\sqrt{\frac{4k^4T^4}{ch^3}\frac{x^4e^x}{\left(e^x-1\right)^2}}$$

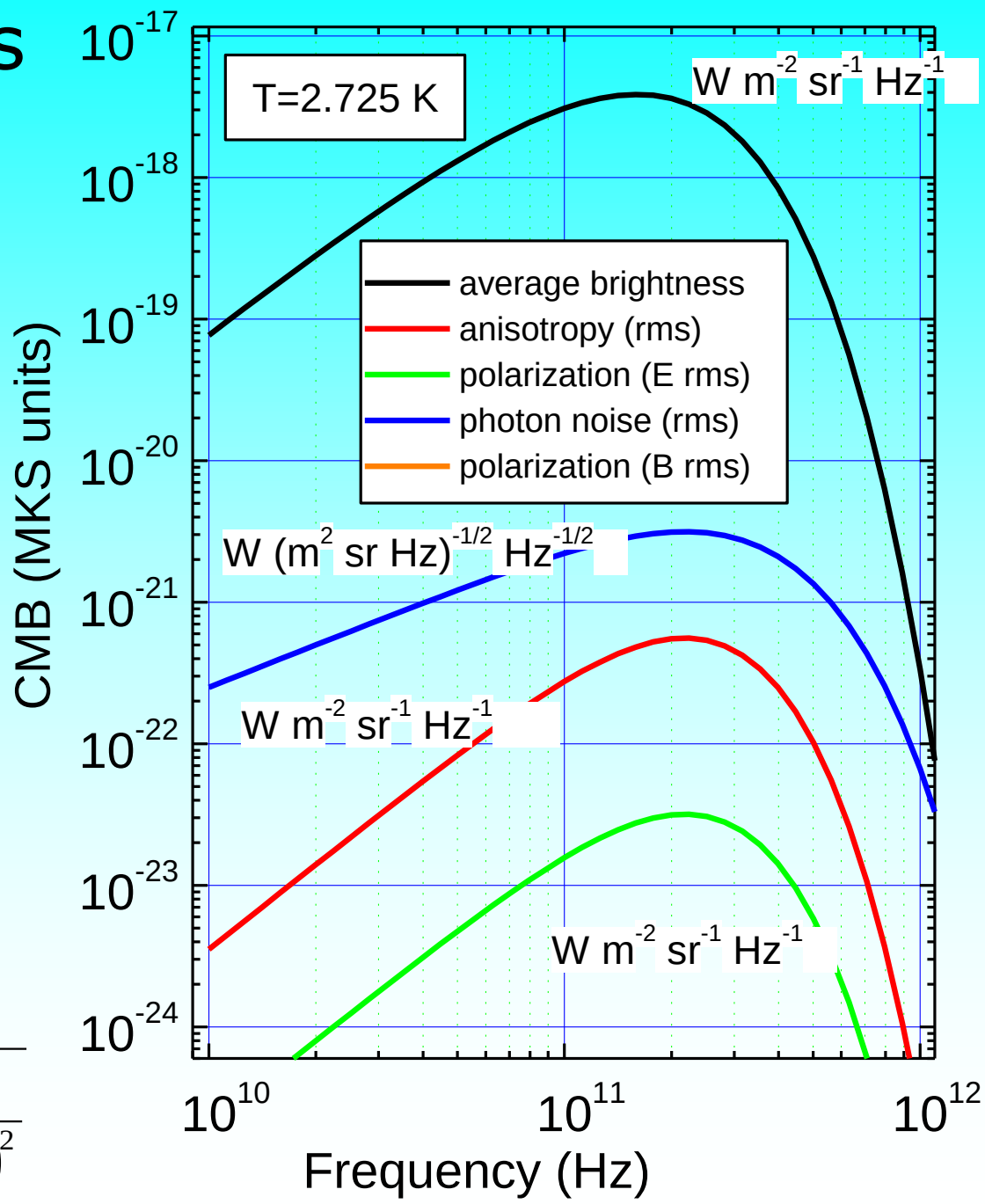

CMB observables

- The CMB is ONLY **slightly anisotropic**.
- The brightness (temperature) fluctuations are due to small density fluctuations present in the primeval fireball, and to their motions:

$$\frac{\Delta T}{T} = \frac{1}{4}\frac{\Delta \rho_\gamma}{\rho_\gamma} + \frac{1}{3}\frac{\Delta \varphi}{c^2} + \frac{\mathrm{v}}{c}$$

Photon Density fluctuations

Gravitational redshift

Scattering against moving e-

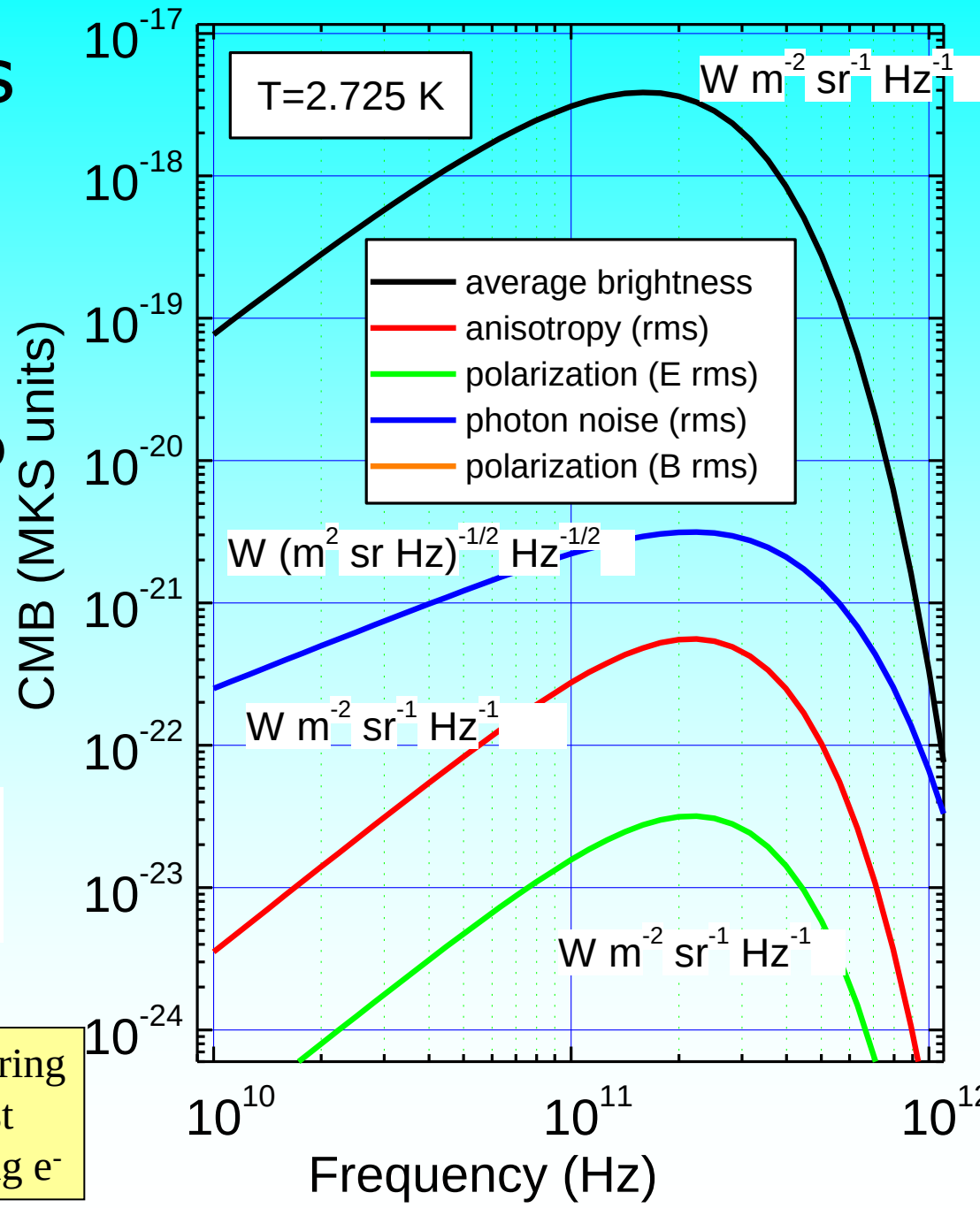

CMB observables

- The **rms anisotropy** has contributions from many angular scales
- The **angular power spectrum** c_l of the anisotropy defines the contribution to the rms from the different multipoles:

$$\Delta T(\theta,\varphi) = \sum_{\ell,m} a_{\ell m} Y_\ell^m(\theta,\varphi)$$

$$c_\ell = \left\langle a_{\ell m}^2 \right\rangle$$

$$\left\langle \Delta T^2 \right\rangle = \frac{1}{4\pi} \sum_\ell (2\ell+1) c_\ell$$

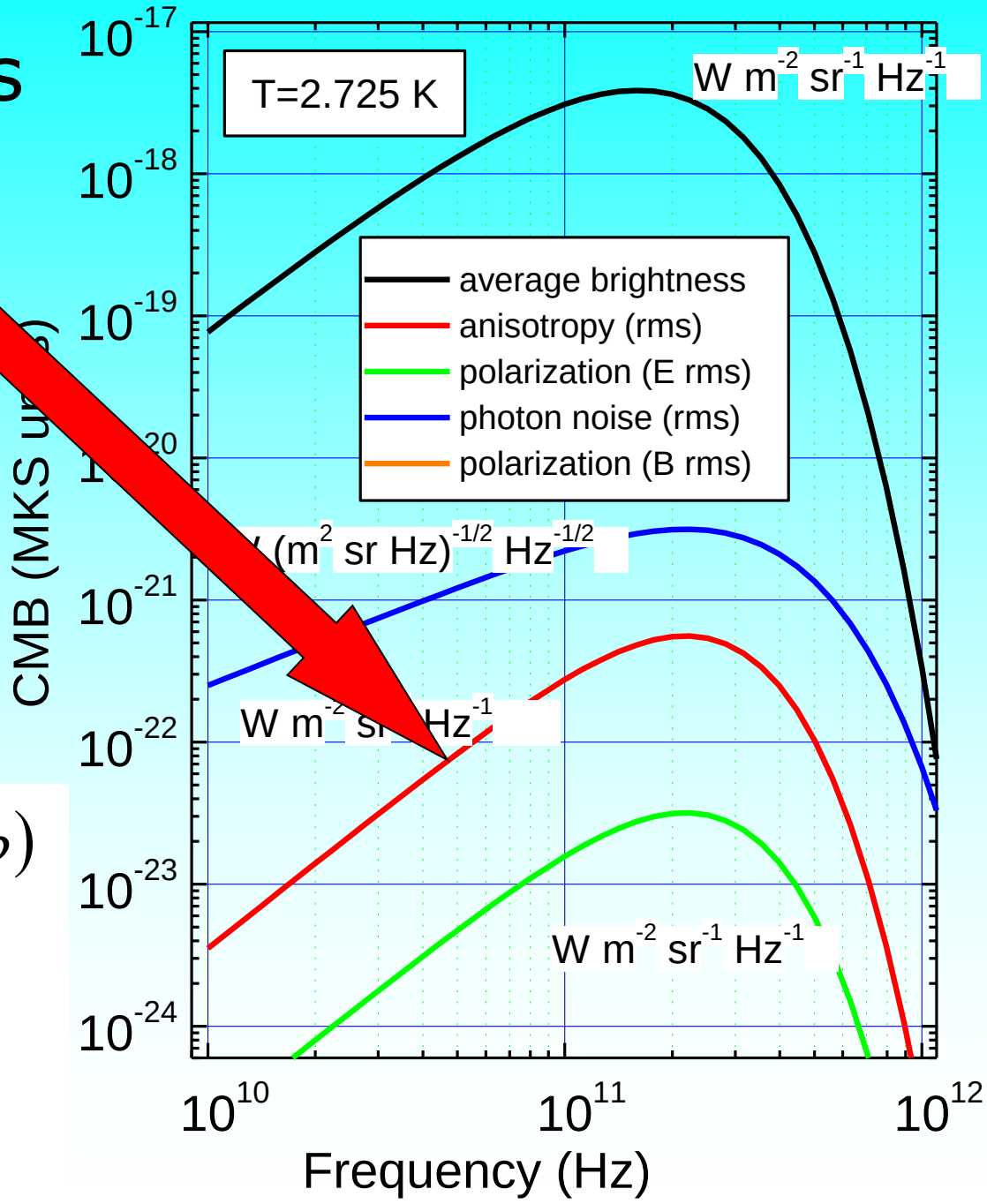

Which is the power spectrum ?

- The angular power spectrum of the CMB depends on the physical processes happening in the early universe, during the primeval fireball phase.
- The primeval fireball is an **expanding plasma**, slowly decreasing its temperature, where photons and matter are in thermal equilibrium
- There are 10^9 photons for each baryon, so photon pressure is very important.
- For T > 0.8 eV the energy density of photons dominates, while at later times the energy density of matter dominates.
- At T = 0.26 eV the plasma neutralizes, H atoms are formed, and the universe becomes transparent to photons (recombination). We see the image of the CMB as it was there, when photons were last scattered.

Image of Solar Granulation

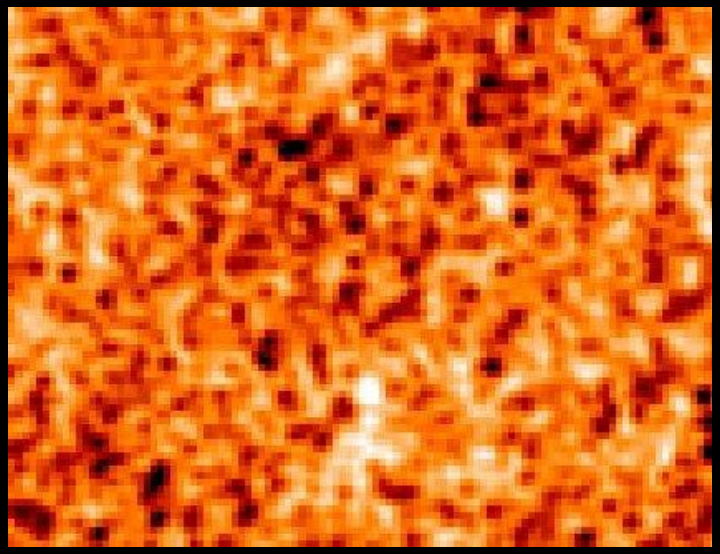

Plasma in the
solar photosphere

(5500 K)

8 light minutes

Here, now

Image of Solar Granulation

Plasma in the
solar photosphere

(5500 K)

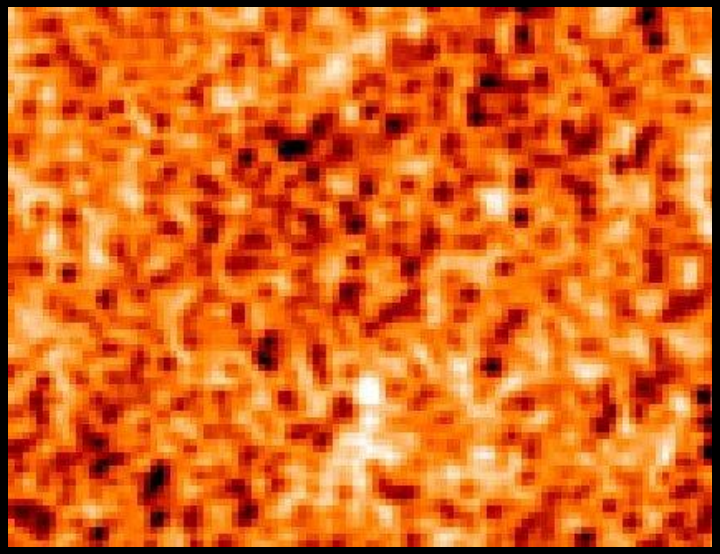

8 light minutes

Here, now

Plasma in the LSS
the cosmic
photosphere

(3000 K)

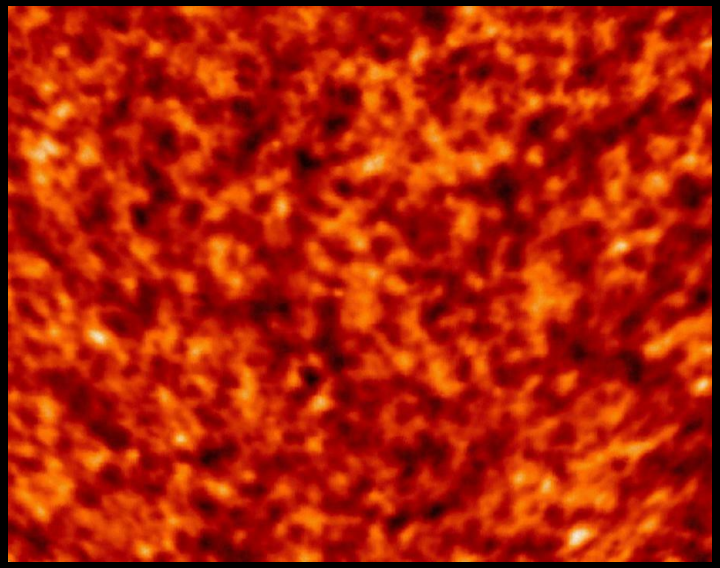

14 billion light years

Here, now

The BOOMERanG map of the last scattering surface

- How is the structure we expect to see in the primeval plasma at recombination ?
- It depends on
  - –the physics of the primeval fireball
  - –the physics of the very early Universe
  - –the geometry of space

Physics of the Primeval fireball and very early universe

Geometry of space

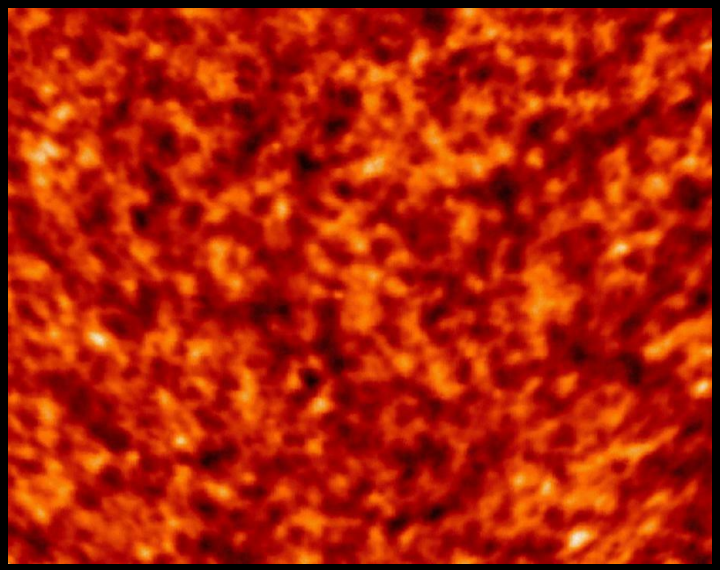

14 billion light years

Here, now

The BOOMERanG map of the last scattering surface

Density perturbations ($\Delta\rho/\rho$) were **oscillating** in the primeval plasma (as a result of the opposite effects of gravity and photon pressure).

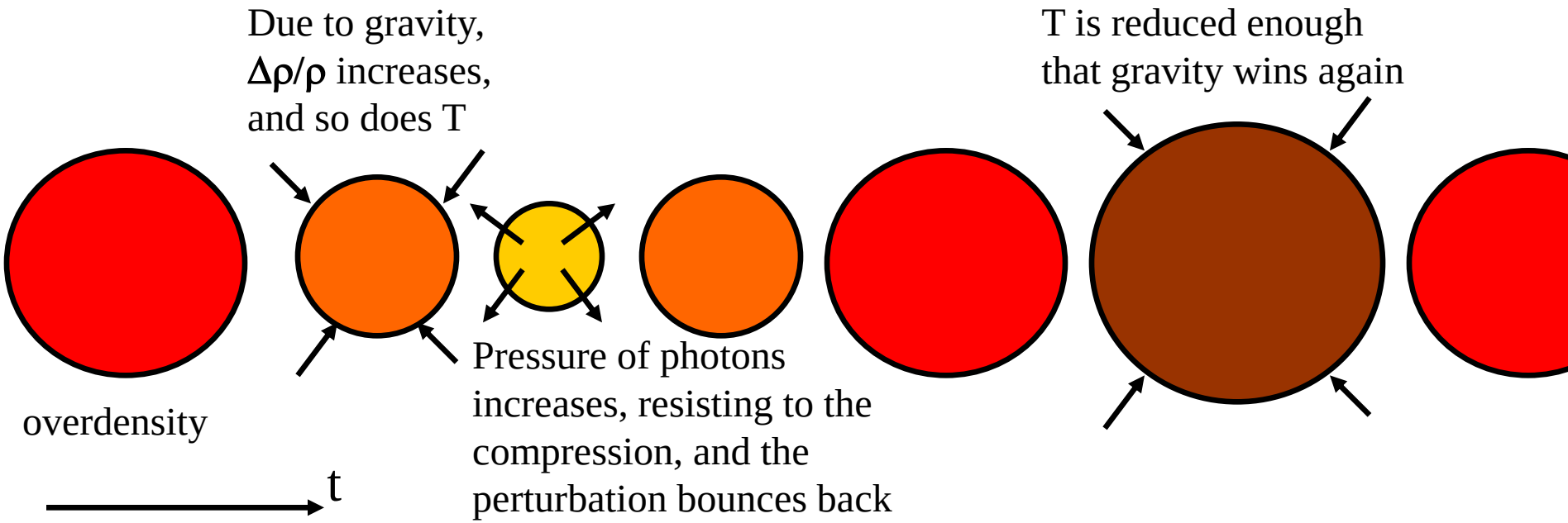

After recombination, density perturbation can **grow** and create the hierarchy of structures we see in the nearby Universe.

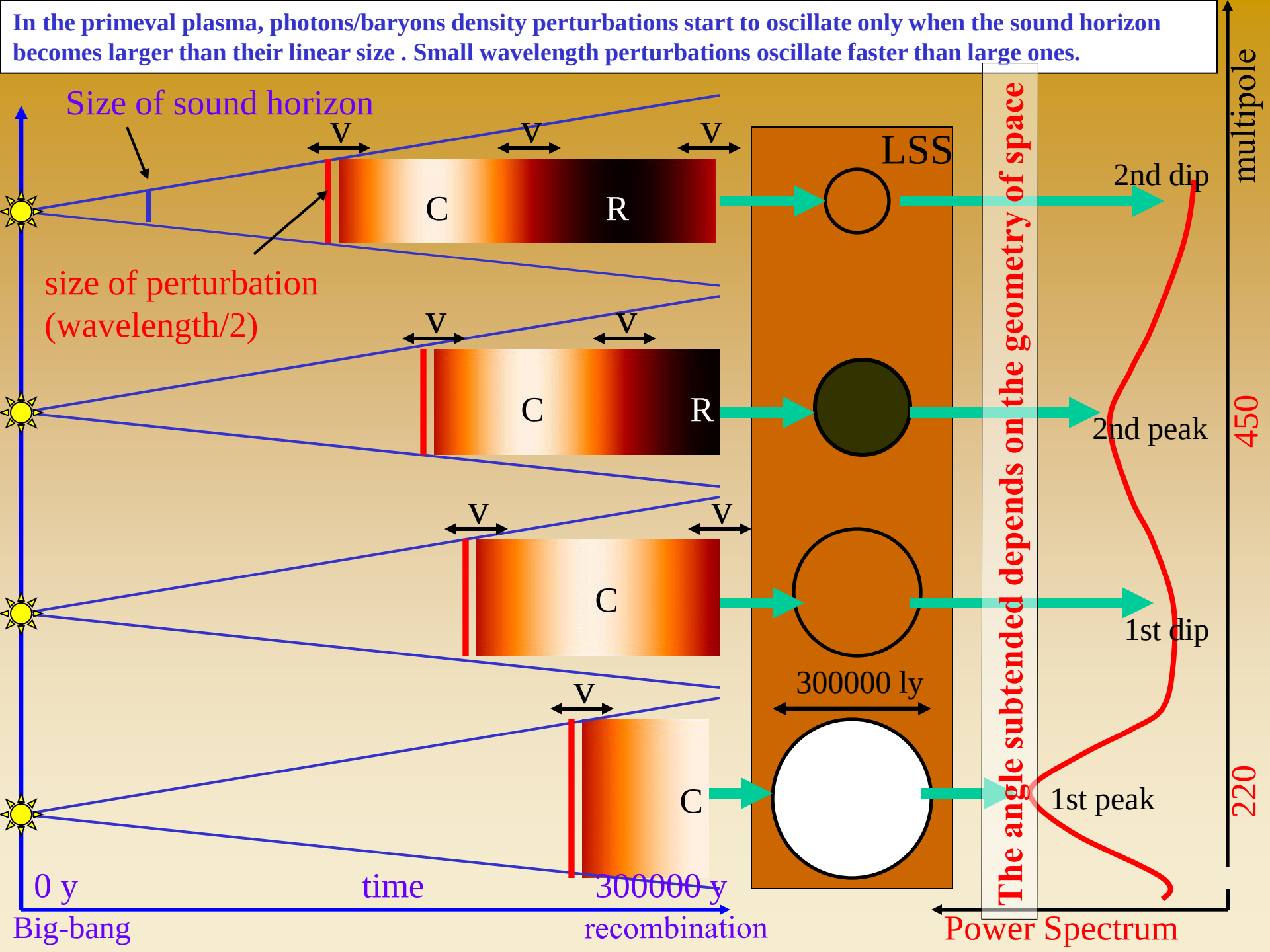
In the primeval plasma, photons/baryons density perturbations start to oscillate only when the sound horizon becomes larger than their linear size . Small wavelength perturbations oscillate faster than large ones.
Size of sound horizon
size of perturbation
(wavelength/2)
V
C
R
LSS
300000 ly
2nd dip
2nd peak
1st dip
1st peak
The angle subtended depends on the geometry of space
multipole
450
220
0 y
time
300000 y
Big-bang
recombination
Power Spectrum

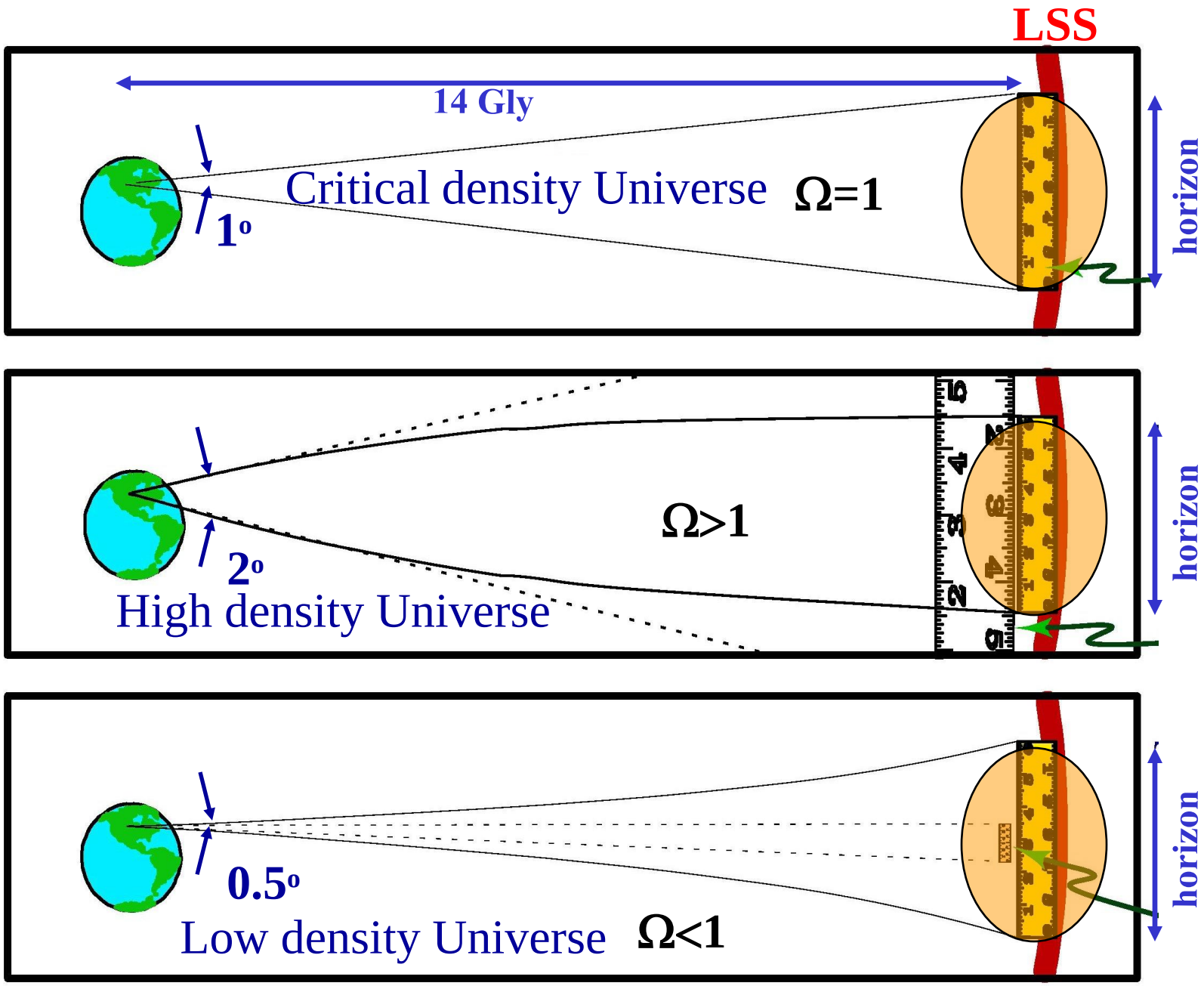
LSS
14 Gly
Critical density Universe Ω=1
1°
horizon
Ω>1
2°
High density Universe
horizon
0.5°
Low density Universe Ω<1
horizon

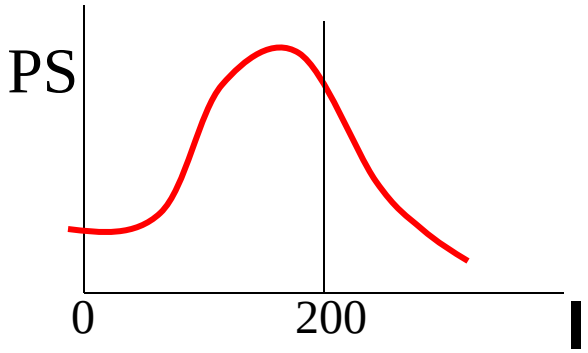

High density Universe

$\Omega>1$

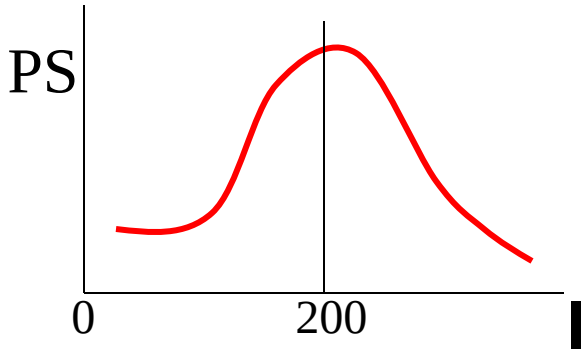

Critical density Universe

$\Omega=1$

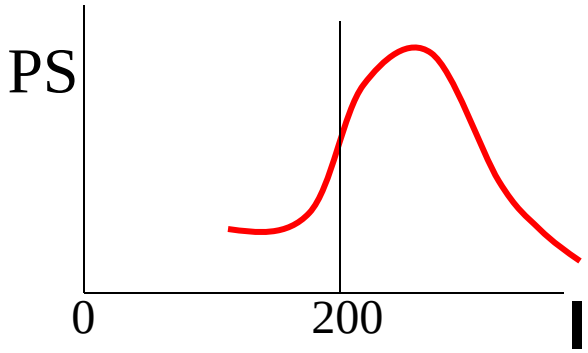

Low density Universe

$\Omega<1$

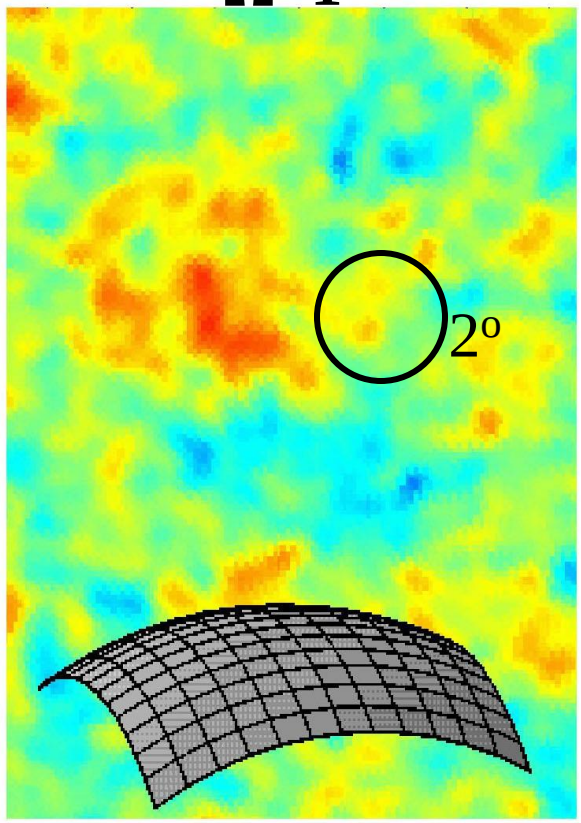

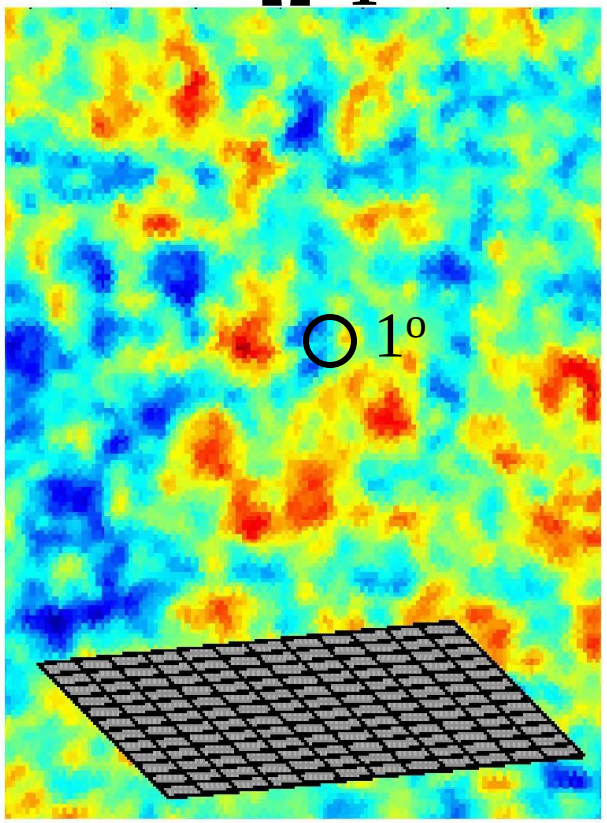

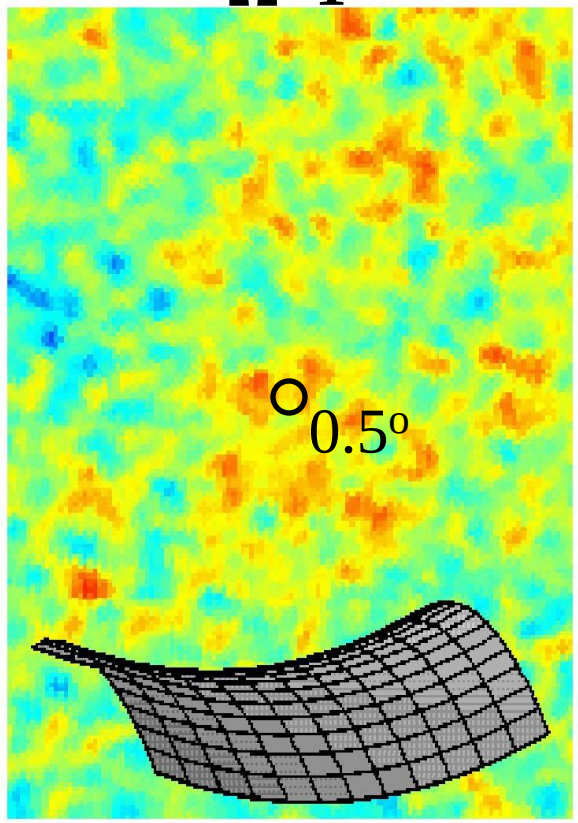

The origin of CMB anisotropies

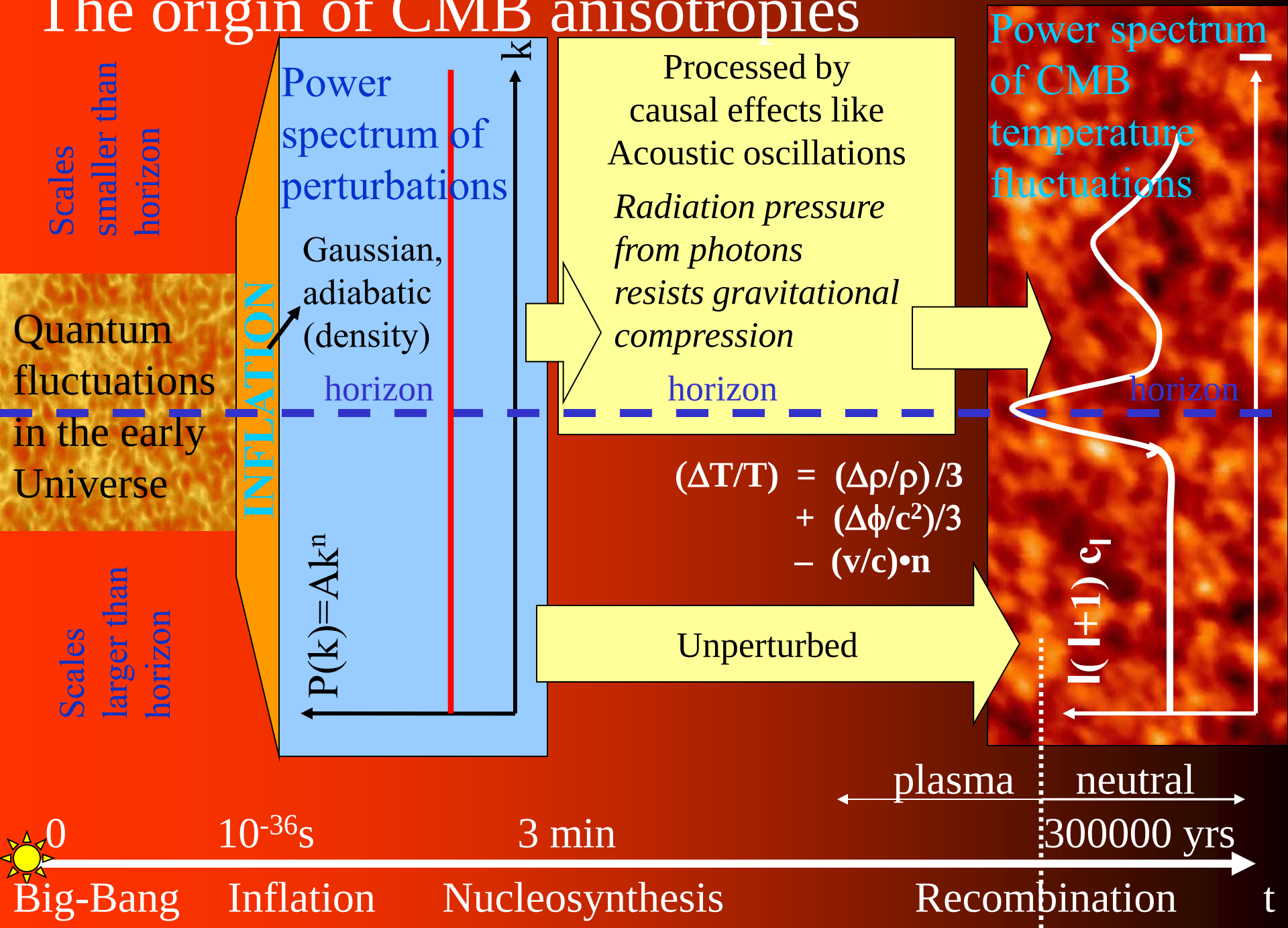

The angular power spectrum depends on the cosmological parameters

Dependance on **Ω** (curvature drives the location of first peak).

Not as simple as in these examples (see S.Weinberg, astro-ph/0006276)

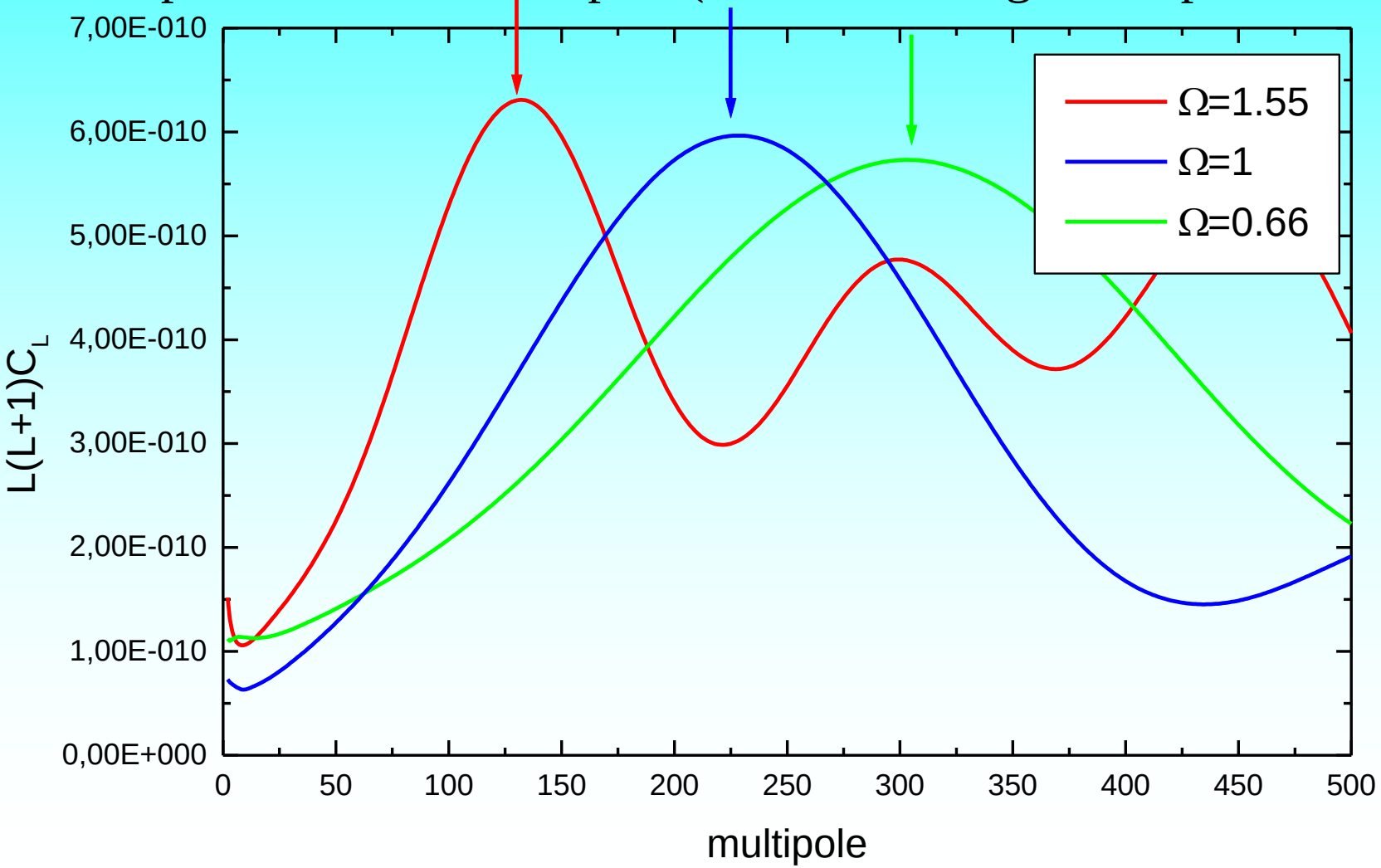

Effect of the baryon density

Dependance on Ω_b (Relative amplitudes second to first peak):
All the spectra are normalized to the first peak.

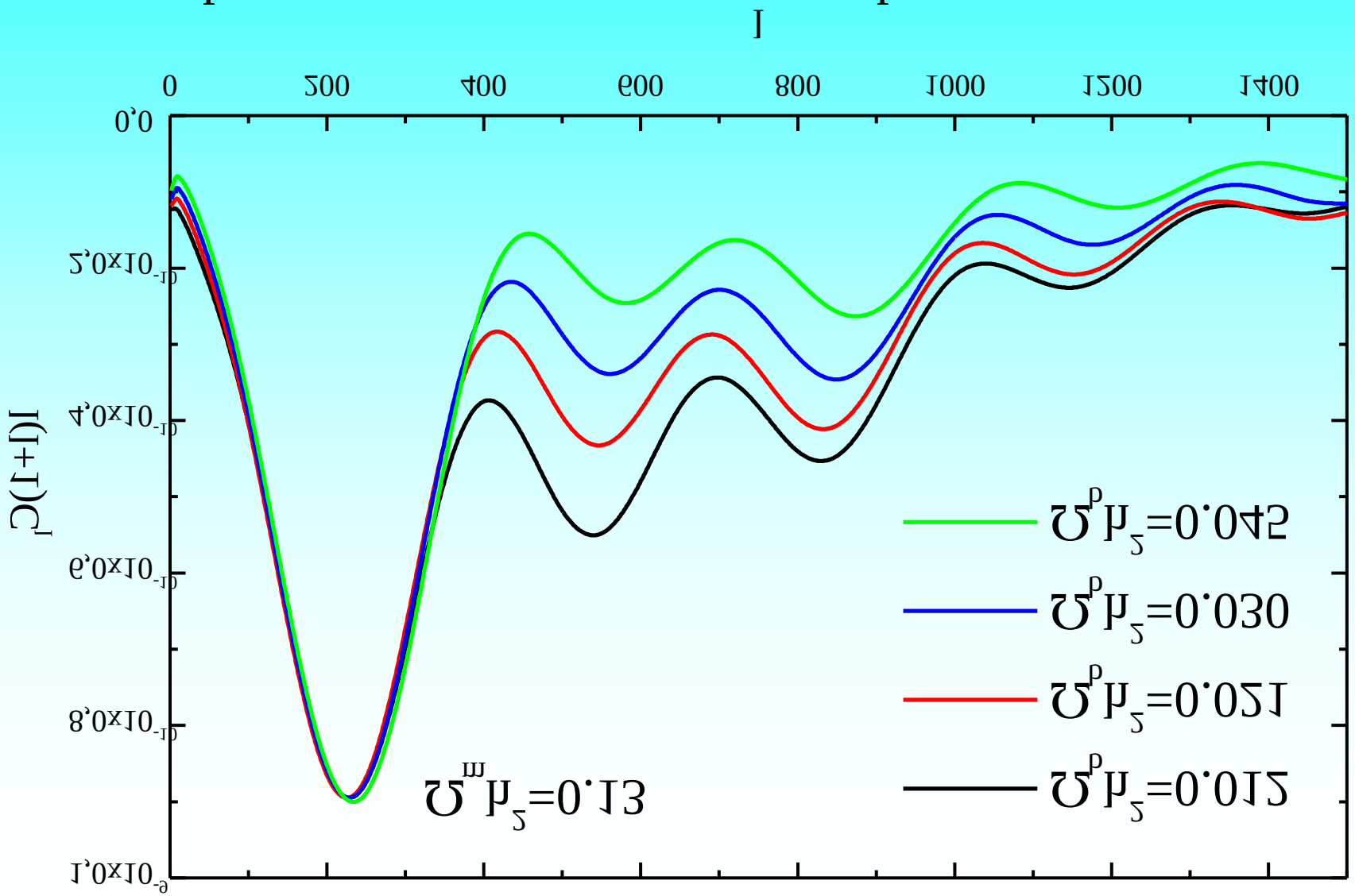

CMB polarization

- CMB radiation is Thomson scattered at recombination.
- If the local distribution of incoming radiation in the rest frame of the electron has a *quadrupole moment*, the scattered radiation acquires some degree of linear polarization.

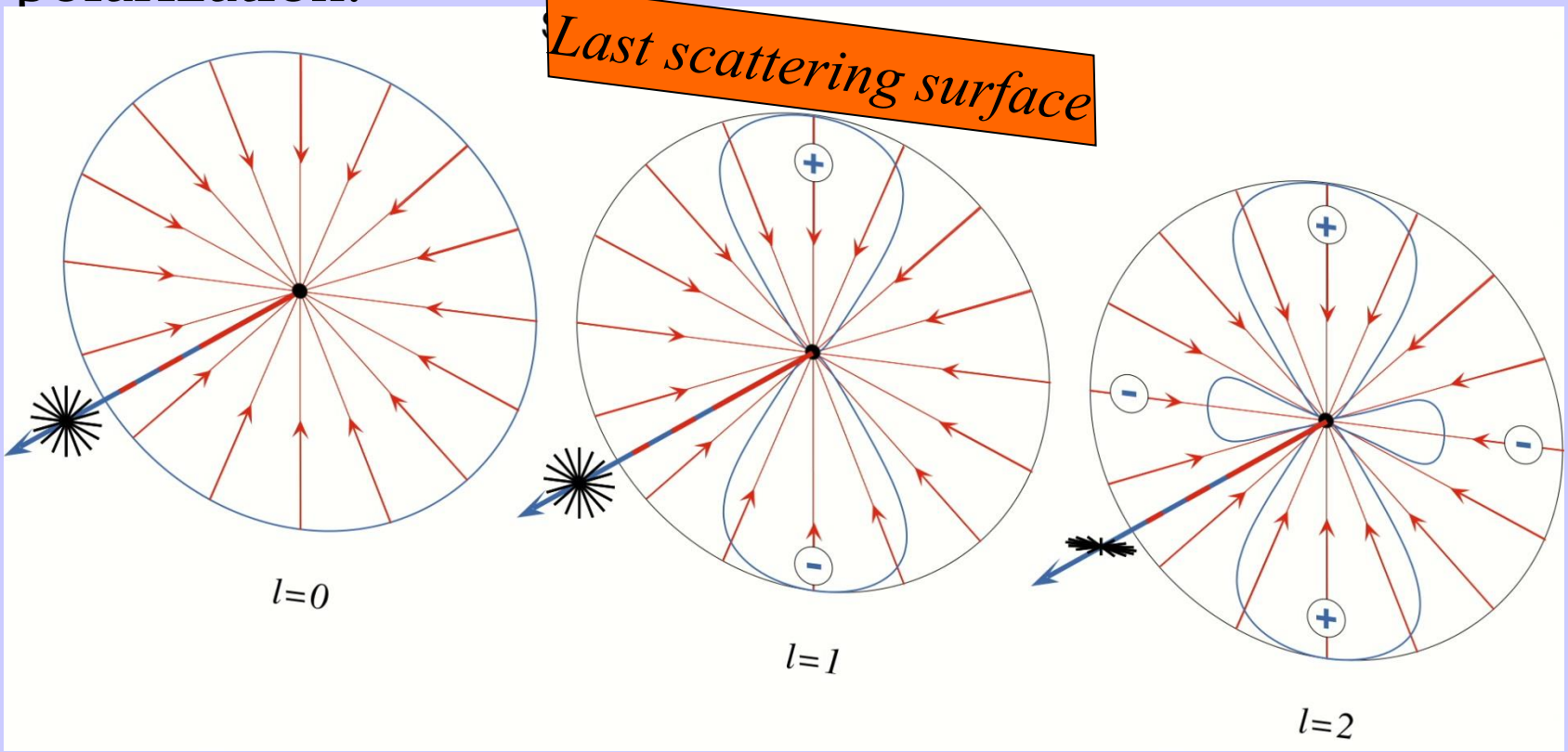

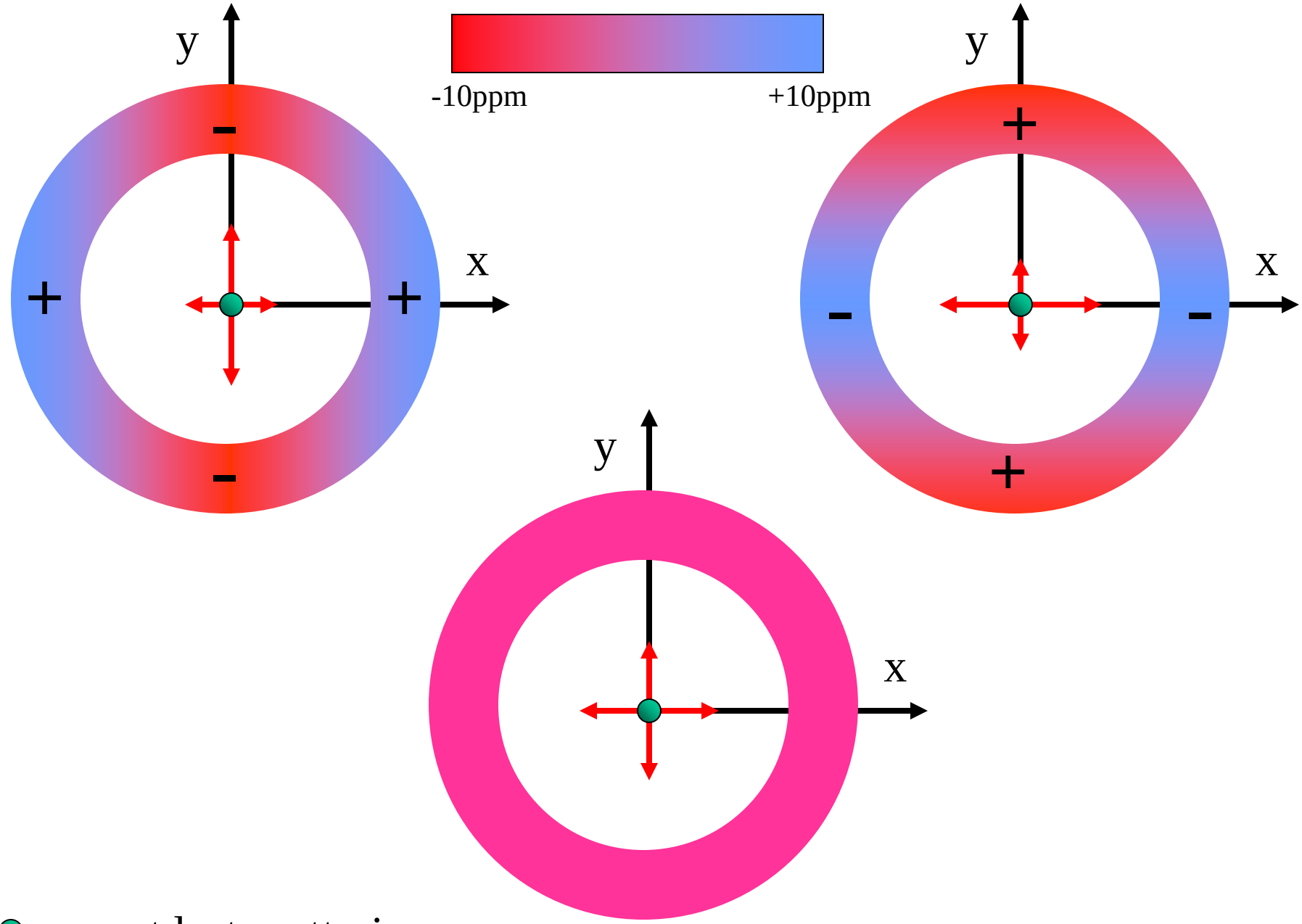

● = e^- at last scattering

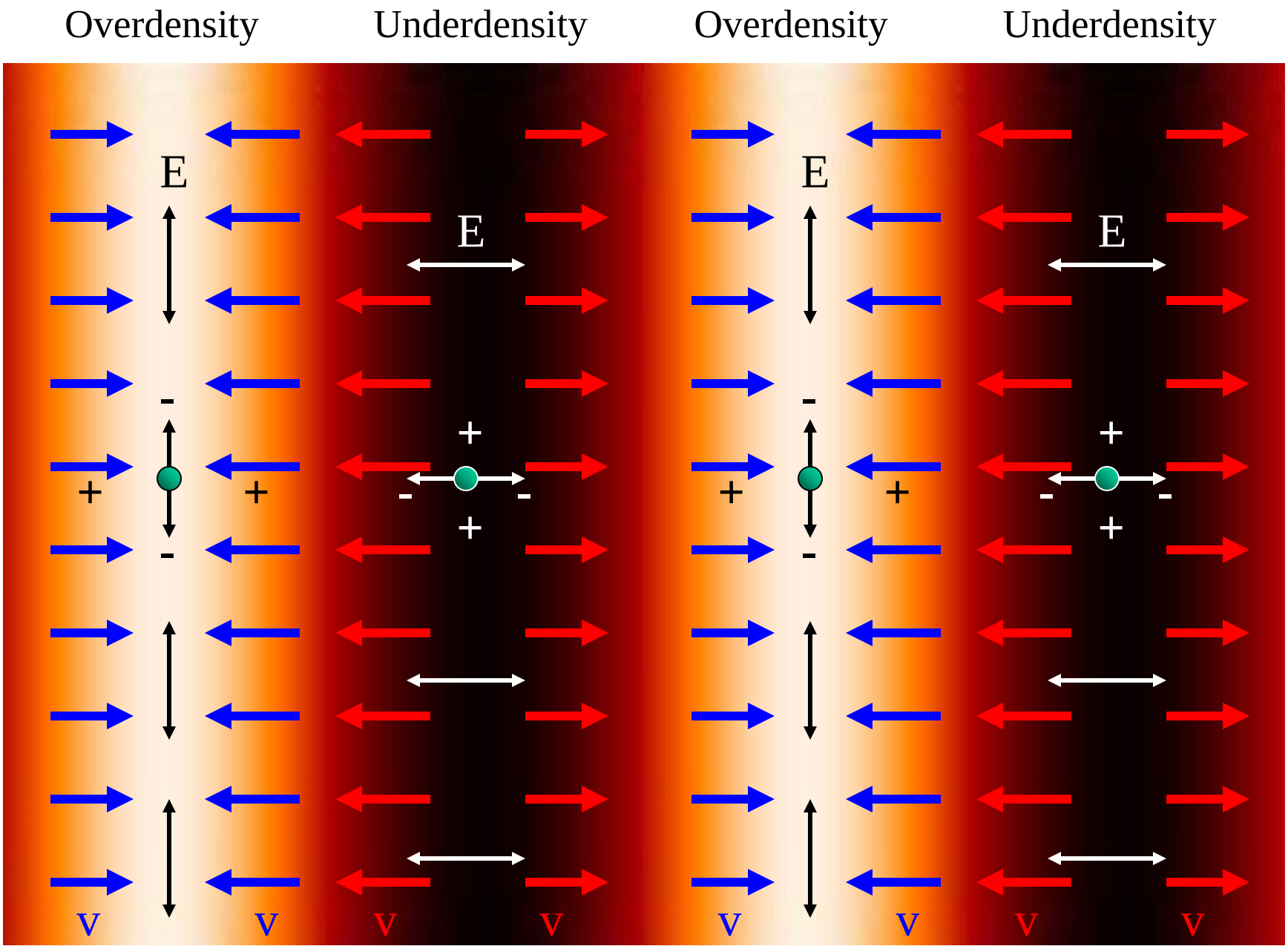

E-modes in the polarization pattern

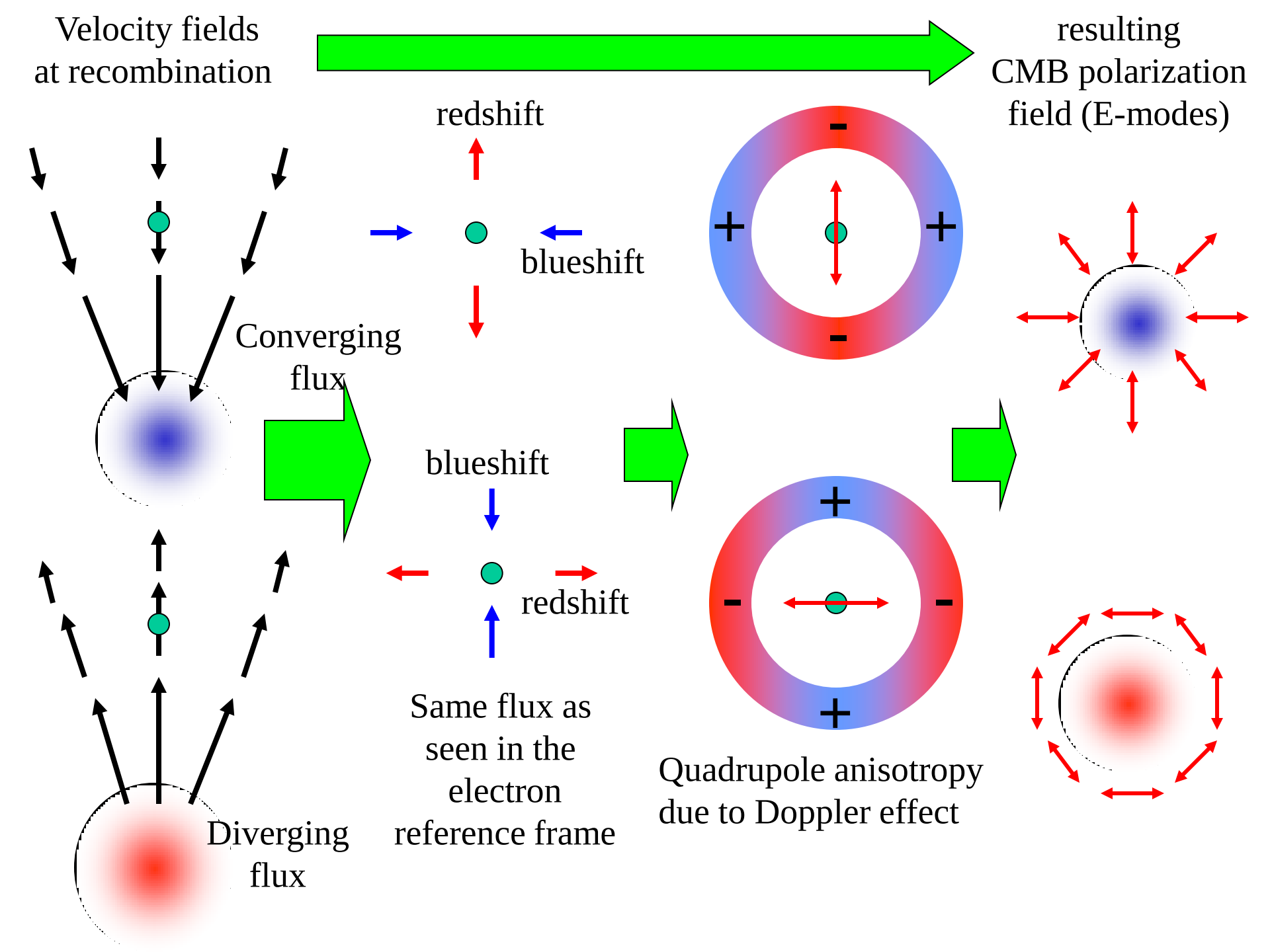
Velocity fields
at recombination
resulting
CMB polarization
field (E-modes)
redshift
blueshift
Converging
flux
blueshift
redshift
Same flux as
seen in the
electron
reference frame
Quadrupole anisotropy
due to Doppler effect
Diverging
flux

- **Tensor perturbations (gravity waves)** also produce quadrupole anisotropy. The generation of a faint stochastic background of gravity waves is a generic feature of all **inflationary processes**.
- The resulting polarization pattern is shear-like.
- The amplitude of the effect is very small.
- This component of the CMB polarization field is called **B-modes** component, or **curl component**.

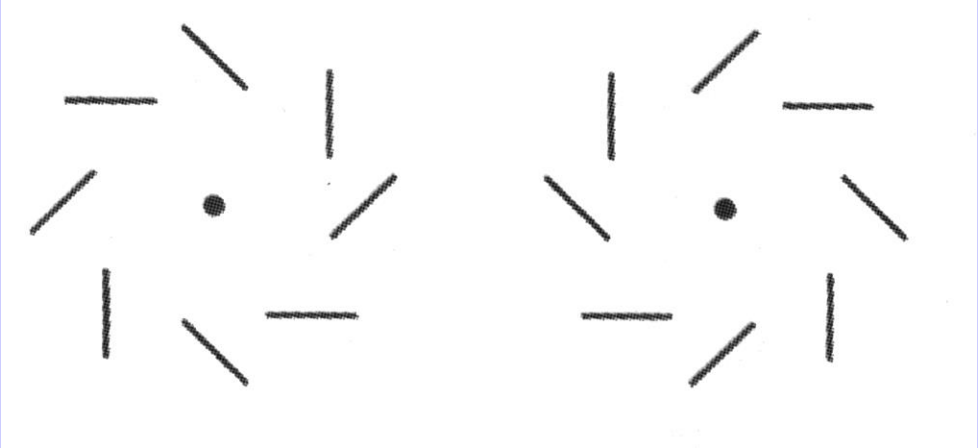

- Velocity fields cannot produce B modes.
- Weak lensing can, but is subdominant at scales larger than 1 deg.
- Mathematical alghoritms exist to separate B modes and E modes.

- The detection of B-modes in the CMB polarization is the only way we have to measure the stochastic background of gravitational waves generated during inflation, a split-second after the Big Bang
- It is the only way to investigate physics at energies of 100…10^{19} GeV
- Incredibly sensitive and polarization pure polarimeters are needed.

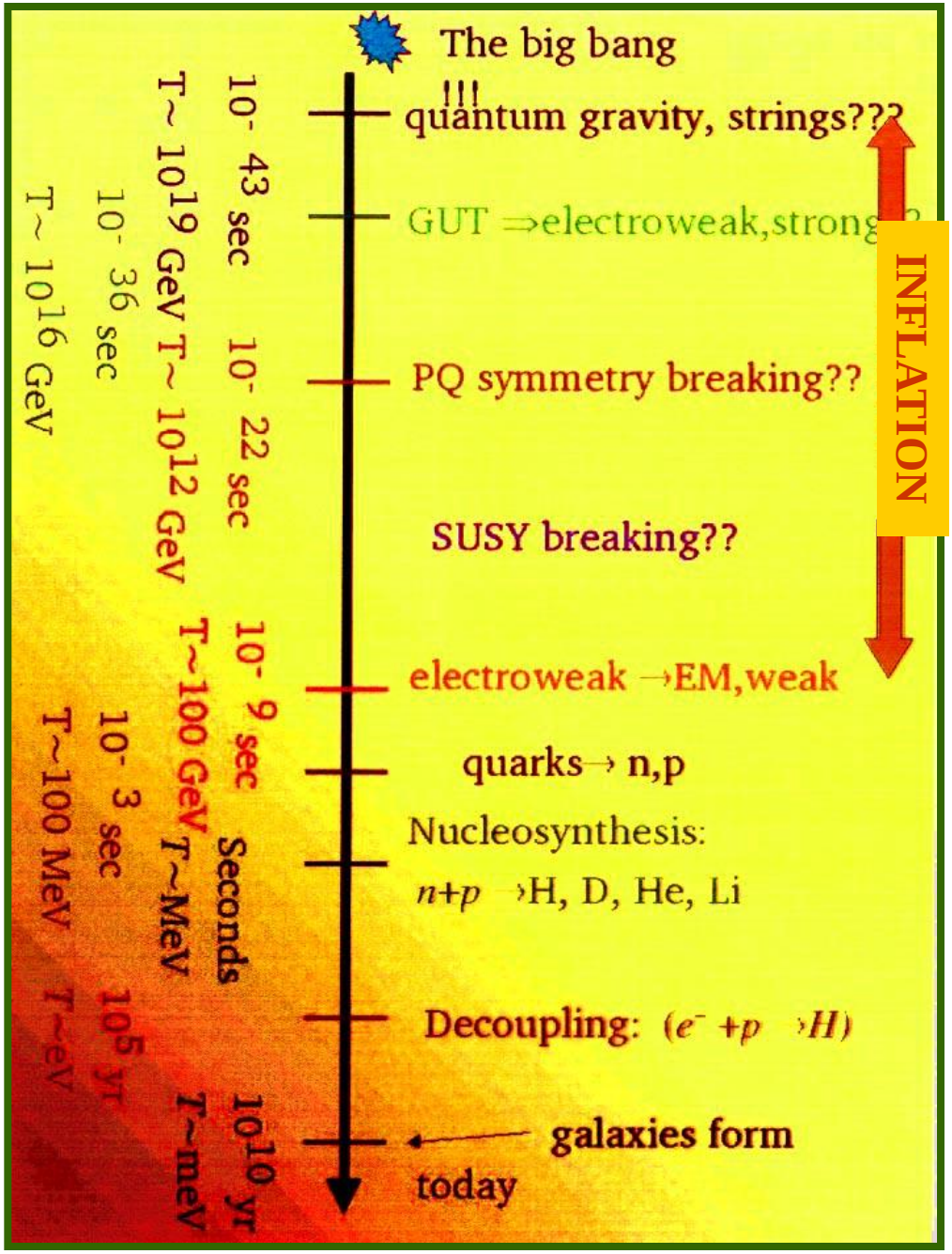

Expected Patterns of Polarization in the Sky

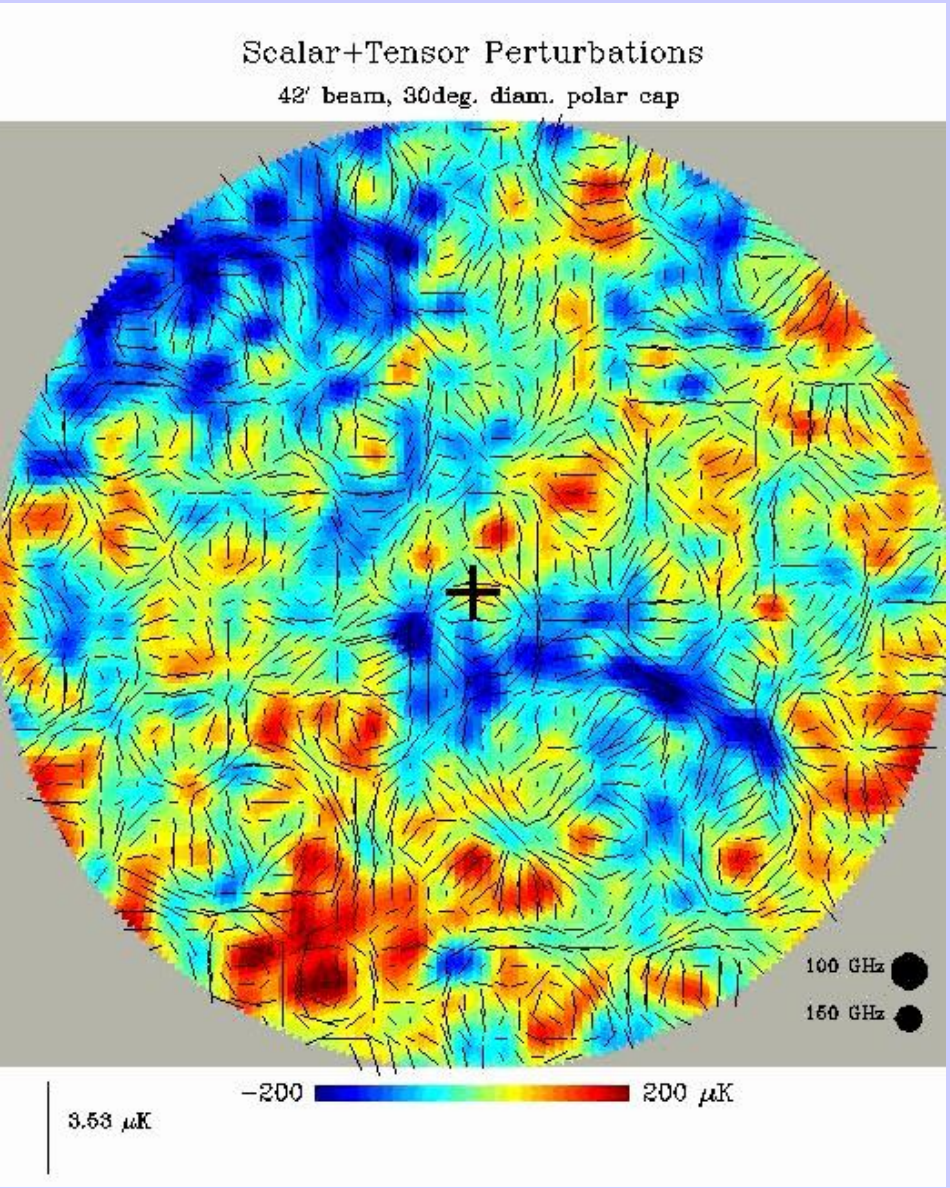

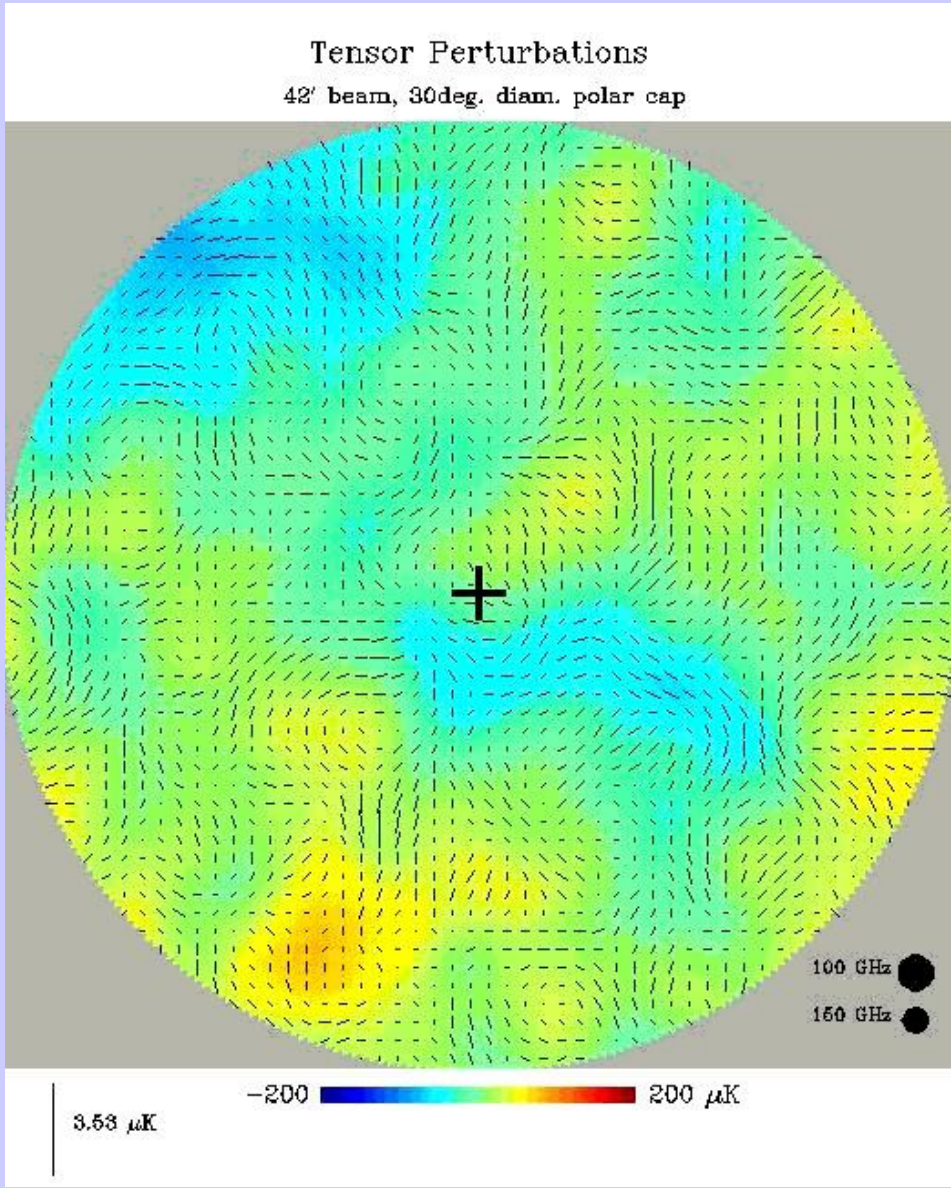

From the BICEP website (Caltech)

CMB observables

- The **angular power spectrum c_l** of the anisotropy defines the contribution to the rms from the different multipoles:

$$\Delta T(\theta,\varphi) = \sum_{\ell,m} a_{\ell m} Y_\ell^m(\theta,\varphi)$$

$$c_\ell = \left\langle a_{\ell m}^2 \right\rangle$$

$$\left\langle \Delta T^2 \right\rangle = \frac{1}{4\pi} \sum_\ell (2\ell+1) c_\ell$$

- A real experiment will not be sensitive to all the multipoles of the CMB.
- The window function w_l defines the sensitivity of the instrument to different multipoles.
- The detected signal will be:

$$\left\langle \Delta T^2 \right\rangle_{meas} = \frac{1}{4\pi} \sum_\ell (2\ell+1) w_\ell c_\ell$$

- For example, if the angular resolution is a gaussian beam with s.d. σ, the corresponding window function is

$$w_\ell^{LP} = e^{-\ell(\ell+1)\sigma^2}$$

Expected power spectrum:

$$\Delta T(\theta,\varphi) = \sum_{\ell,m} a_{\ell m} Y_\ell^m(\theta,\varphi)$$

$$c_\ell = \left\langle a_{\ell m}^2 \right\rangle$$

$$\left\langle \Delta T^2 \right\rangle = \frac{1}{4\pi} \sum_\ell (2\ell+1) c_\ell$$

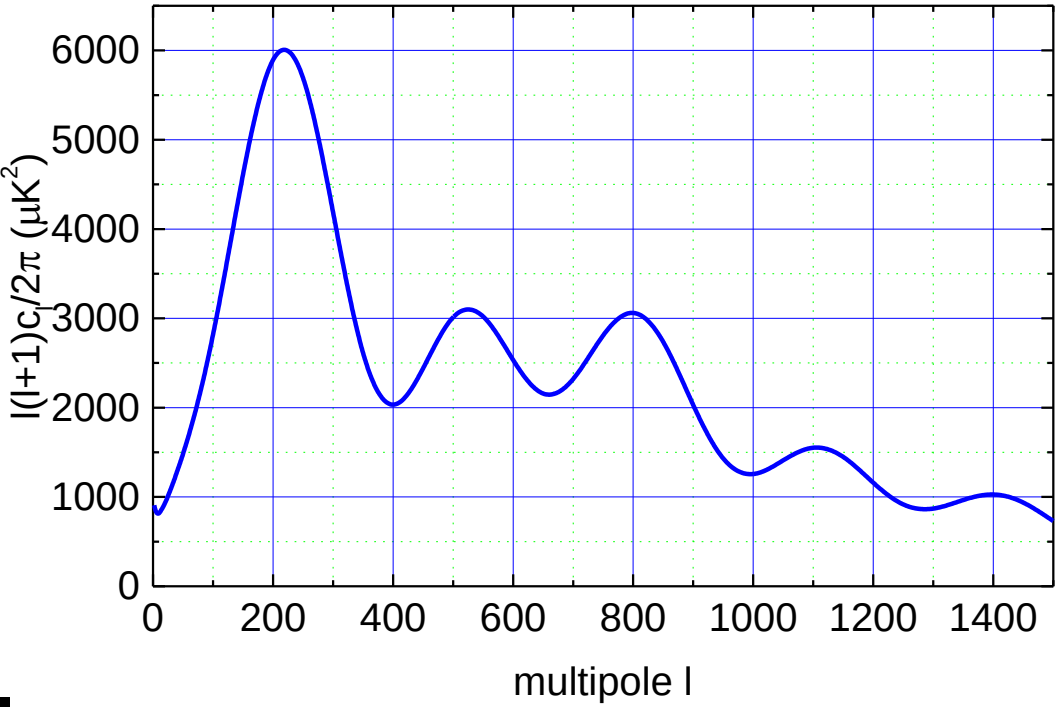

An instrument with finite angular resolution is not sensitive to the smallest scales (highest multipoles). For a gaussian beam with s.d. σ:

$$w_\ell^{LP} = e^{-\ell(\ell+1)\sigma^2}$$

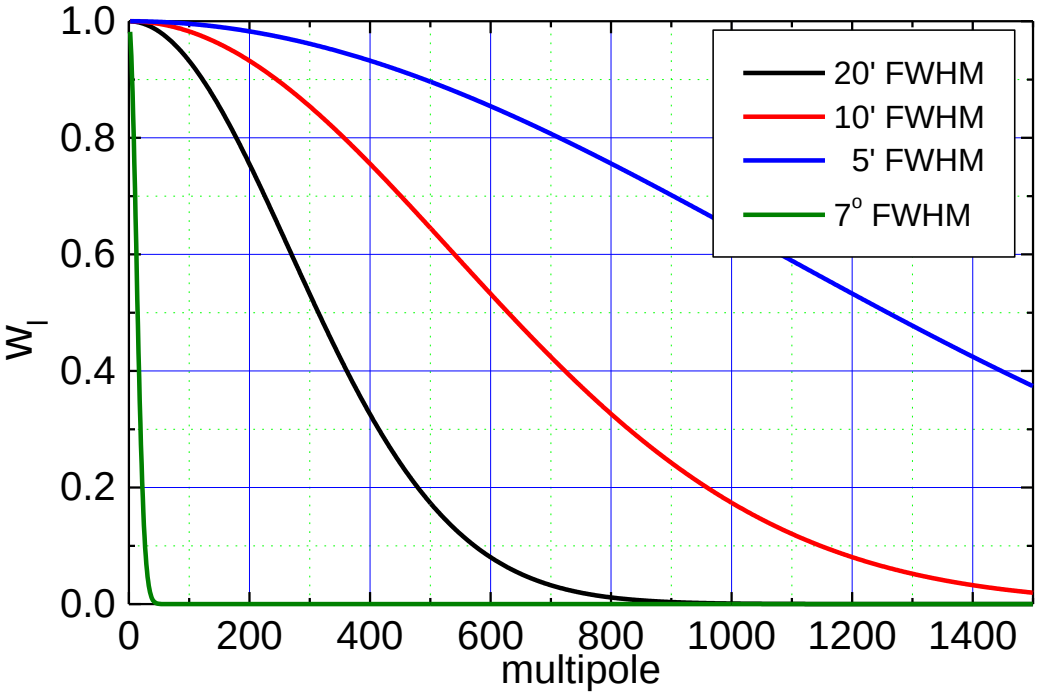

Expected power spectrum:

$$\Delta T(\theta,\varphi) = \sum_{\ell,m} a_{\ell m} Y_\ell^m(\theta,\varphi)$$

$$c_\ell = \left\langle a_{\ell m}^2 \right\rangle$$

$$\left\langle \Delta T^2 \right\rangle = \frac{1}{4\pi} \sum_\ell (2\ell+1) c_\ell$$

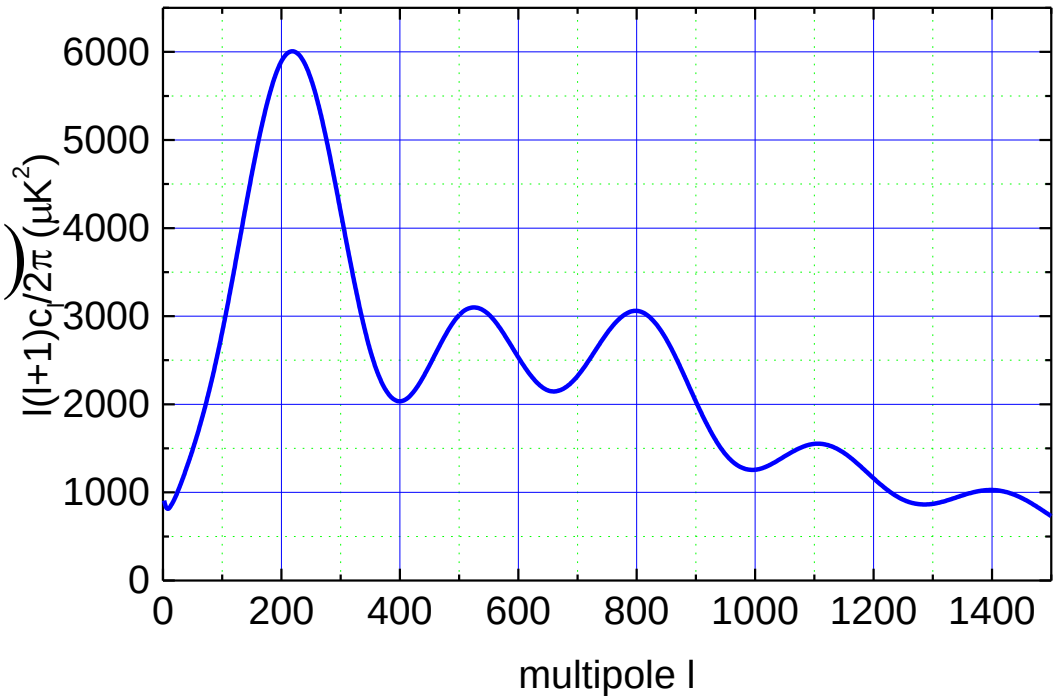

rms signal in an instrument with gaussian beam σ :

$$\left\langle \Delta T^2 \right\rangle_{meas} = \frac{1}{4\pi} \sum_\ell (2\ell+1) w_\ell^{LP} c_\ell$$

$$w_\ell^{LP} = e^{-\ell(\ell+1)\sigma^2}$$

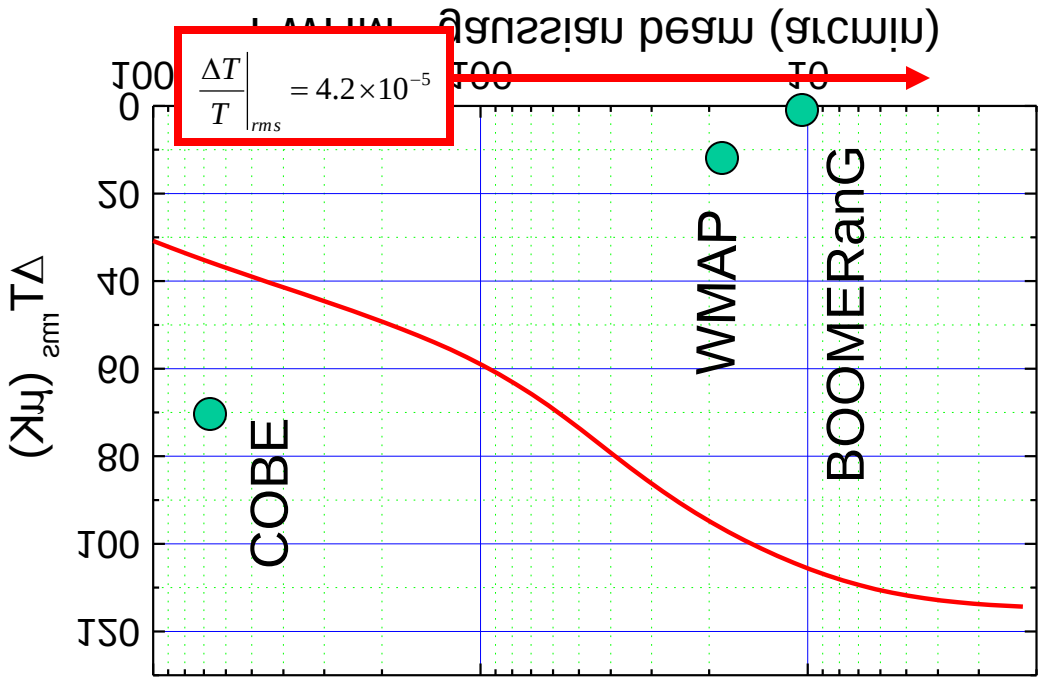

CMB observables

- The **rms anisotropy** has contributions from many angular scales
- The **angular power spectrum c_l** of the anisotropy defines the contribution to the rms from the different multipoles:

$$\Delta T(\theta,\varphi) = \sum_{\ell,m} a_{\ell m} Y_\ell^m(\theta,\varphi)$$

$$c_\ell = \left\langle a_{\ell m}^2 \right\rangle$$

$$\left\langle \Delta T^2 \right\rangle = \frac{1}{4\pi} \sum_\ell (2\ell+1) c_\ell$$

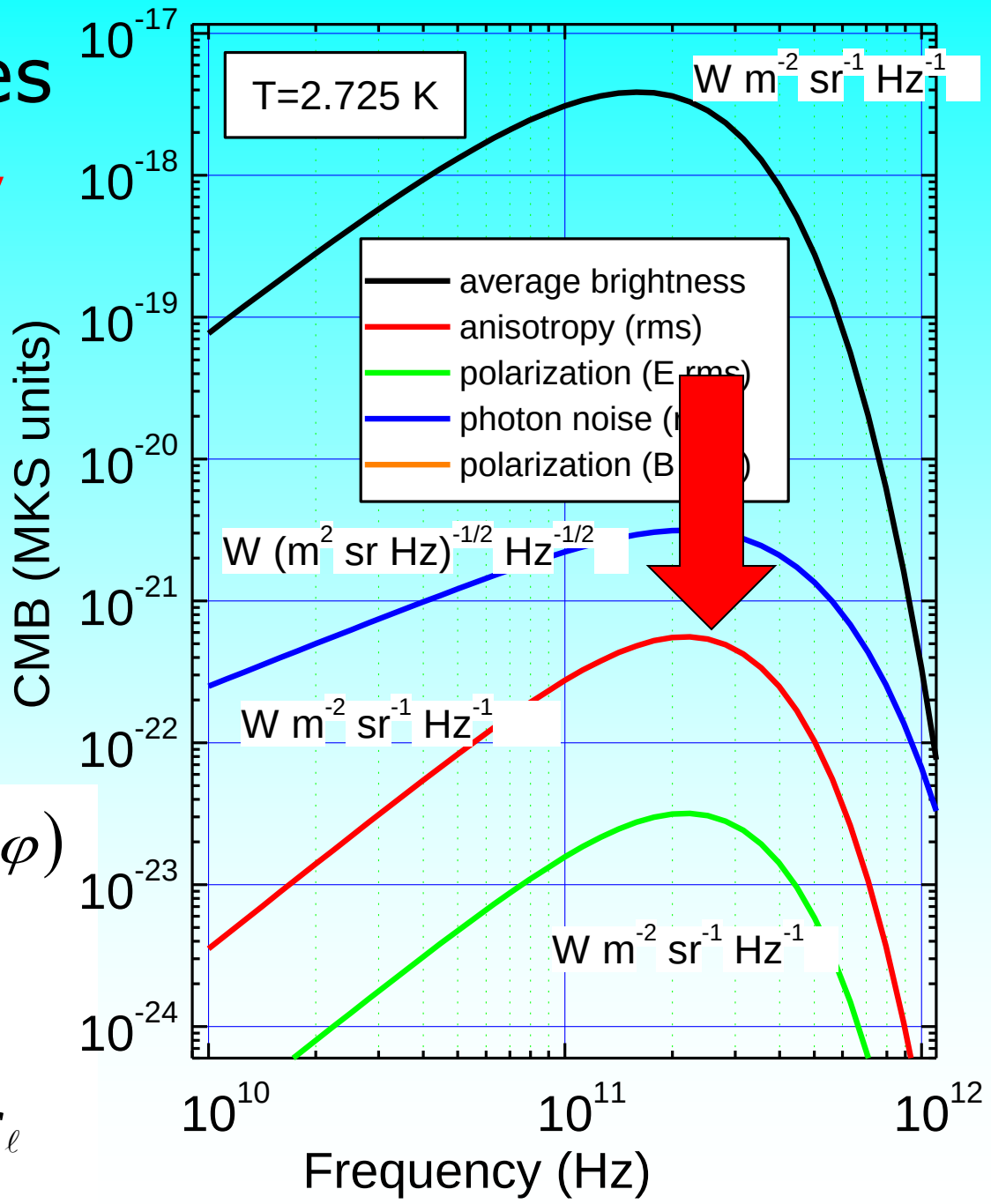

CMB observables

- **The polarization state**

$$\Delta B_P(\nu,T) = \frac{xe^x}{e^x-1} B(\nu,T) \frac{\Delta T_P}{T}$$

$$\left.\frac{\Delta T_P}{T}\right|_{rmsE} \approx 4\times10^{-6}$$

$$\left.\frac{\Delta T_P}{T}\right|_{rmsB} \approx 2\times10^{-7}$$

- **Extremely weak !**

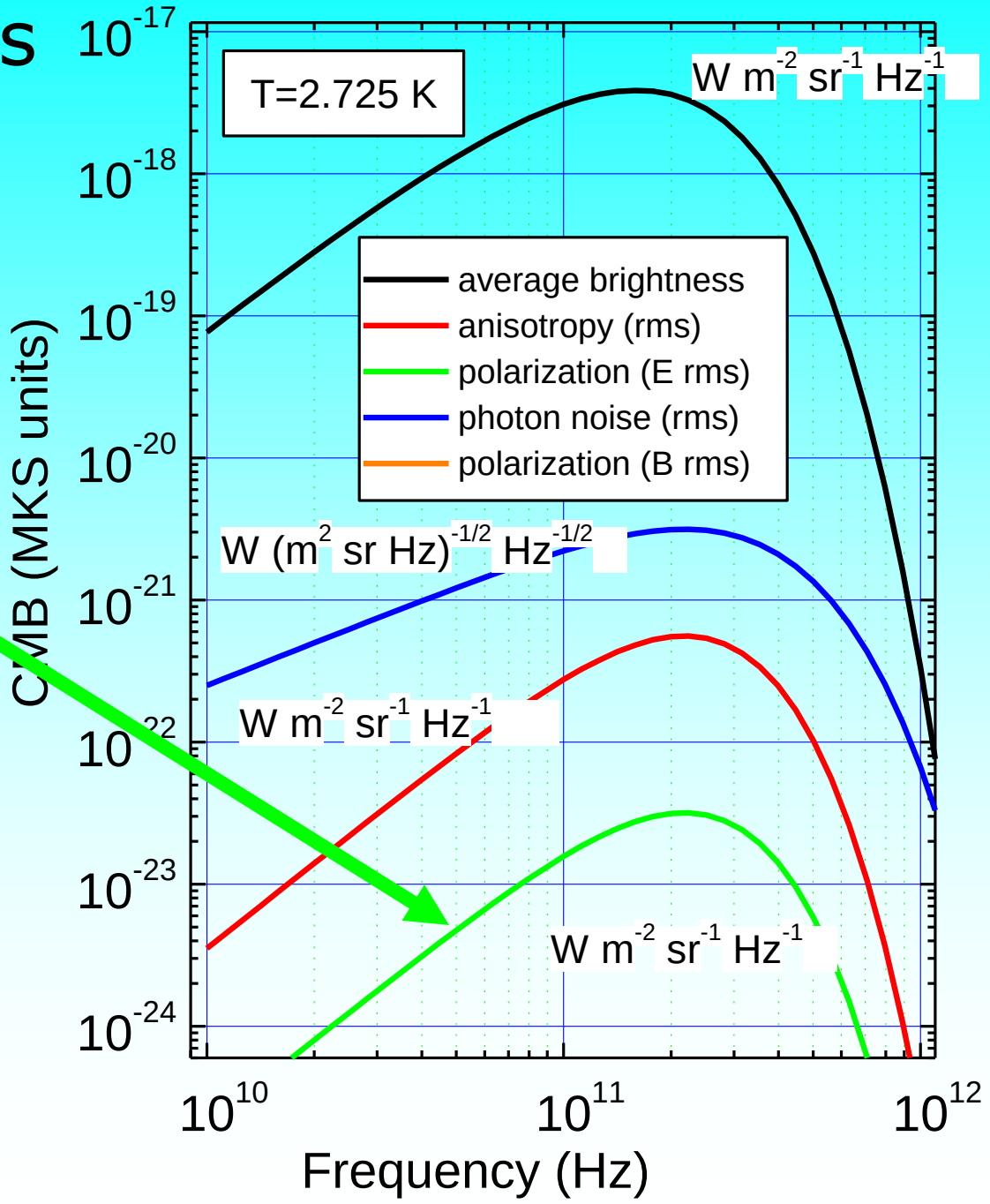

Experimental Approach

CMB observables

- These signals are **faint** with respect to:
  - **detector** noise
  - background emission of the **instrument** and of the earth **atmosphere**
  - background emission of the **astrophysical** environment.

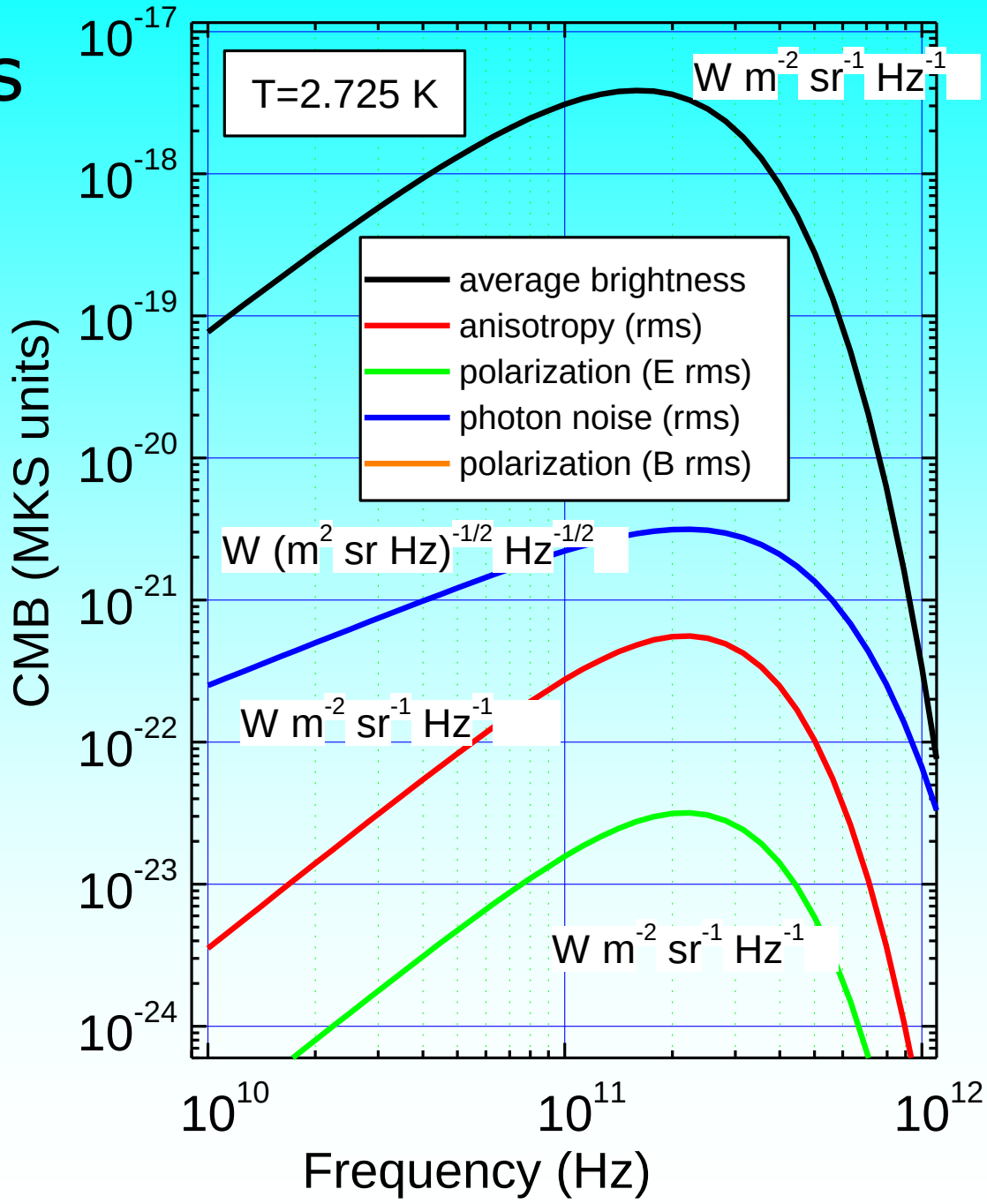

CMB observables

- The spectrum peaks at 150 GHz
- The anisotropy, polarization and noise peak at 210-220 GHz
- These frequencies are high for coherent detectors, and low for thermal detectors.

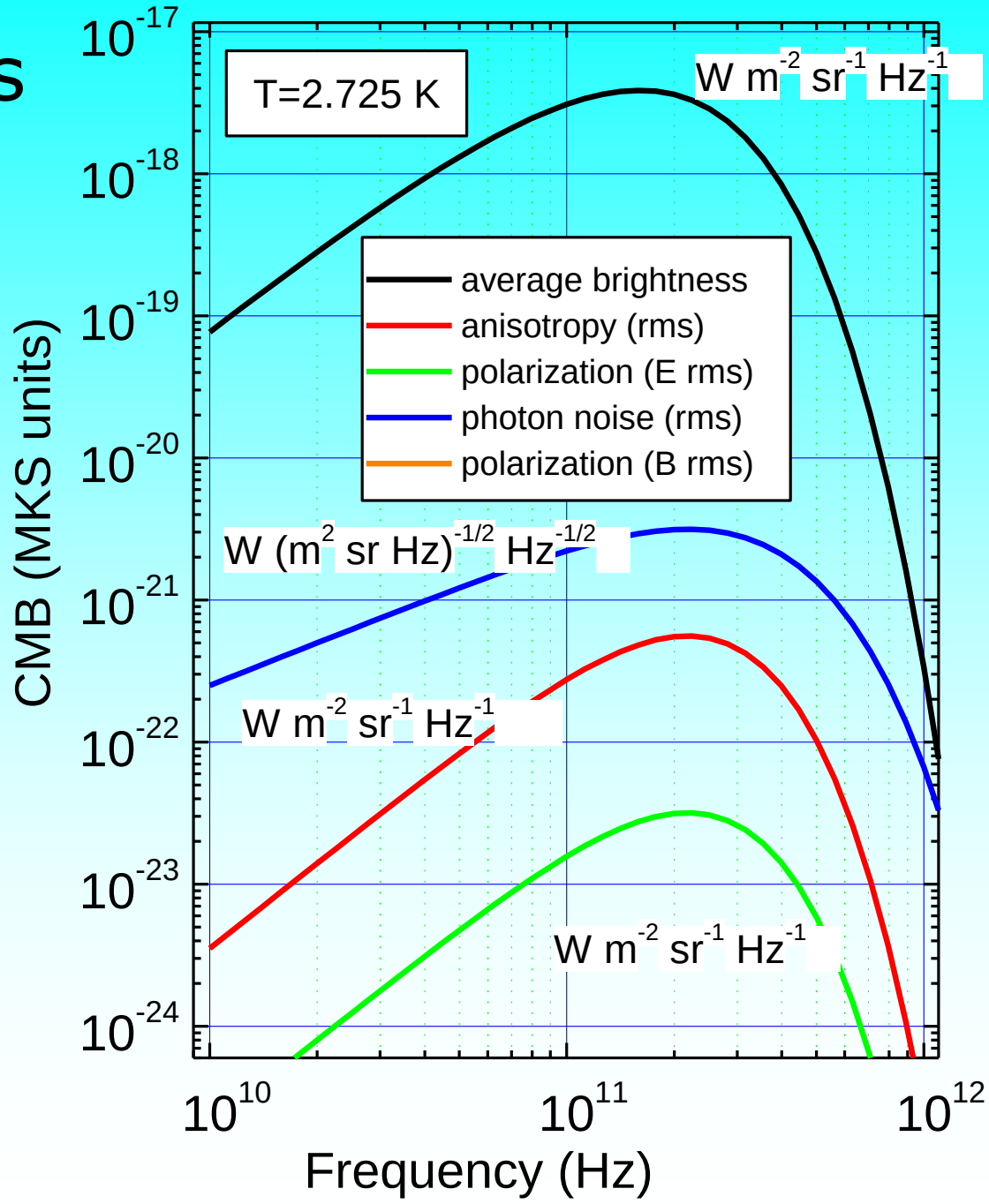

Detectors

Detectors

- Coerent detectors measure amplitude and phase of the em wave
- Thermal detectors measure the energy of the em wave
- On both sides, CMB research drove the development of new devices:
  - Cryogenic, ultra-low noise HEMT amplifiers (coherent)
  - Cryogenic "Spider Web" and "Polarization Sensitive" Bolometers (thermal)
  - Low sidelobe corrugated antennas …..
- Also, the two worlds are progressively mixed: for example waveguides and striplines are now used with cryogenic bolometers

Cryogenic Bolometers

- The CMB spectrum is continuum and bolometers are wide band detectors. That's why they are so sensitive.

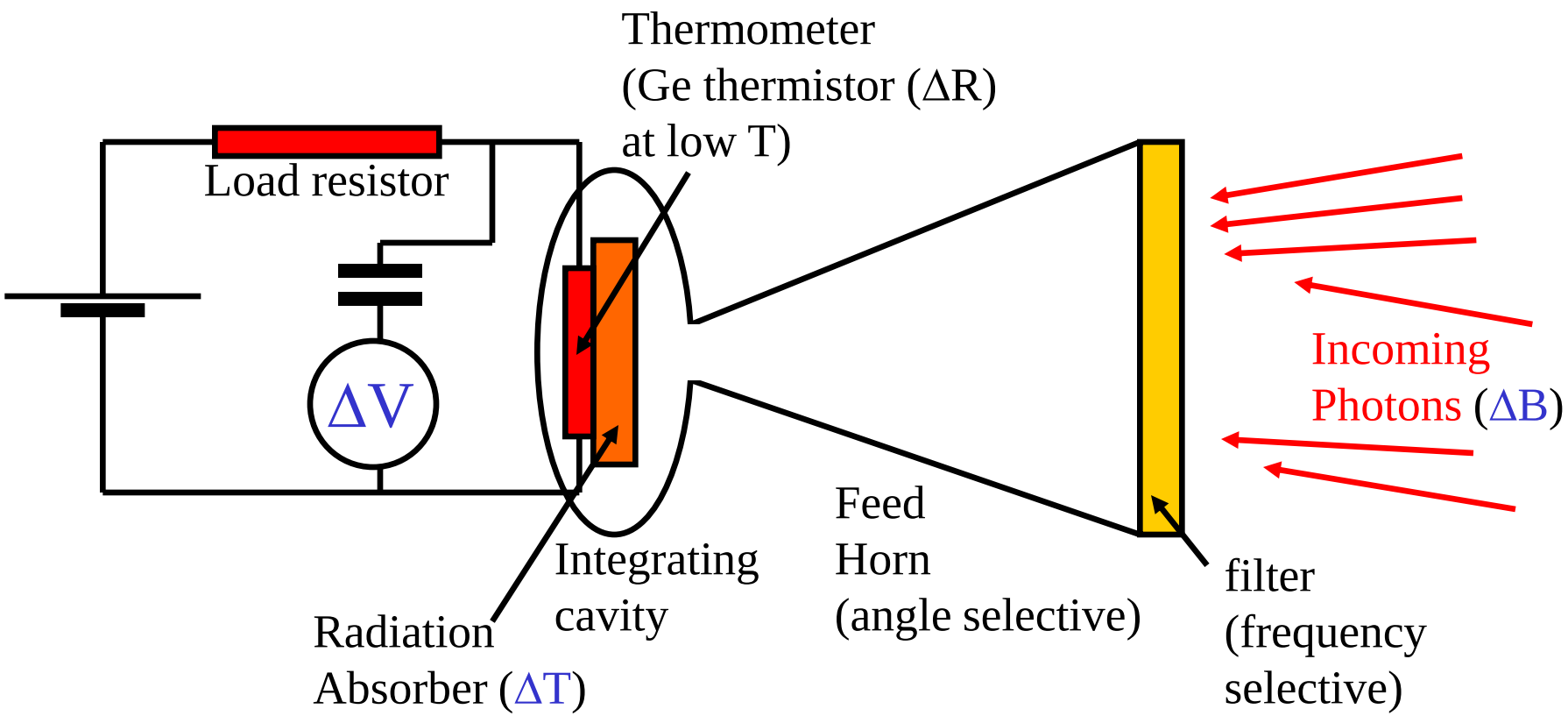

- Fundamental noise sources are Johnson noise in the thermistor ($<\Delta V^2> = 4kTR$), temperature fluctuations in the thermistor ($(<\Delta W^2> = 4kGT^2$), background radiation noise (T_{bkg}^5) → need to reduce the temperature of the detector and the radiative background.

Cryogenic Bolometers

- In steady conditions the temperature rise of the sensor is due to the background radiative power absorbed Q and to the electrical bias power P:

$$G(T - T_0) = Q + P$$

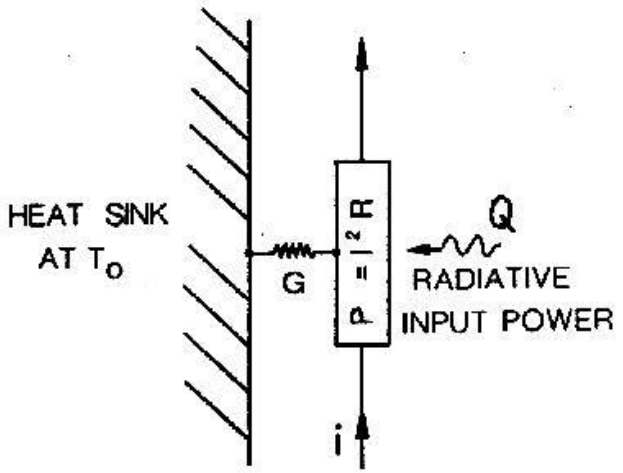

- The effect of the background power is thus equivalent to an increase of the reference temperature:

$$P = G\left[T - (T_0 + \frac{Q}{G})\right] = G(T - T_0')$$

$$T_0' = T_0 + \frac{Q}{G}$$

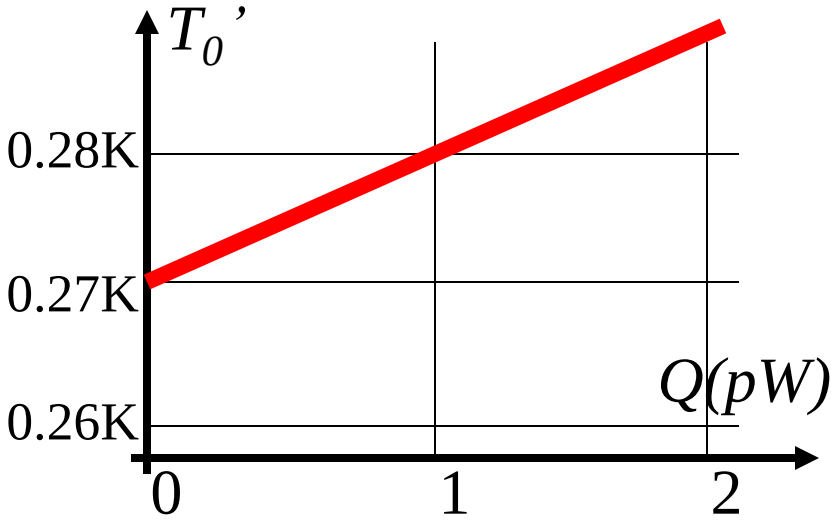

Cryogenic Bolometers

- In presence of an additional signal $\Delta Q\, e^{j\omega t}$ (from the sky)

$$C\frac{d\Delta T}{dt}+G_{eff}\Delta T=\Delta Q$$

$$\left|\frac{dT}{dQ}\right|=\frac{1}{G_{eff}\sqrt{1+\tau^2\omega^2}}$$

$$\tau=\frac{C}{G}$$

- There is a tradeoff between high sensitivity and fast response. **The heat capacity C should be minimized** to optimize both.

Small sensor at **low temperature**

- Using a current biased thermistor to readout the temperature change:

$$\alpha=\frac{1}{R(T)}\frac{dR(T)}{dT}\quad\Rightarrow\quad dV=idR=i\alpha R dT$$

Responsivity

$$\Re=\frac{dV}{dQ}=i\alpha R\frac{dT}{dQ}=\frac{i\alpha R}{G_{eff}\sqrt{1+\tau^2\omega^2}}$$

Cryogenic Bolometers

$$\alpha = \frac{1}{R(T)}\frac{dR(T)}{dT}$$

$$\Re = \frac{i\alpha R}{G_{eff}\sqrt{1+\tau^2\omega^2}}$$

- A large α is important for high responsivity.
- Ge thermistors: $\alpha \approx 10K^{-1}$
- Superconducting transition thermistors: $\alpha \approx 1000K^{-1}$

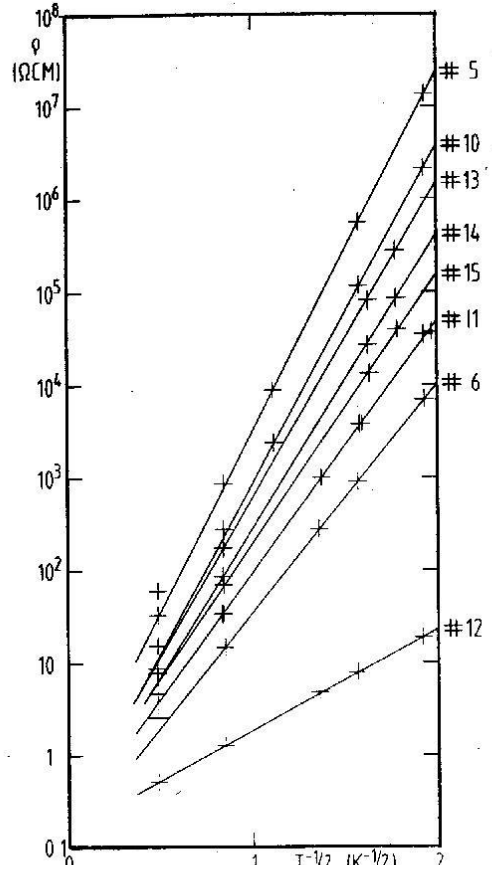

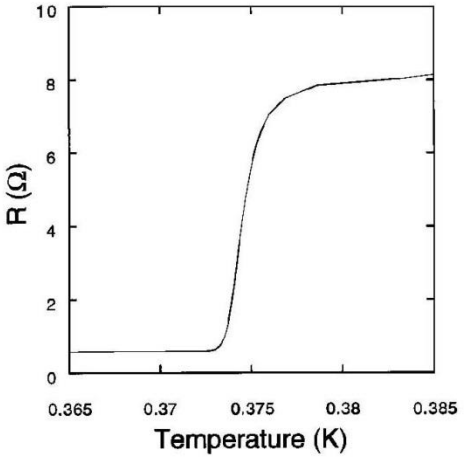

S.F. Lee et al. Appl.Opt. **37** 3391 (1998)

Cryogenic Bolometers

- Johnson noise in the thermistor

$$\frac{d\left\langle \Delta V_J^2 \right\rangle}{df} = 4kTR$$

- Temperature noise

$$\frac{d\left\langle \Delta W_T^2 \right\rangle}{df} = \frac{4kT^2 G_{eff}}{G_{eff}^2 + (2\pi f C)^2}$$

- Photon noise

$$\frac{d\left\langle \Delta W_{Ph}^2 \right\rangle}{df} = \frac{4k^5 T_{BG}^5}{c^2 h^3} \int \varepsilon \frac{x^4 \left(e^x - 1 + \varepsilon\right)}{\left(e^x - 1\right)^2} dx$$

- Total NEP (fundamental):

$$NEP^2 = \frac{1}{\Re^2} \frac{d\left\langle \Delta V_J^2 \right\rangle}{df} + \frac{d\left\langle \Delta W_T^2 \right\rangle}{df} + \frac{d\left\langle \Delta W_{Ph}^2 \right\rangle}{df}$$

Again, need of low Temperature And low Background

Q

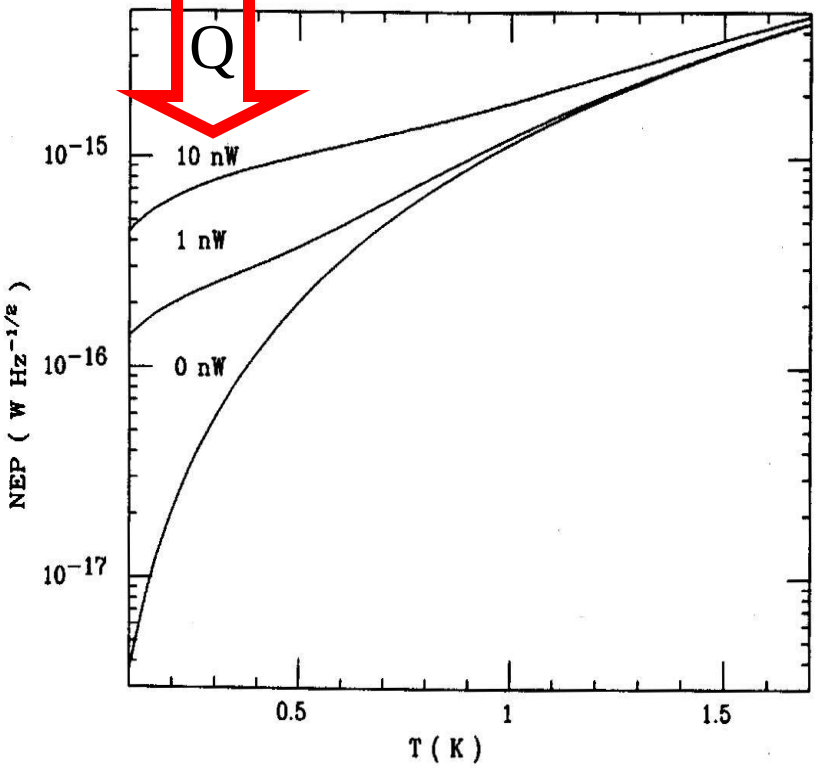

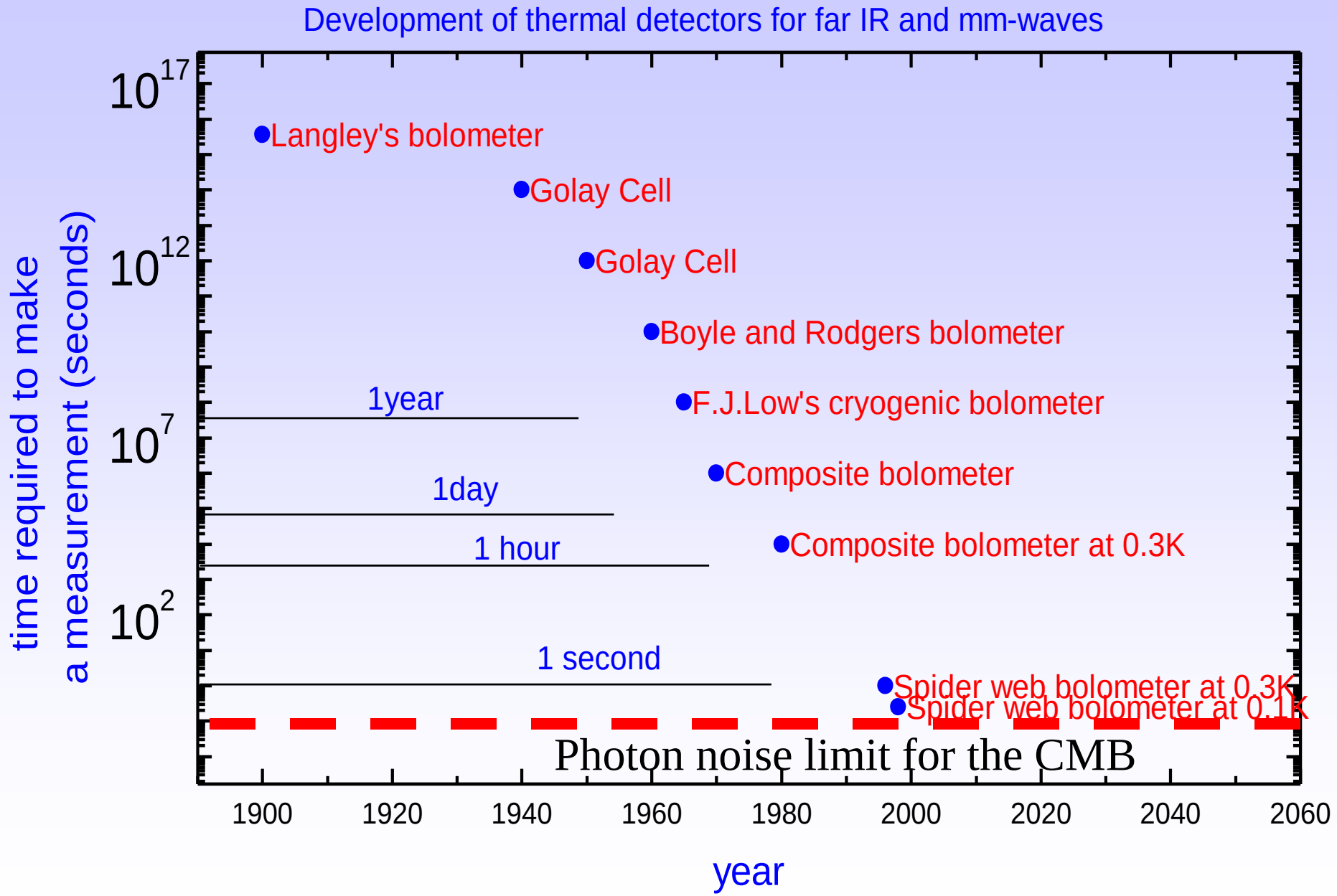
Development of thermal detectors for far IR and mm-waves
time required to make a measurement (seconds)
10^{17}
10^{12}
10^{7}
10^{2}
Langley's bolometer
Golay Cell
Golay Cell
Boyle and Rodgers bolometer
F.J.Low's cryogenic bolometer
Composite bolometer
Composite bolometer at 0.3K
Spider web bolometer at 0.3K
Spider web bolometer at 0.1K
1year
1day
1 hour
1 second
Photon noise limit for the CMB
1900
1920
1940
1960
1980
2000
2020
2040
2060
year

Spider-Web Bolometers

- The absorber is micro machined as a web of metallized Si_3N_4 wires, 2 μm thick, with 0.1 mm pitch.
- This is a good absorber for mm-wave photons and features a very low cross section for cosmic rays. Also, the heat capacity is reduced by a large factor with respect to the solid absorber.
- NEP ~ $2\ 10^{-17}$ W/$Hz^{0.5}$ is achieved @0.3K
- 150μK_{CMB} in 1 s
- Mauskopf *et al.* Appl.Opt. **36**, 765-771, (1997)

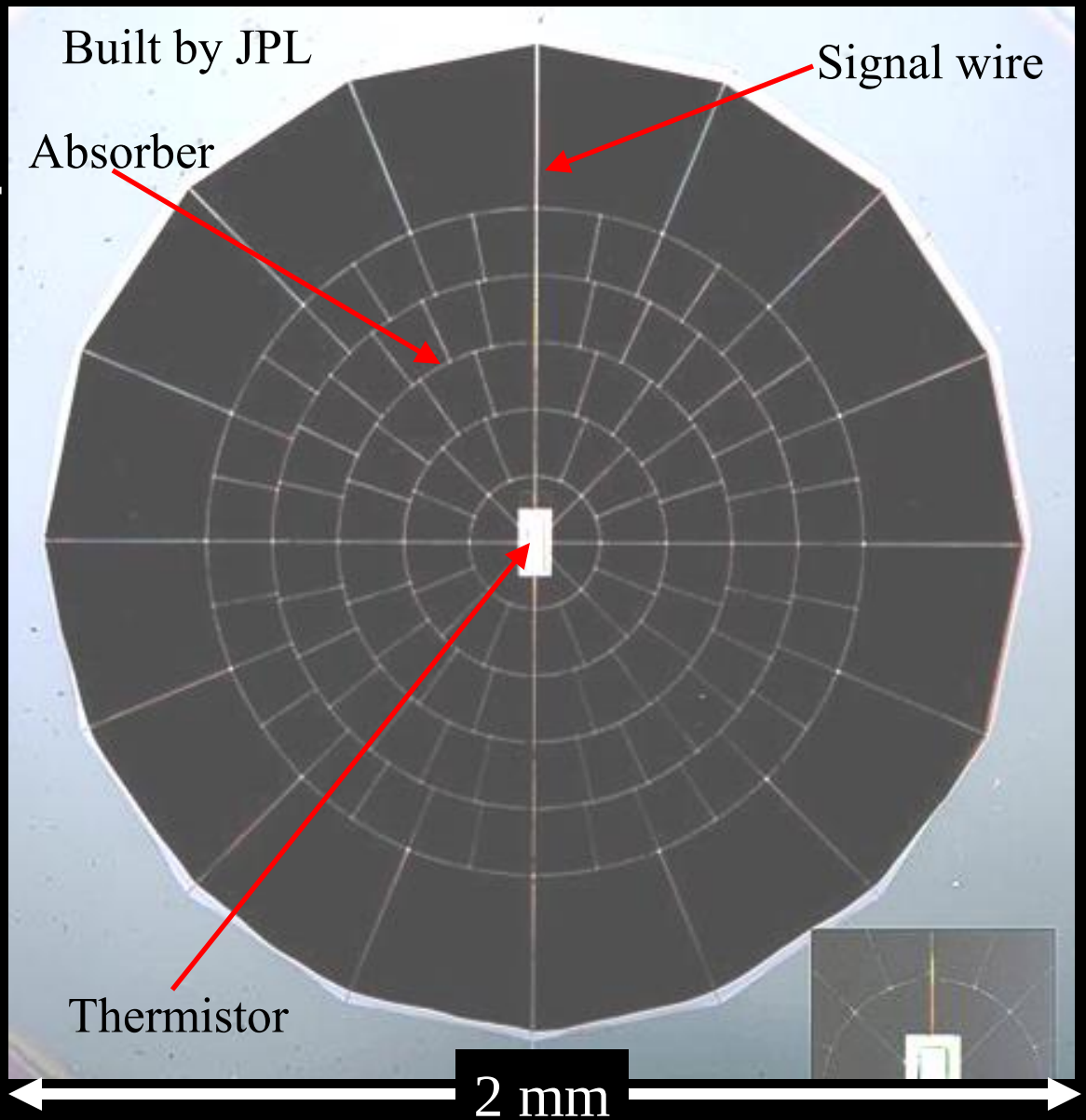

Table 5. In-flight bolometer performance

ν_0 (GHz)	τ (ms)	η_{opt}	G (pW K^{-1})	R (MΩ)	NEP (1 Hz) (10^{-17} W/$\sqrt{\text{Hz}}$)	NET$_{CMB}$ (μK$\sqrt{\text{s}}$)
90	22	0.30	82	5.5	3.2	140
150sm	12.1	0.16	85	5.9	4.2	140
150mm	15.7	0.10	88	5.5	4.0	190
240	8.9	0.07	190	5.7	5.7	210
410	5.7	0.07	445	5.4	12.1	2700

Note. — In-flight bolometer performance. The 150 GHz channels are divided into single mode (150sm) and multimode(150mm). The optical efficiency of the channels decreased significantly from the measured efficiency of each feed structure due to truncation by the Lyot stop. The NEP is that measured in flight, and includes contributions from detector noise, amplifier noise, and photon shot noise.

Crill et al., 2003 – BOOMERanG 1998 bolometers

The launch: Dec. 29, 1998

- The instrument is flown above the Earth atmosphere, at an altitude of 37 km, by means of a stratospheric balloon.
- Long duration flights (LDB, 1-3 weeks) are performad by NASA-NSBF over Antarctica
- BOOMERanG has been flown LDB two times:
- From Dec.28, **1998** to Jan.8, 1999, for CMB anisotropy measurements
- In **2003**, from Jan.6 to Jan.20, for CMB polarization measurements (B2K).

  Talk at SS2, July 18

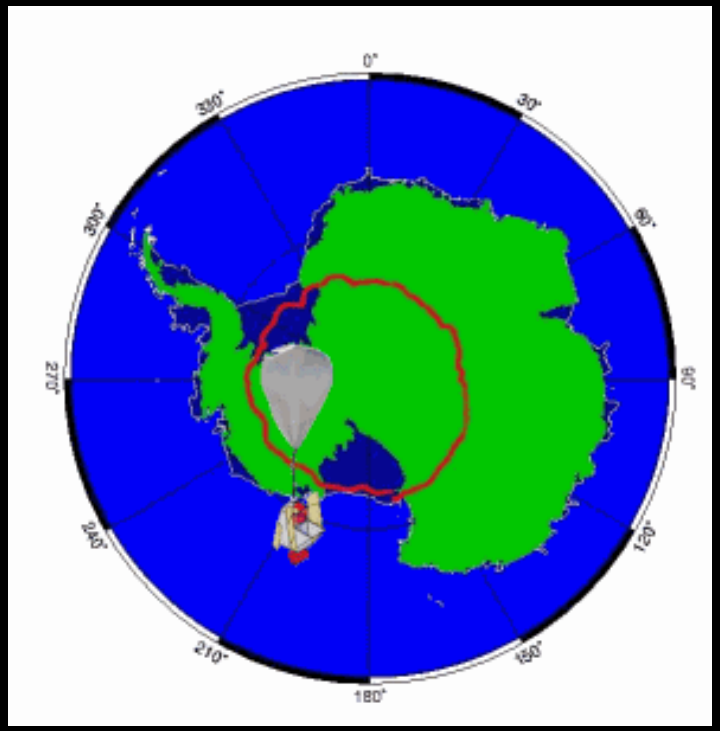

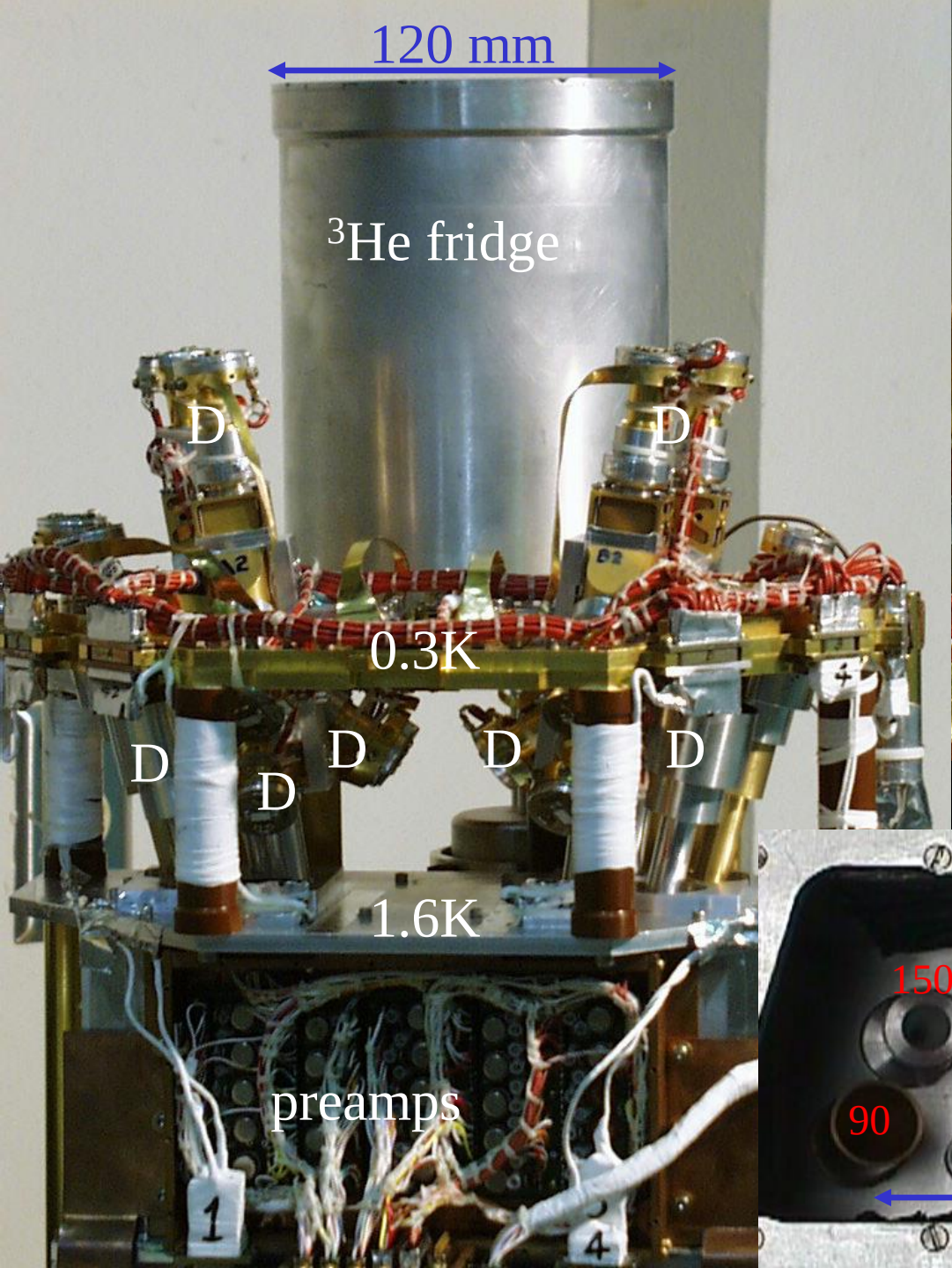

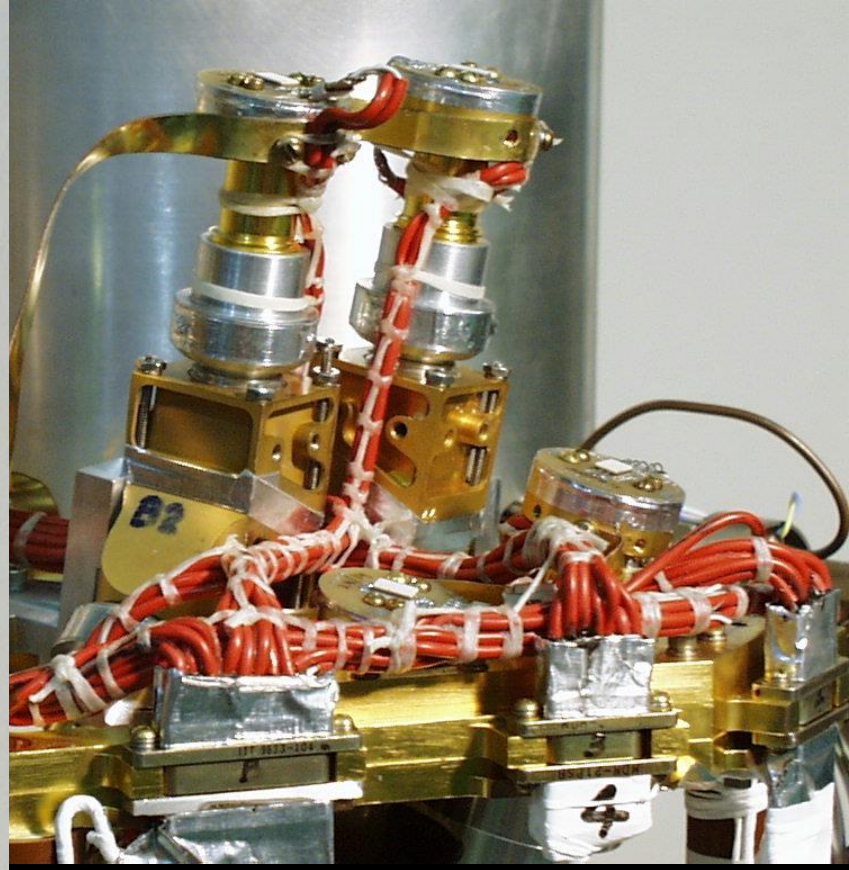

Focal plane assembly

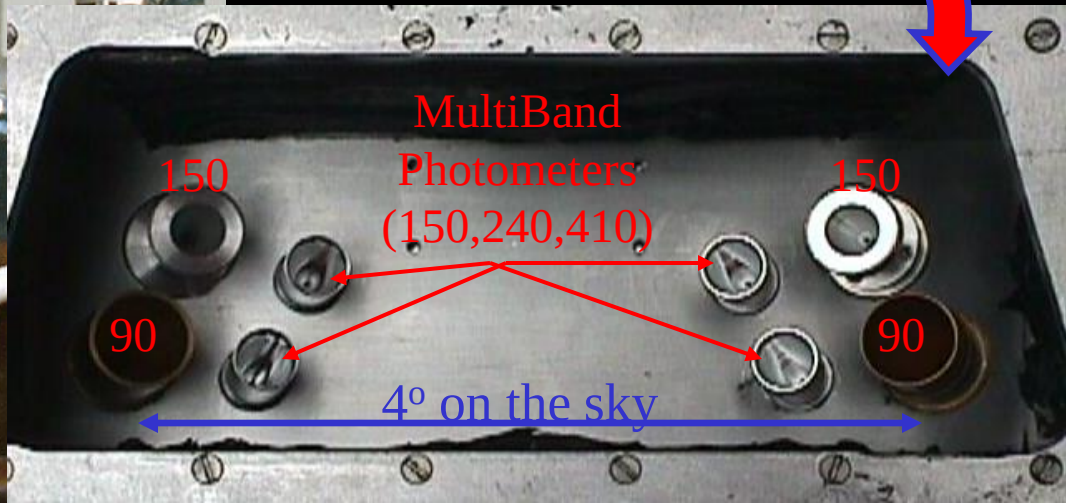

BOOMERanG

- 1998: BOOMERanG mapped the temperature fluctuations of the CMB at sub-horizon scales (<1^{O}).
- The signal was well above the noise:

2 indep. det. at 150 GHz

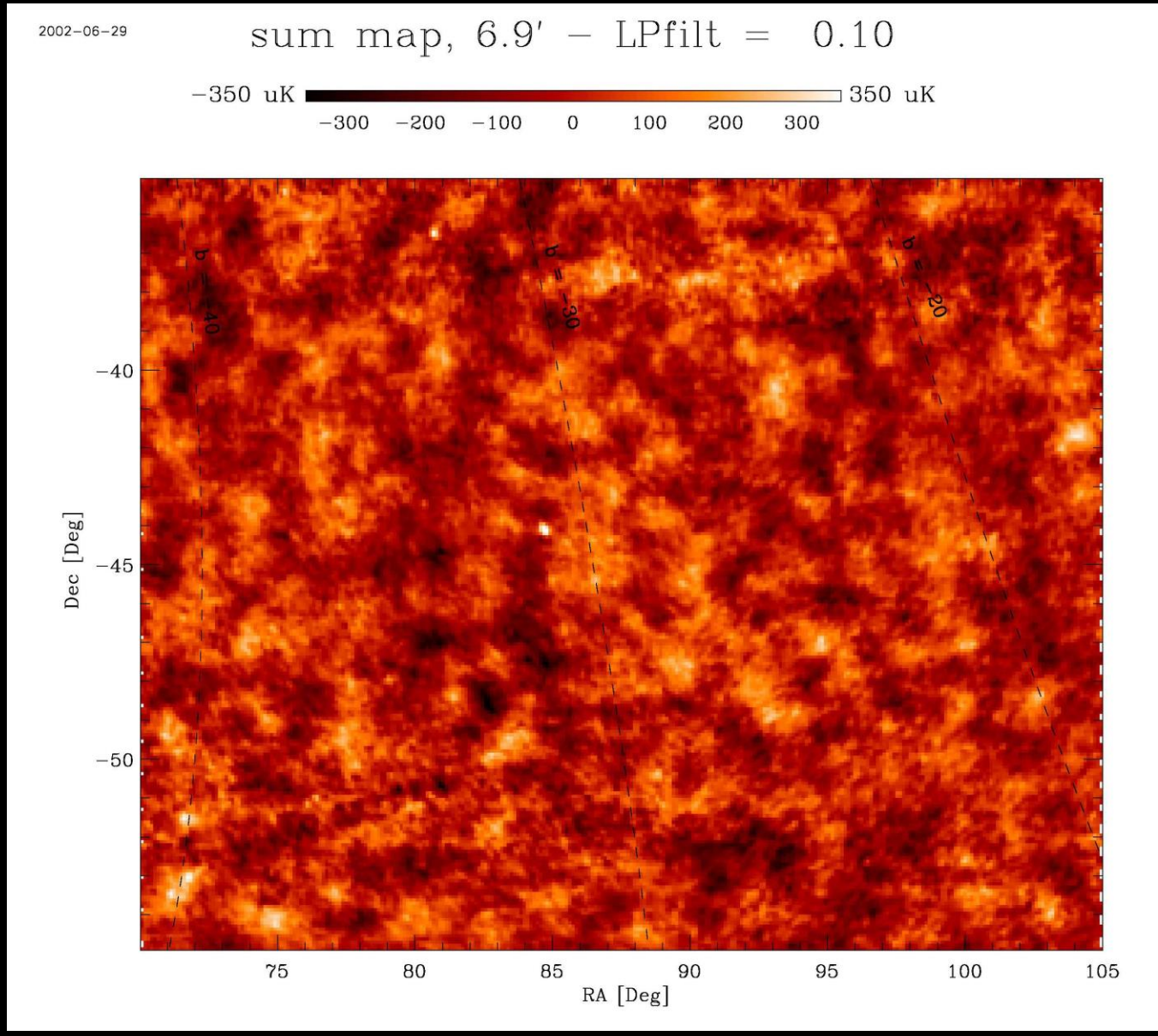

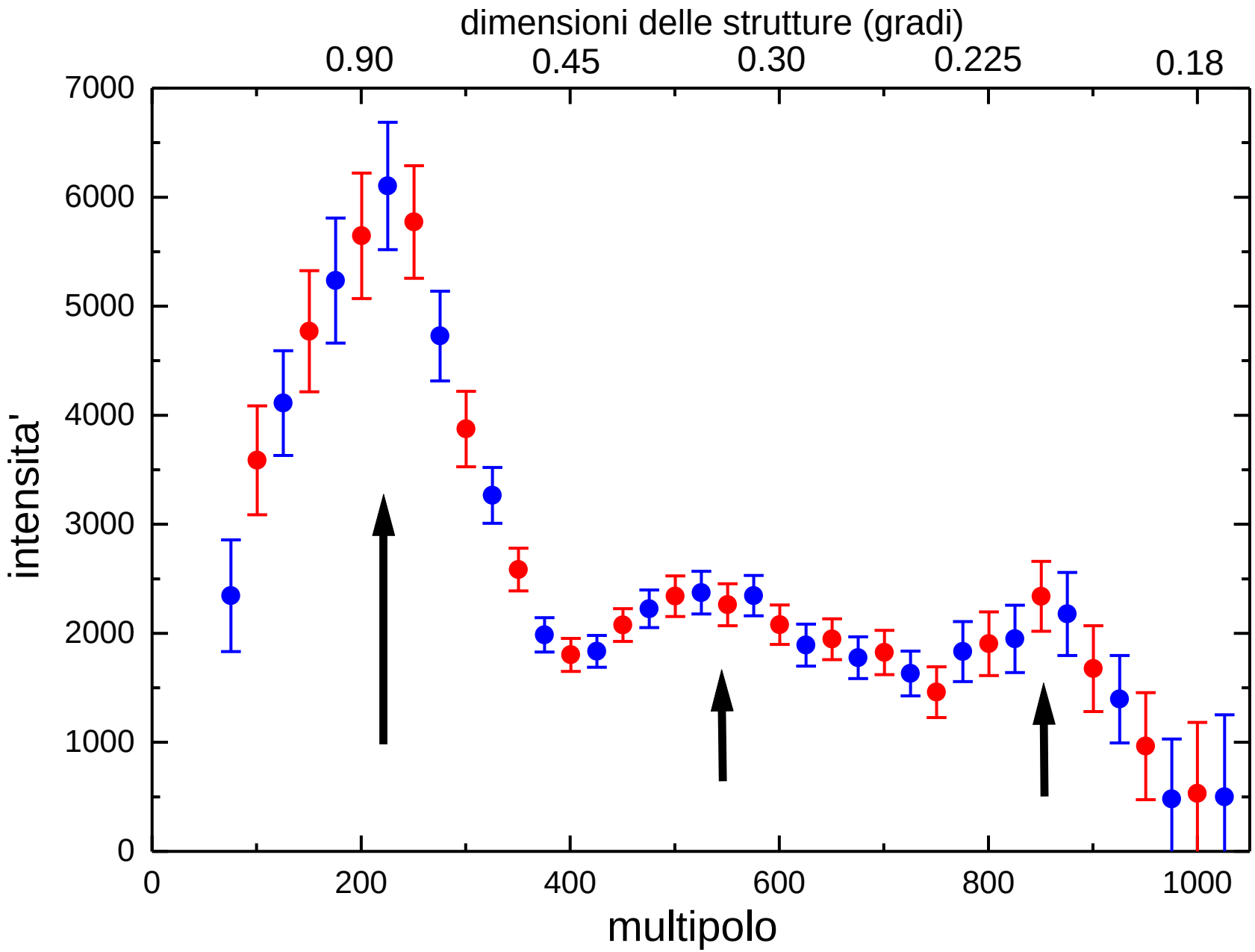
dimensioni delle strutture (gradi)
0.90
0.45
0.30
0.225
0.18
7000
6000
5000
4000
3000
2000
1000
0
intensita'
0
200
400
600
800
1000
multipolo

Parameters III: Concordance Cosmology
(CMB + LSS + Type 1a Supernovae)

$\Omega_{tot} = 0.99 \pm 0.03$

$n_s = 1.00 \pm 0.08$

} **+ gaussianity =Inflation (!) (?)**

$\Omega_b h^2 = 0.021 \pm 0.003$

$\Omega_{cdm} h^2 = 0.14 \pm 0.02$

$\Omega_\Lambda = 0.65 \pm 0.05$

} 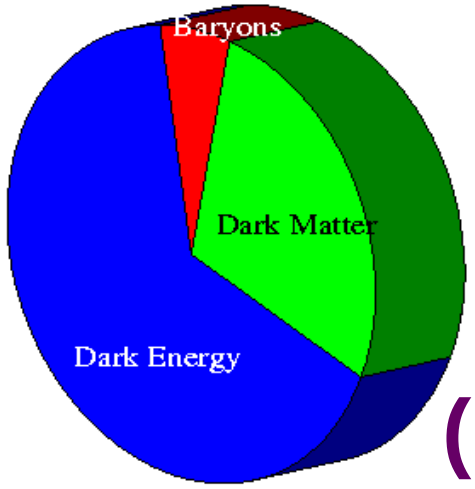

(?)

$h = 0.67 \pm 0.09$

Age: 13.7 ± 1.3 GYr

} **OK !**

MICROWAVE ANISOTROPY PROBE

MAP

NASA-2001

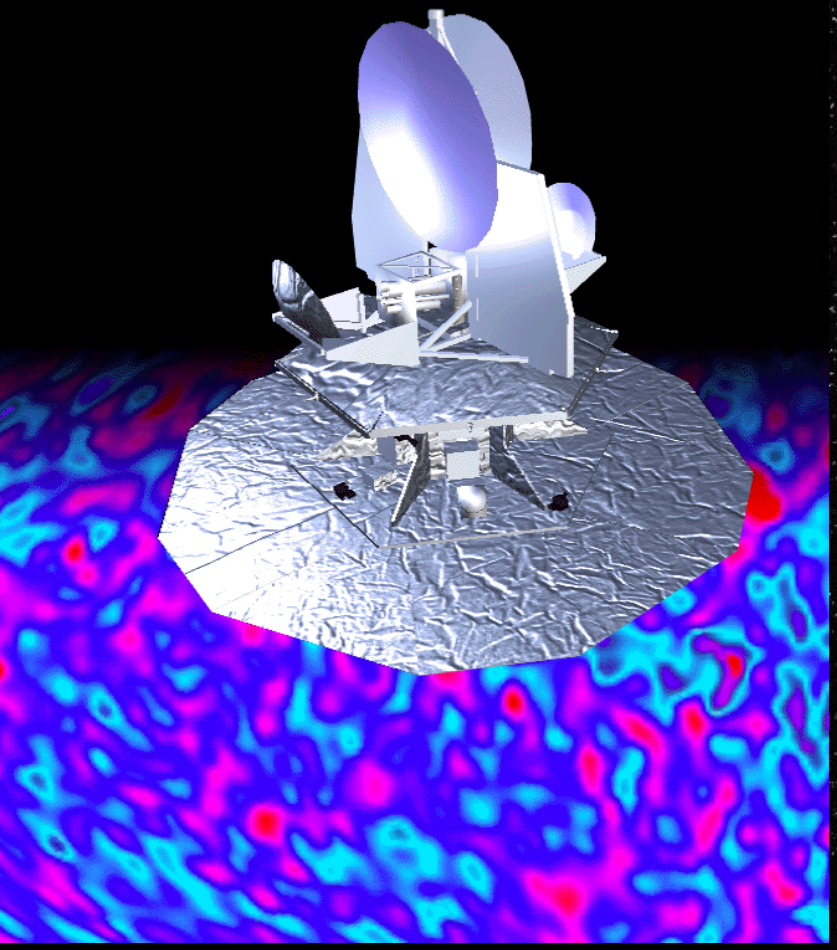

ESA-2007

Planck Surveyor

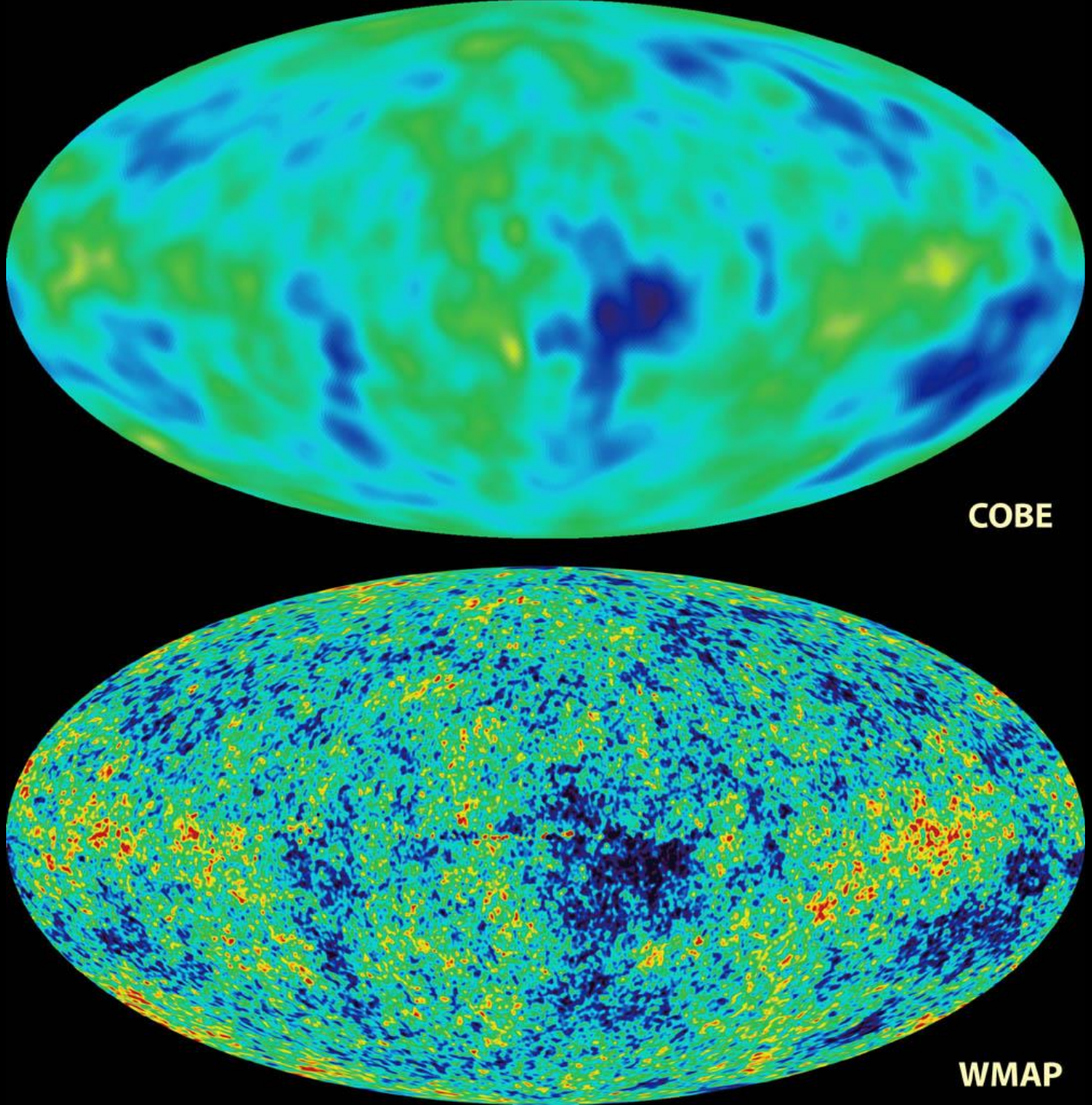
COBE
WMAP

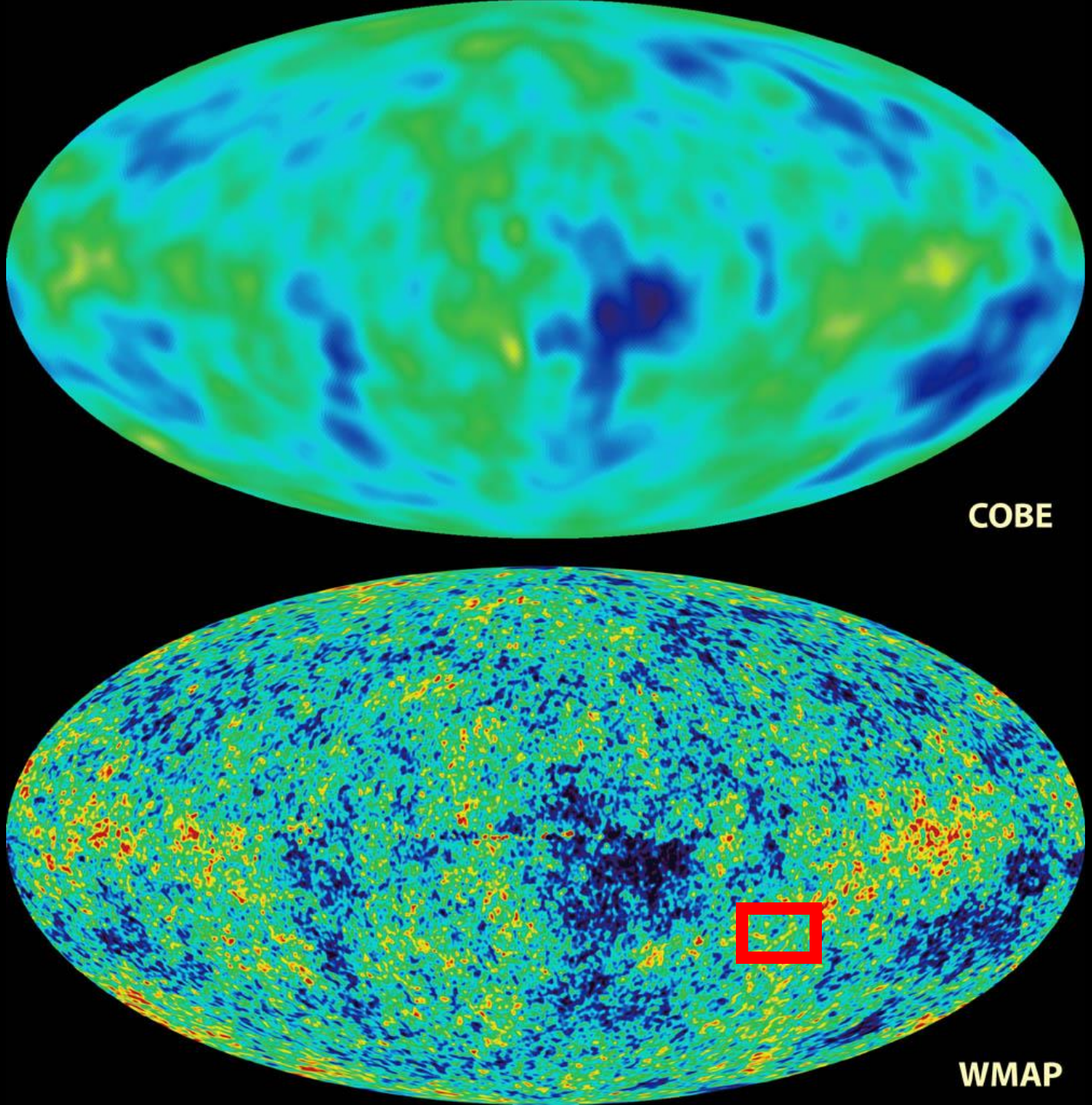
COBE
WMAP

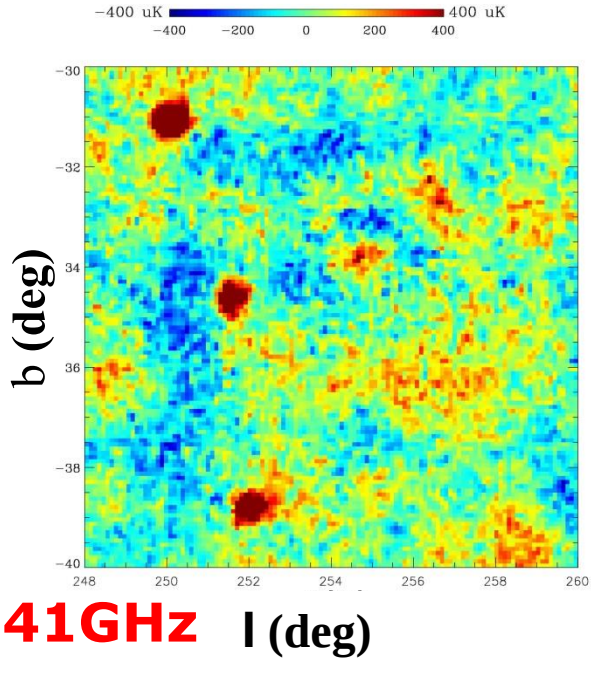

41GHz l (deg)

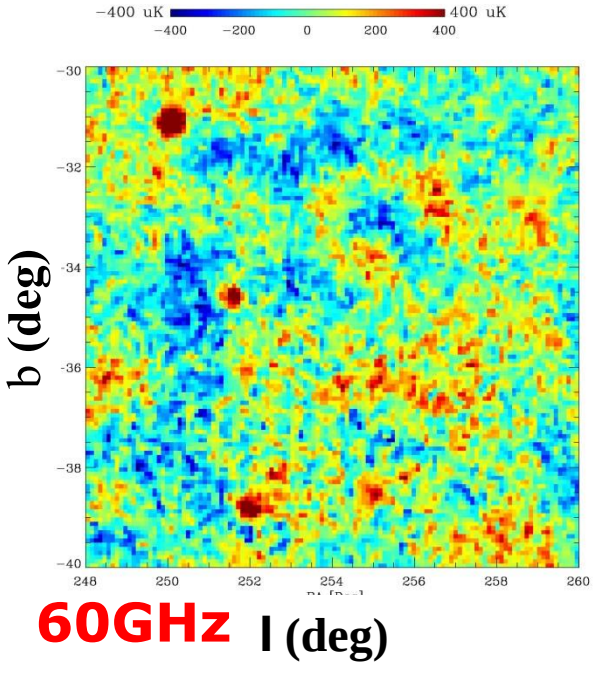

60GHz l (deg)

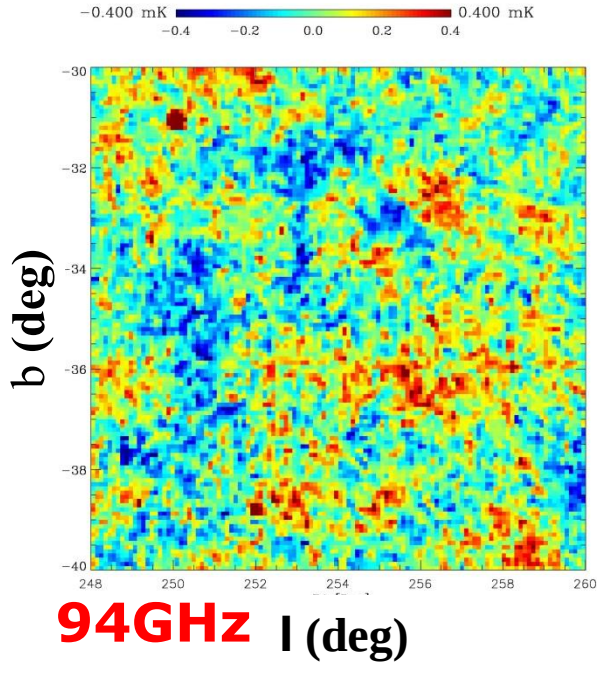

94GHz l (deg)

WMAP 1st yr

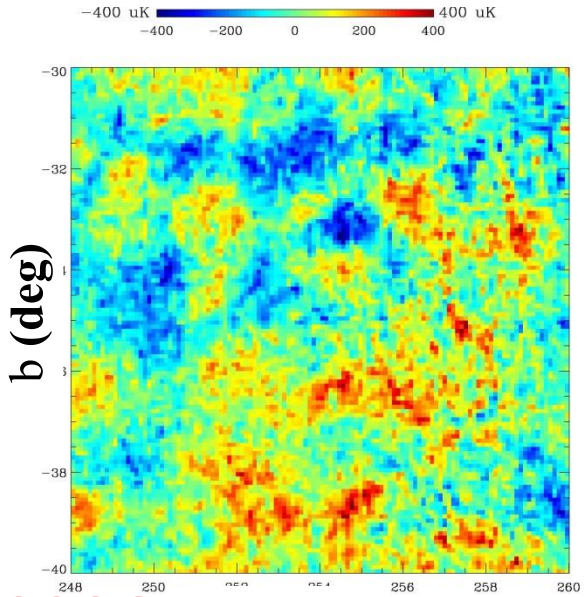

220GHz l (deg)

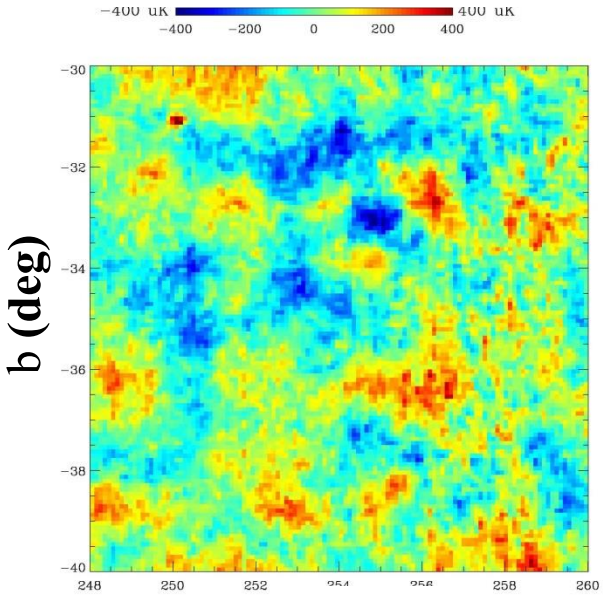

150GHz l (deg)

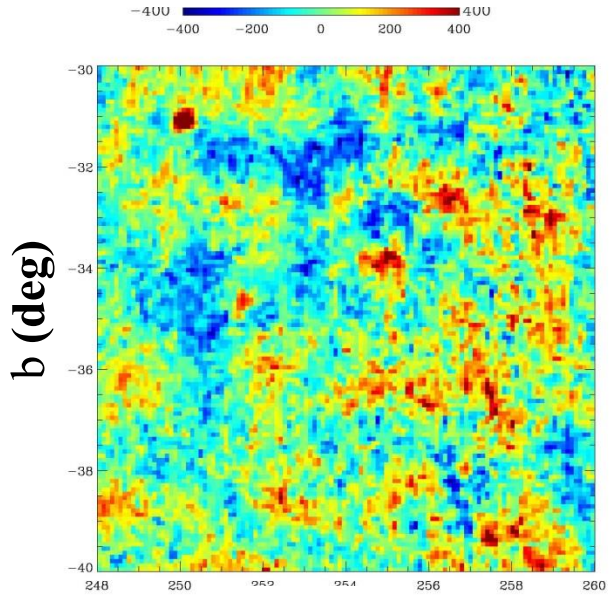

90GHz l (deg)

BOOMERanG 98

Spectrum of CMB anisotropy

[from the correlations map(ν) vs map(94GHz), corrected for beam and sky coverage]

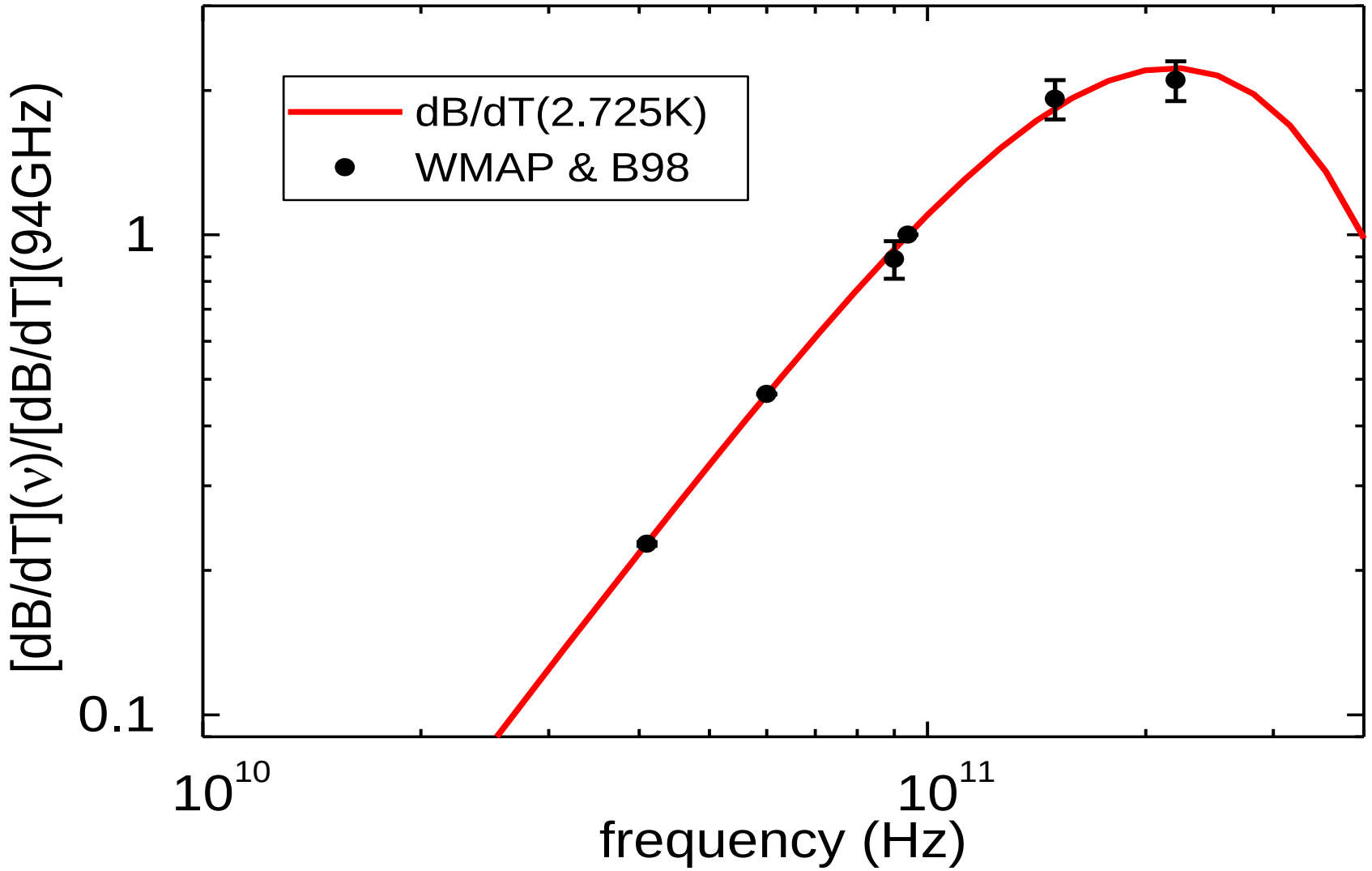

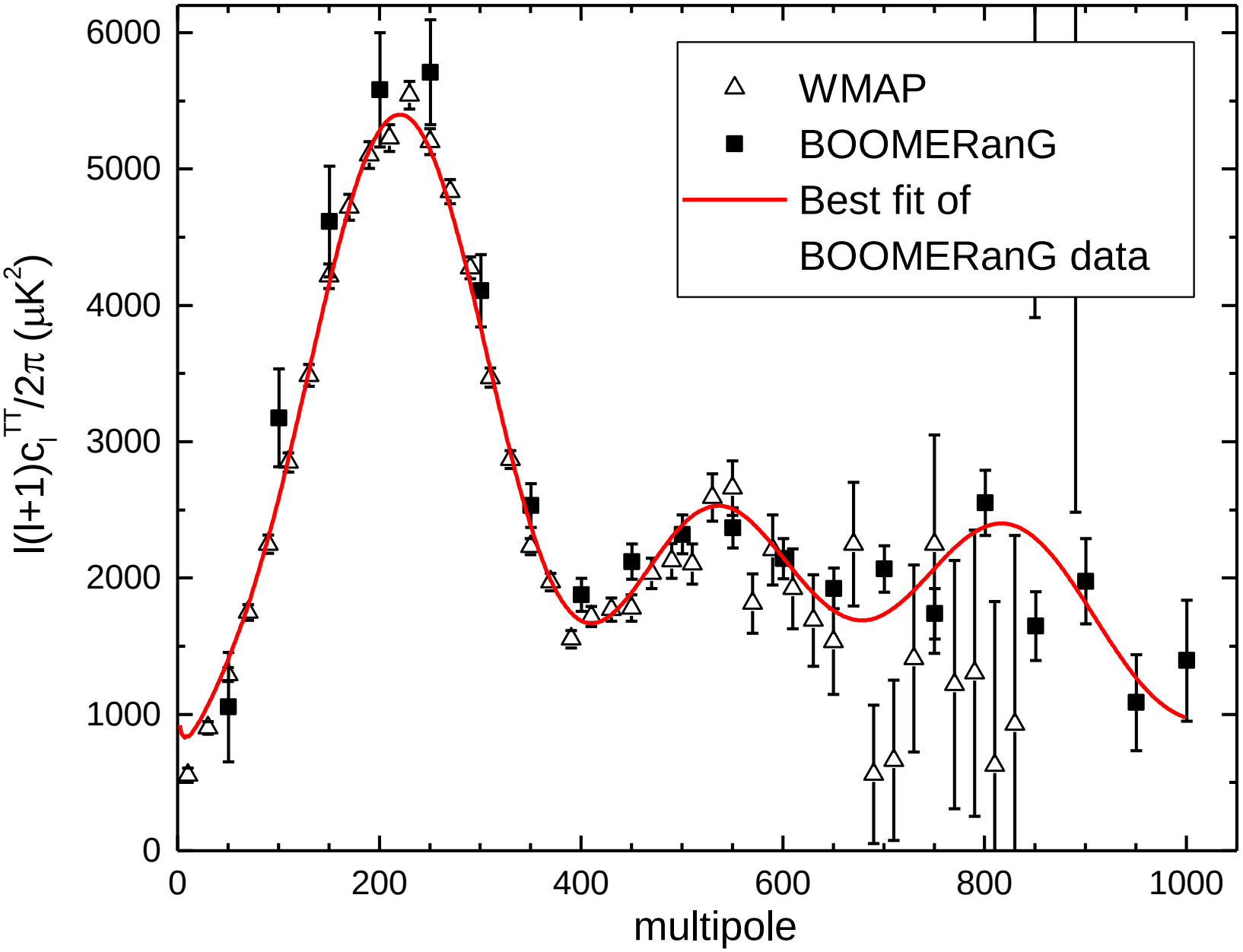
WMAP
BOOMERanG
Best fit of
BOOMERanG data
$l(l+1)c_l^{TT}/2\pi\ (\mu K^2)$
multipole
0
1000
2000
3000
4000
5000
6000
0
200
400
600
800
1000

Cosmological Parameters

Compare with same weak prior on $0.5<h<0.9$

WMAP

(100% of the sky, <1% gain calibration, <1% beam, multipole coverage 2-700)

Bennett et al. 2003

- $\Omega = 1.02 \pm 0.02$
- $n_s = 0.99 \pm 0.04$ *
- $\Omega_b h^2 = 0.022 \pm 0.001$
- $\Omega_m h^2 = 0.14 \pm 0.02$
- $T = 13.7 \pm 0.2$ Gyr
- $\tau_{rec} = 0.166 \pm 0.076$

BOOMERanG

(4% of the sky, 10% gain calibration, 10% beam, multipole coverage 50-1000)

Ruhl et al. astro-ph/0212229

- $\Omega = 1.03 \pm 0.05$
- $n_s = 1.02 \pm 0.07$
- $\Omega_b h^2 = 0.023 \pm 0.003$
- $\Omega_m h^2 = 0.14 \pm 0.04$
- $T = 14.5 \pm 1.5$ Gyr
- $\tau_{rec} = ?$

Polarization-sensitive bolometers JPL-Caltech

3 μm thick wire grids, Separated by 60 μm, in the same groove of a circular corrugated waveguide

Planck-HFI testbed

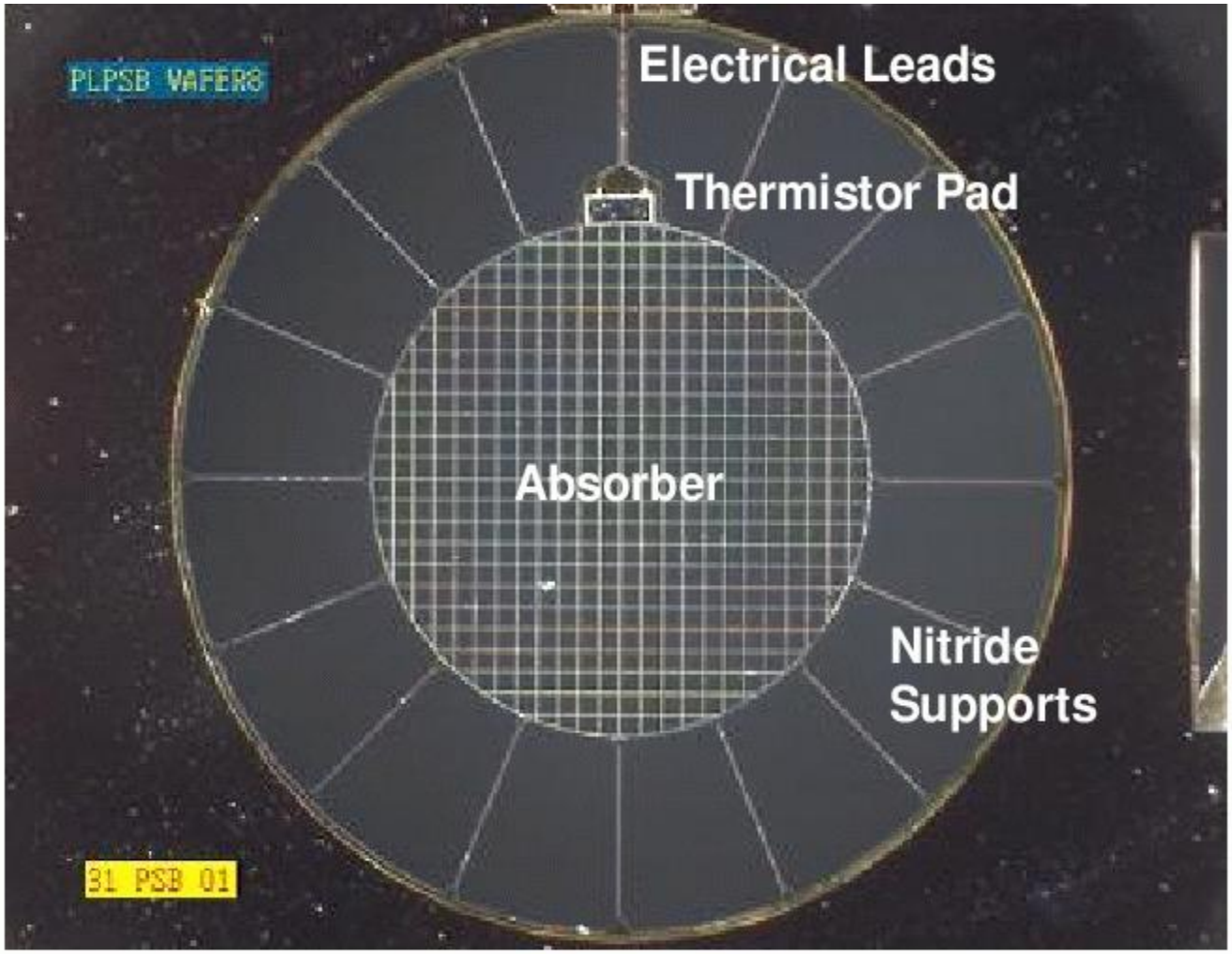

Polarization Sensitive Bolometers

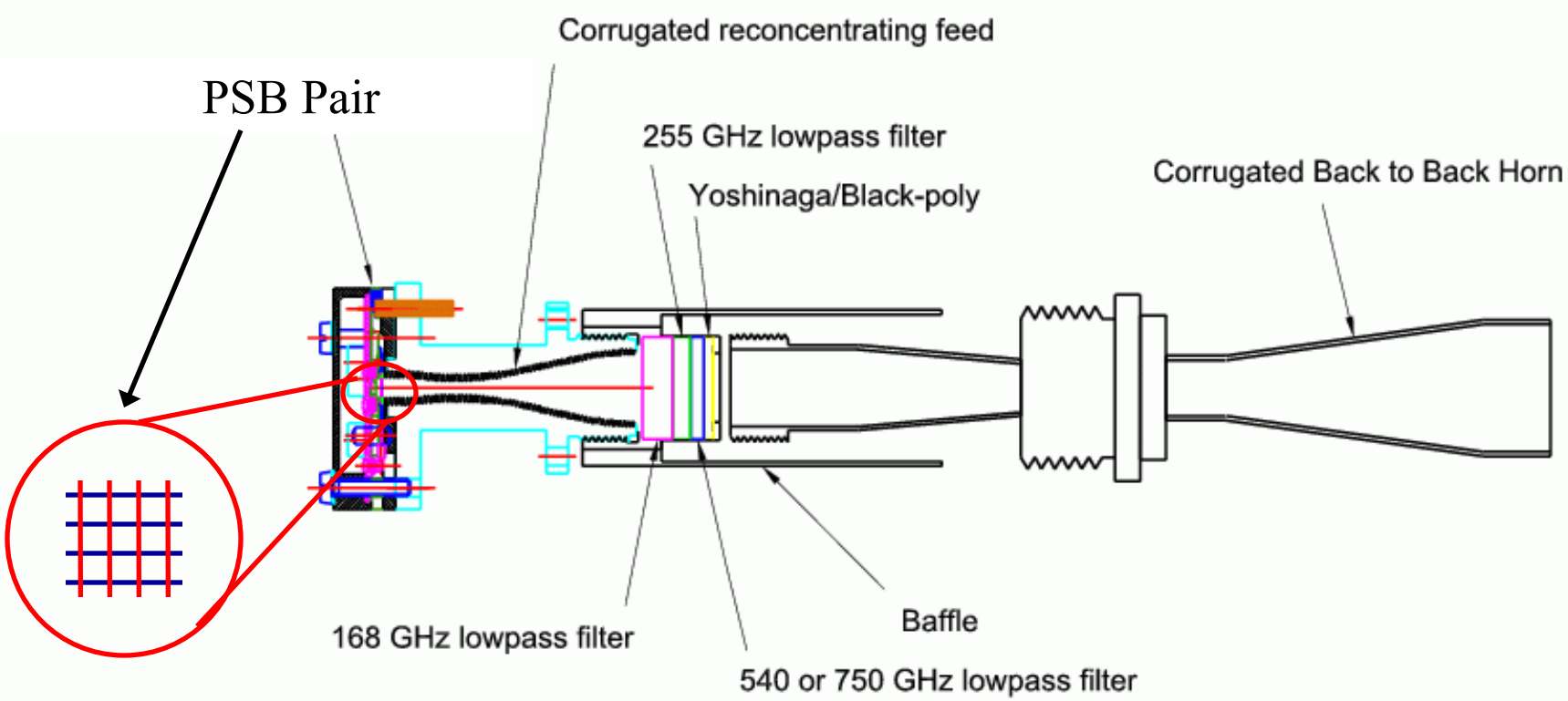

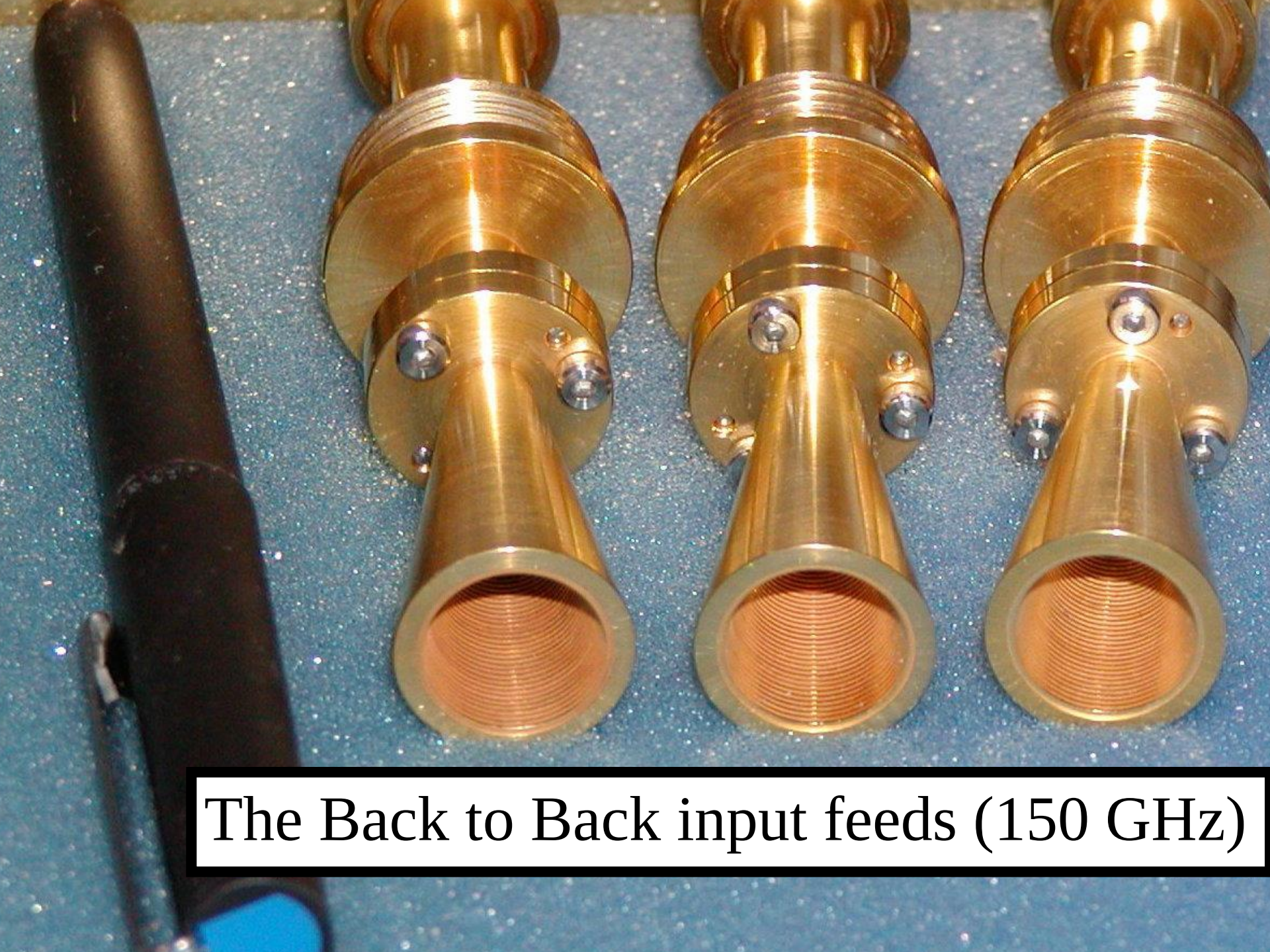

The Back to Back input feeds (150 GHz)

2-Color Photometer

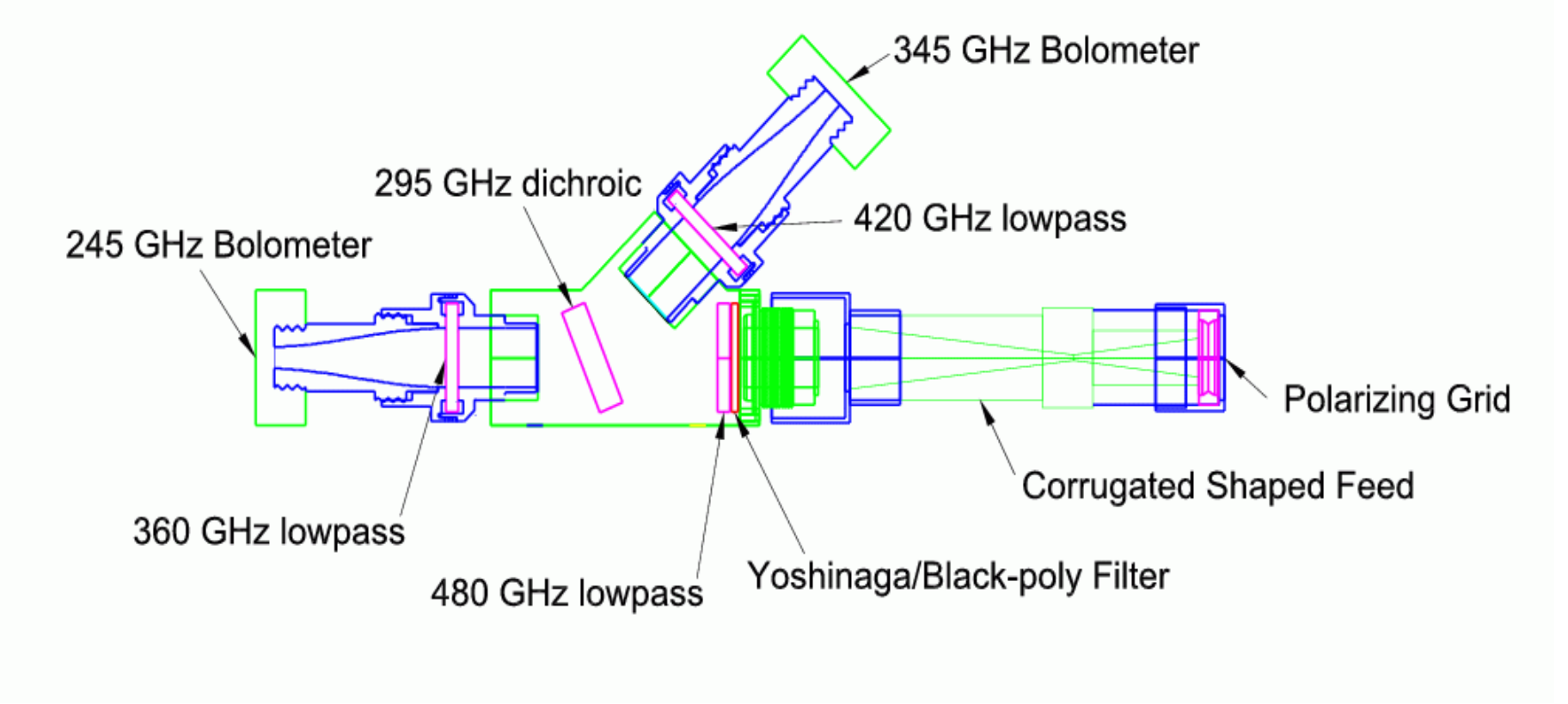

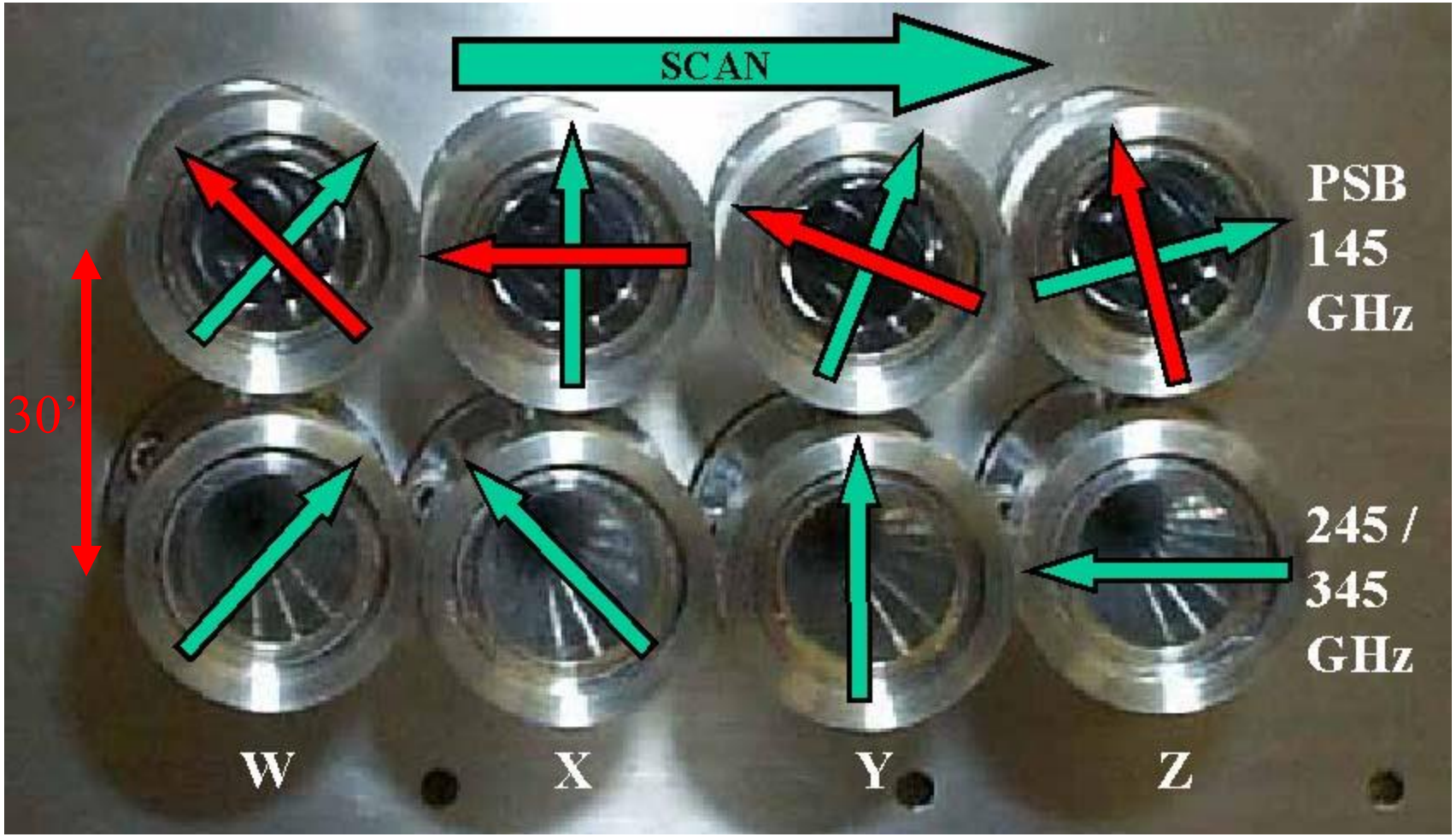
SCAN
PSB
145
GHz
245 /
345
GHz
W
X
Y
Z
30’
30’
30’
30’
elevation
azimuth


2

06/Jan/2003


BOOMERanG
06/Jan/2003

06/Jan/2003

Scan Strategy

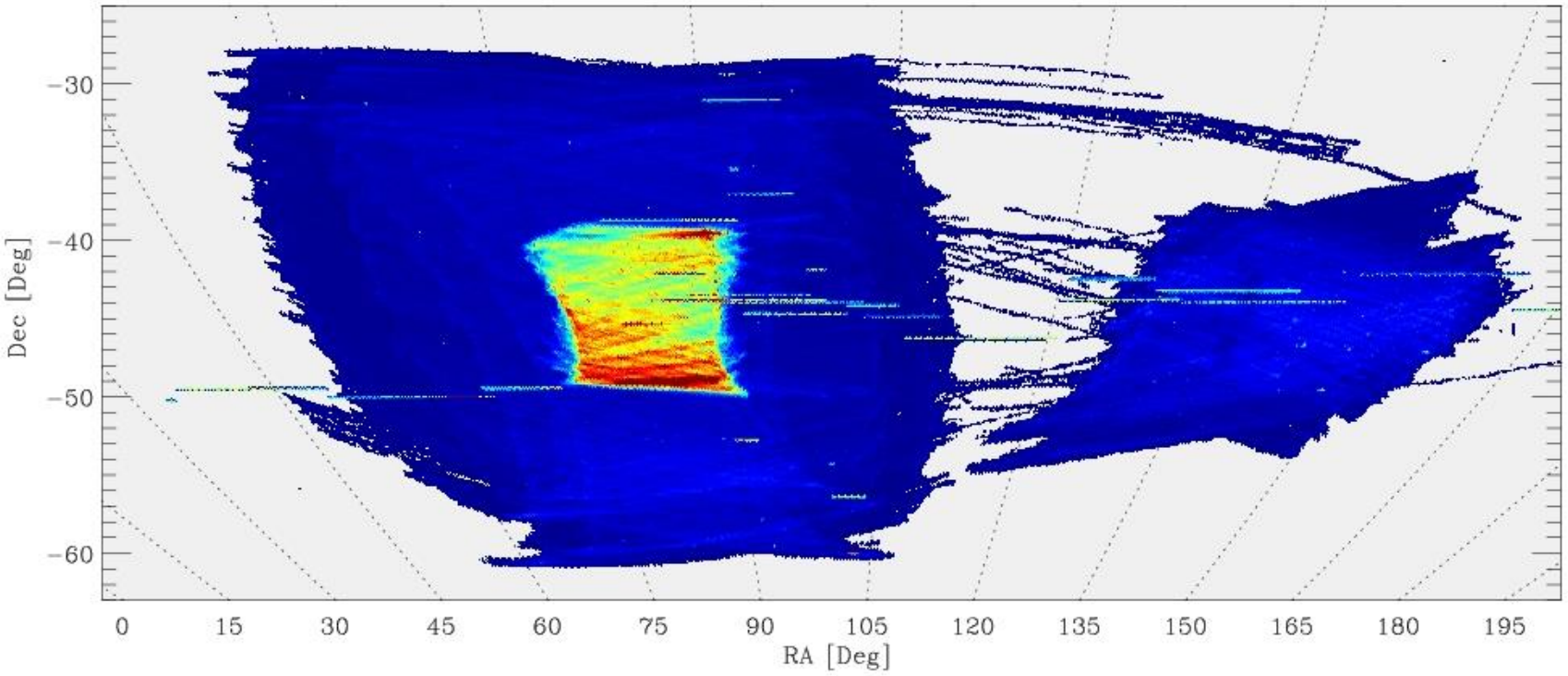

Region	Size (sq deg)	Goal	Time per 7’ pixel
Deep CMB	115	<EE>	60 sec
Shallow CMB	1130	<TE> and <TT>	3.3 sec
Galactic Plane	390	Polarized Foregrounds	4.7 sec

Imaging the CMB in the Sub-mm!

140 GHz (Coadd of 8 detectors)

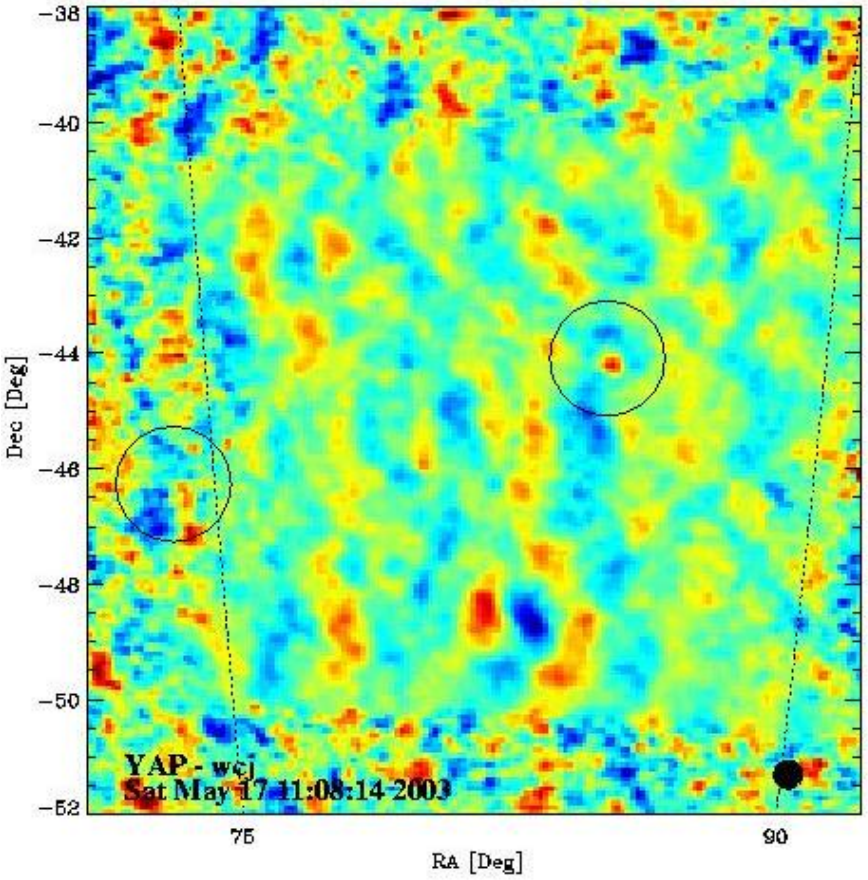

340 GHz (single detector: X)

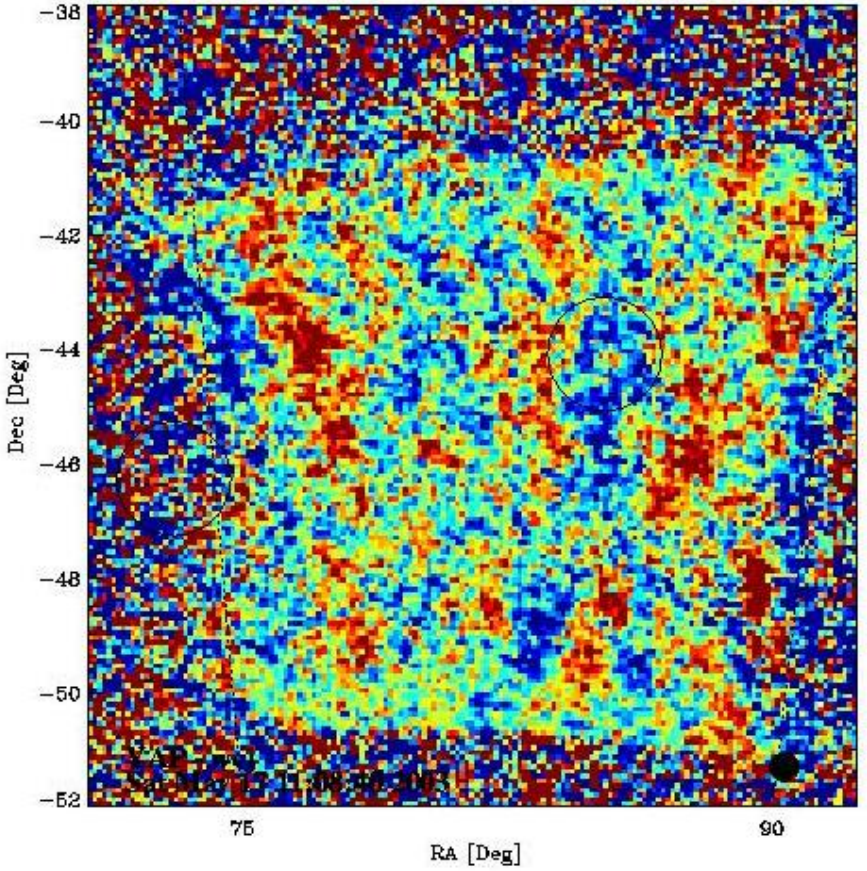

Polarization Maps:

Quick-look data / single pair (of 4) of 143 GHz PSBs /raw data (no compensation for gain drifts!)/ coarse attitude solution

Noise ~ 3μK/20’ pixel in 100 square degree “deep” region

Resolution ~ 10’

Polarized dust emission evident near galactic plane

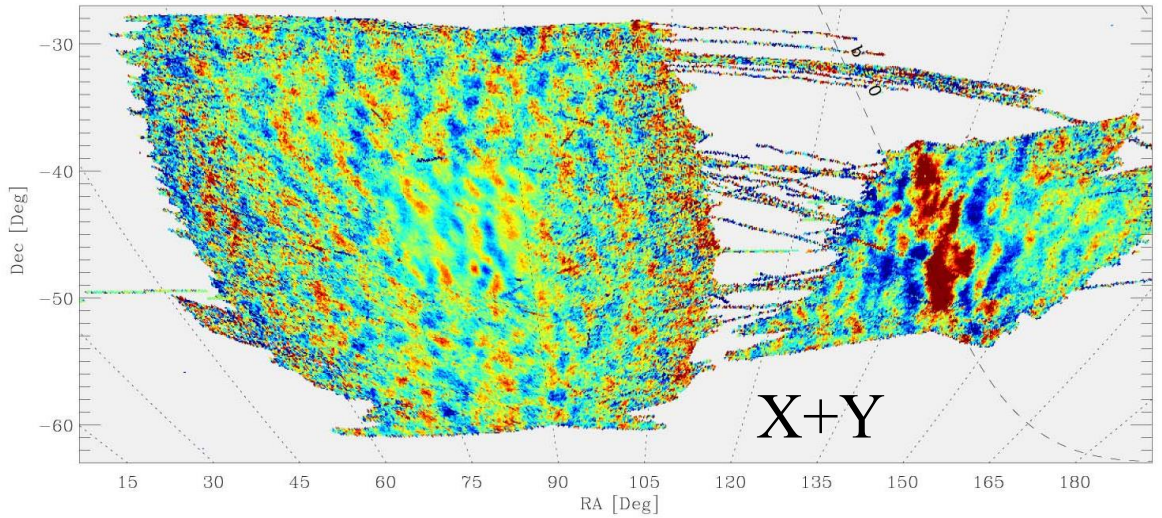

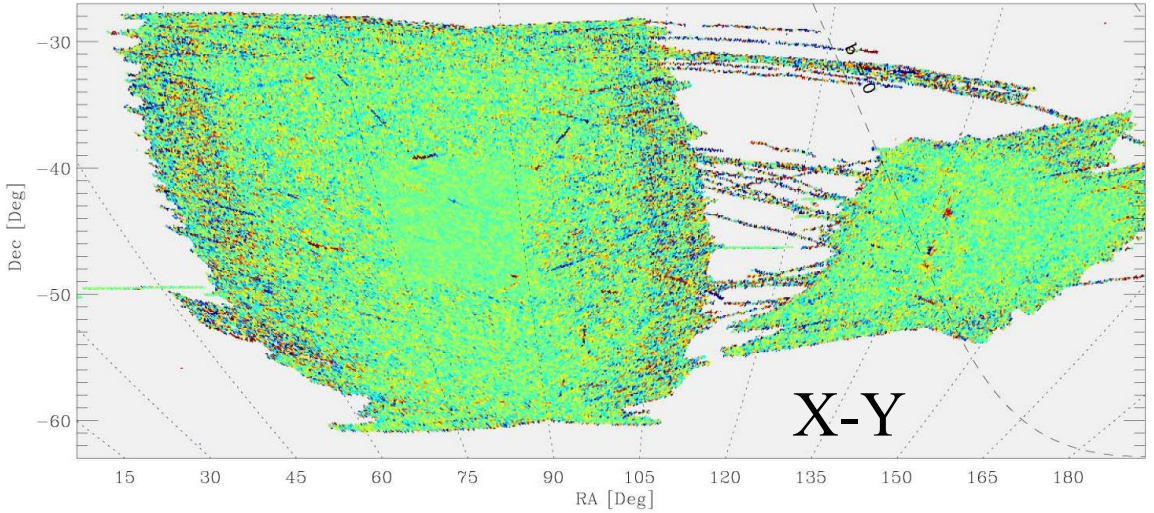

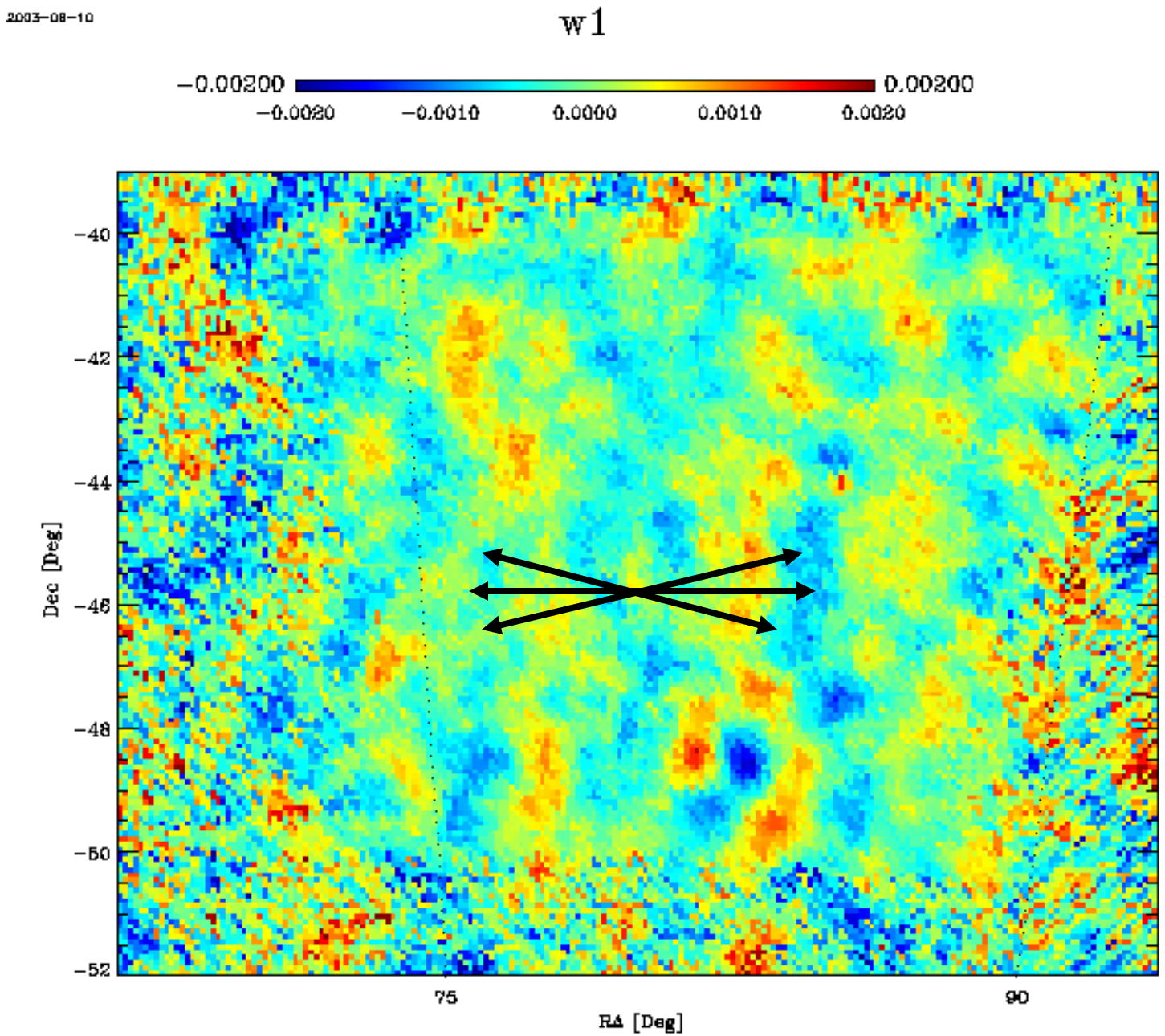

Optimal maps obtained with IGLS, the Rome pipeline (Natoli et al. 2001)

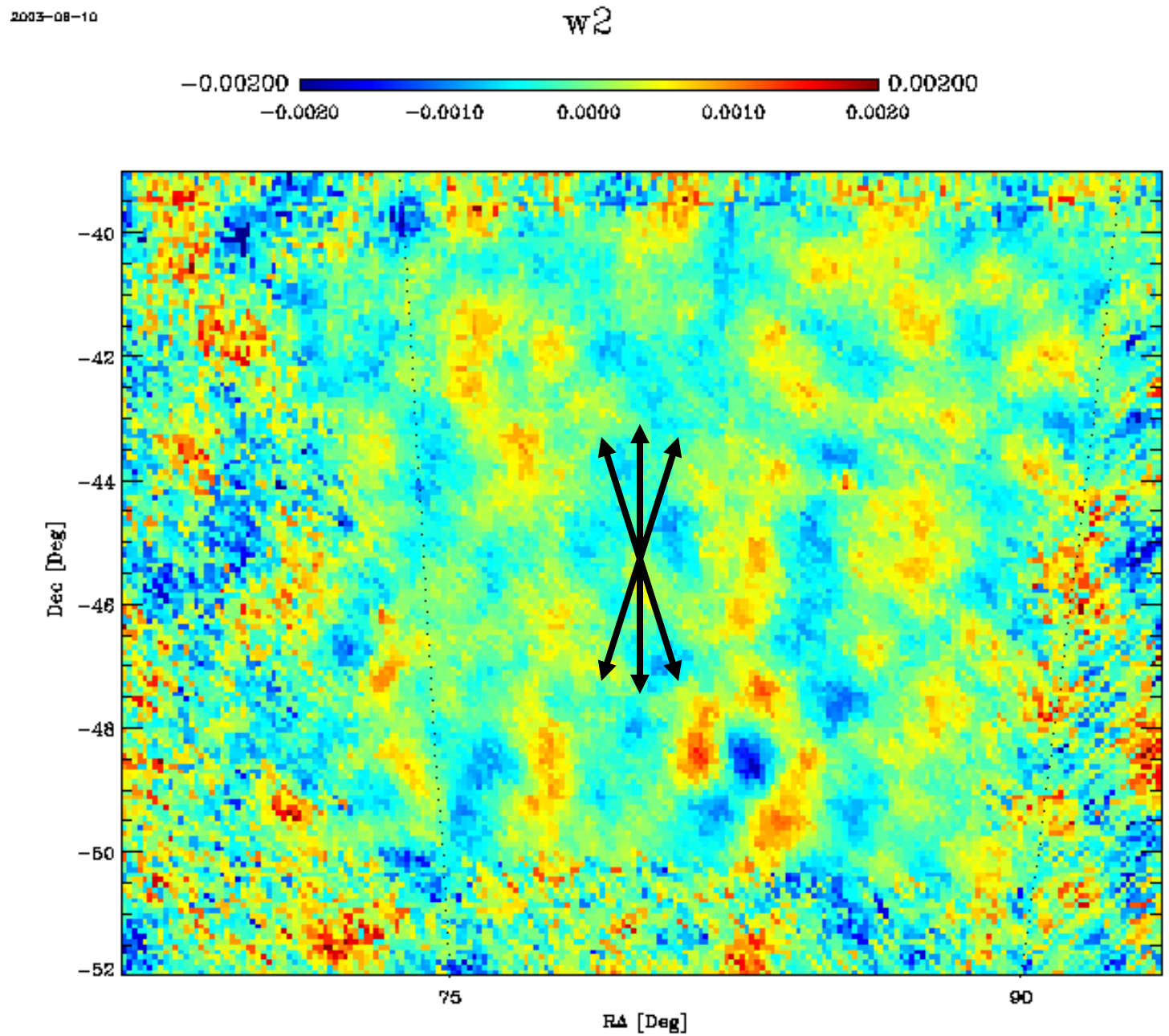

Optimal maps obtained with IGLS, the Rome pipeline (Natoli et al. 2001)

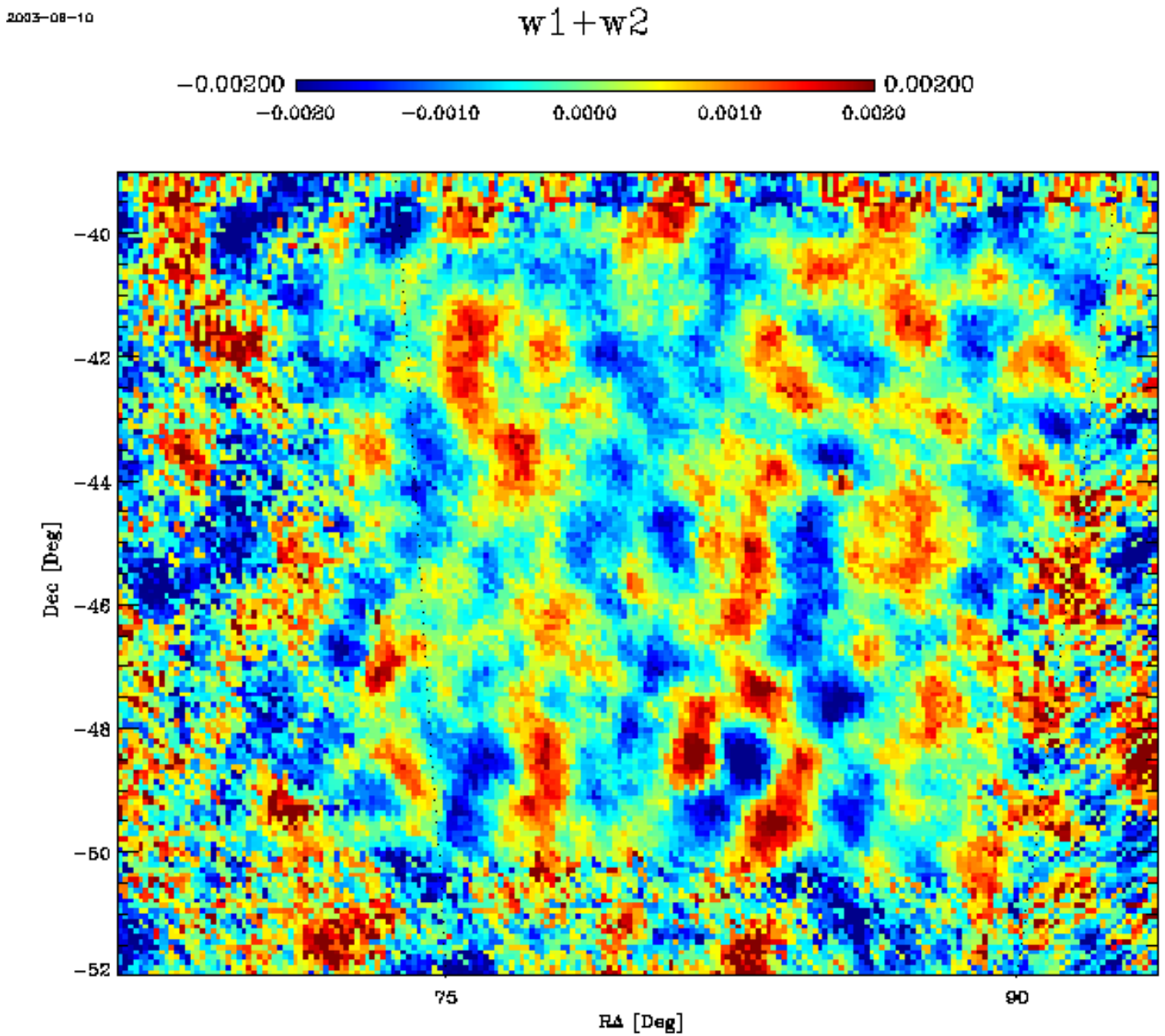

Optimal maps obtained with IGLS, the Rome pipeline (Natoli et al. 2001)

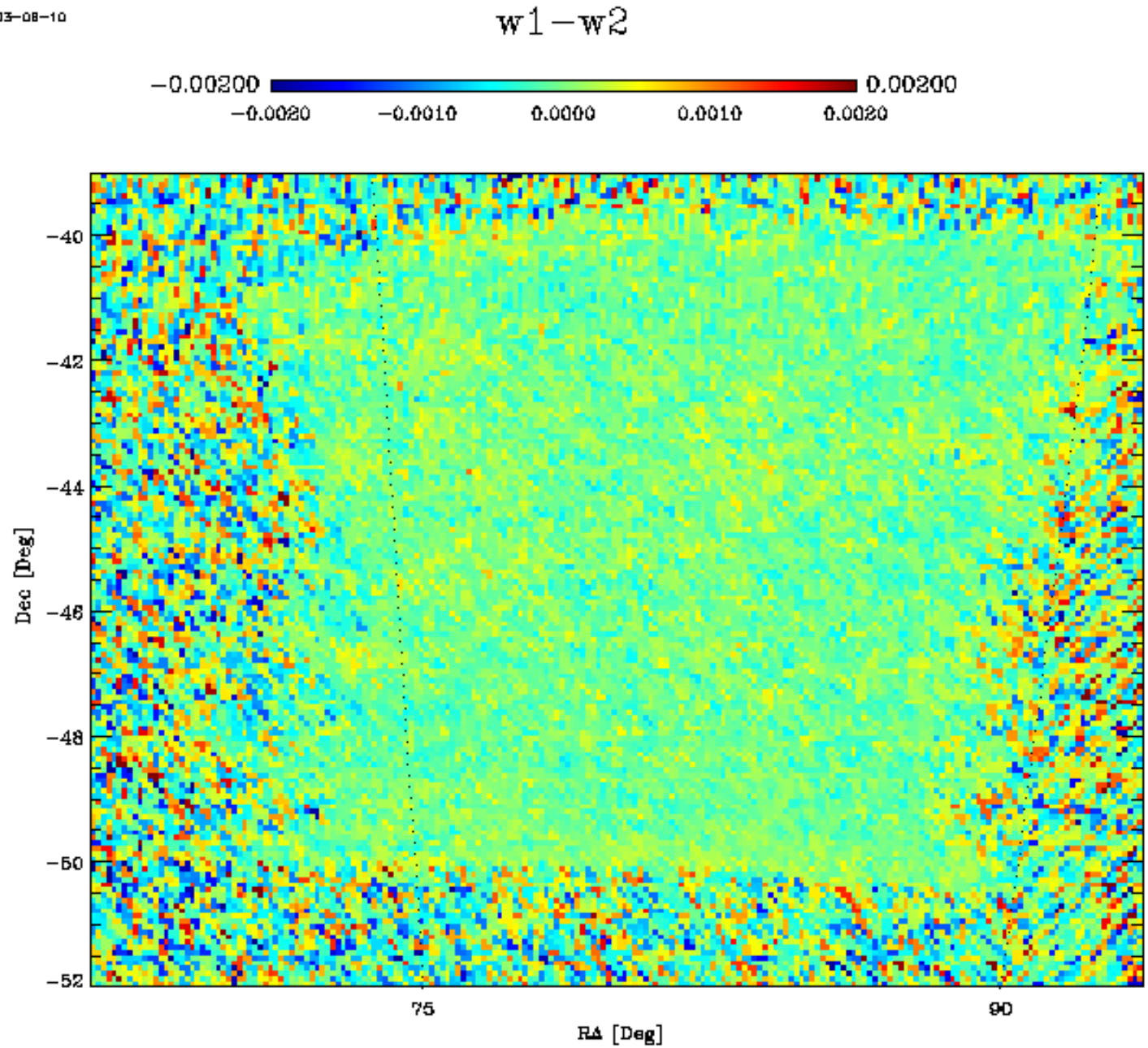

Optimal maps obtained with IGLS, the Rome pipeline (Natoli et al. 2001)

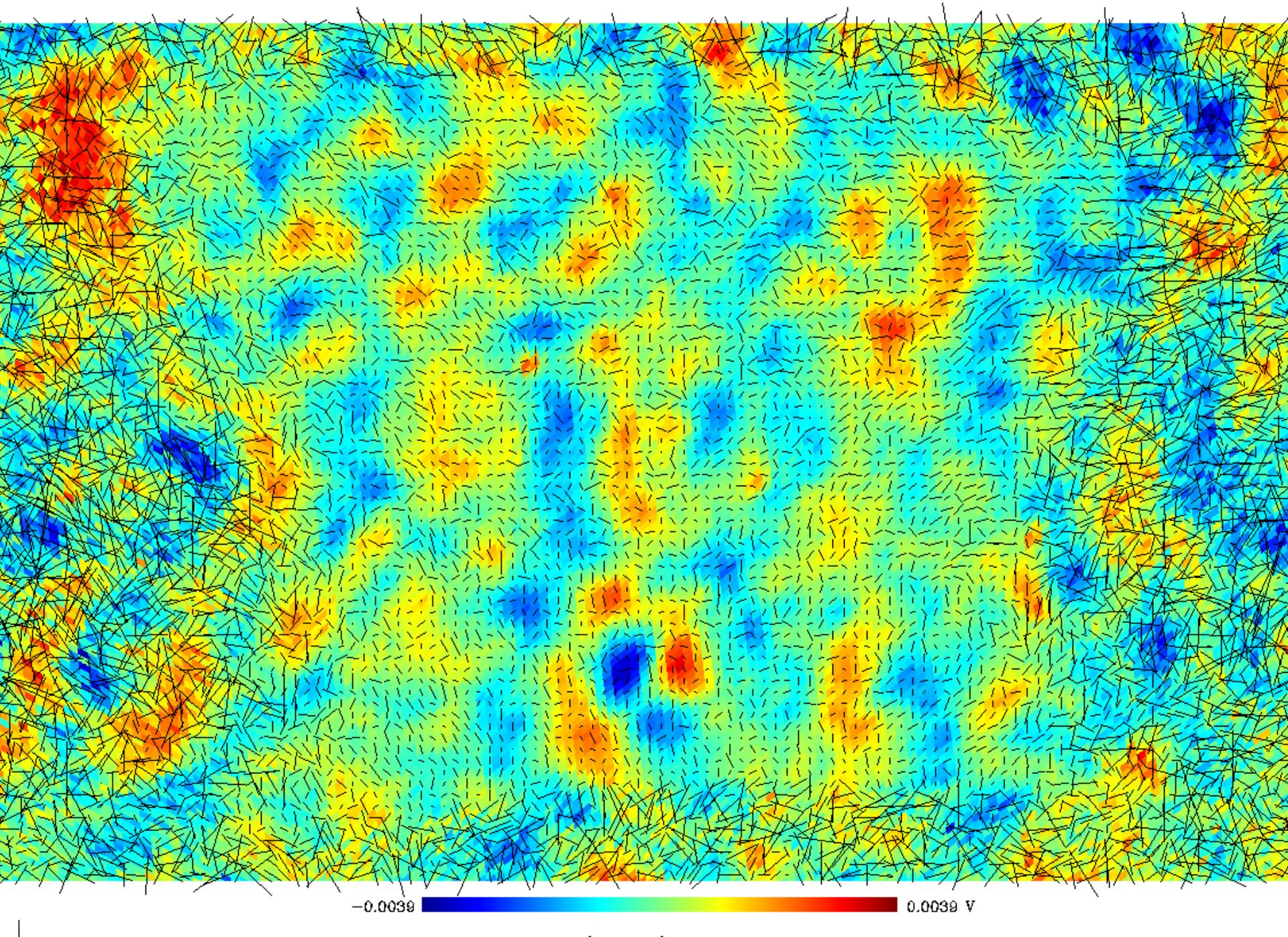
−0.0039
0.0039 V

- **Planck** is a satellite launched in the lagrangian point L2 of the Earth-Sun system, 1.5Mkm away from the Earth, beyond the moon orbit.
- From this advantage location it will map the Universe with unprecedented sensitivity and resolution in the range 20-800 GHz

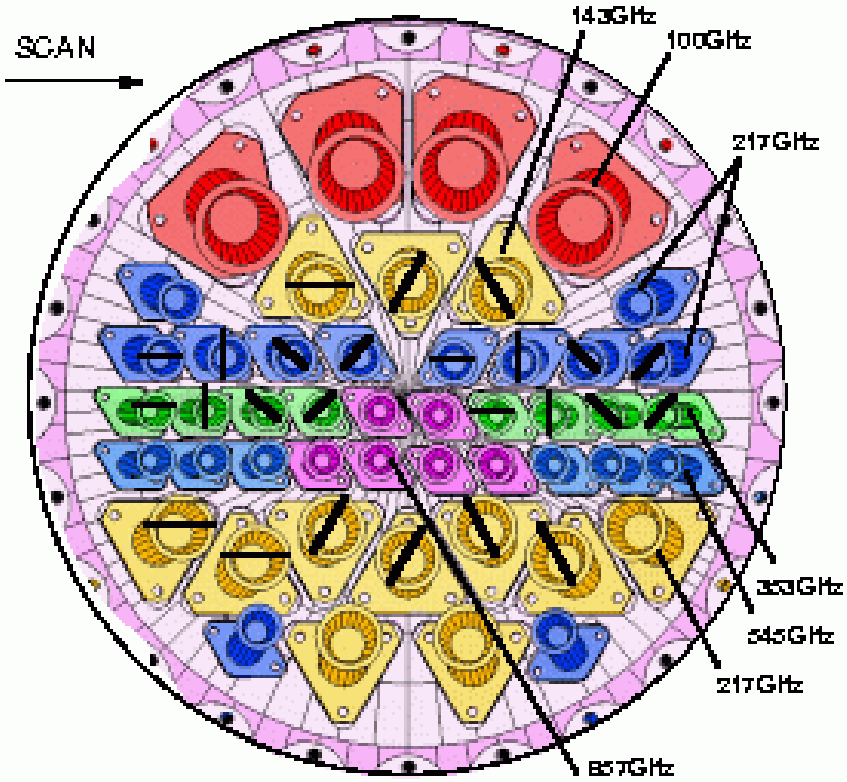

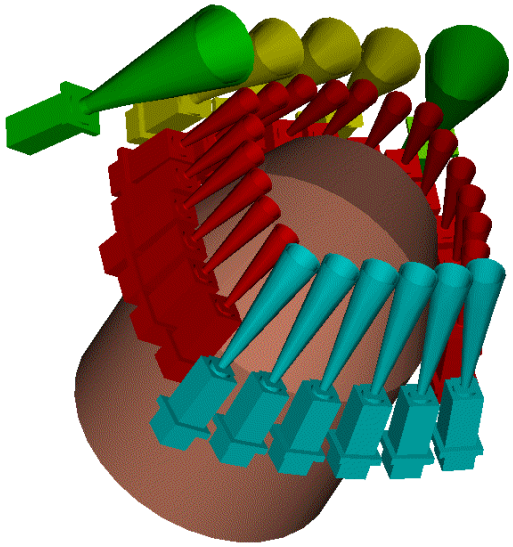

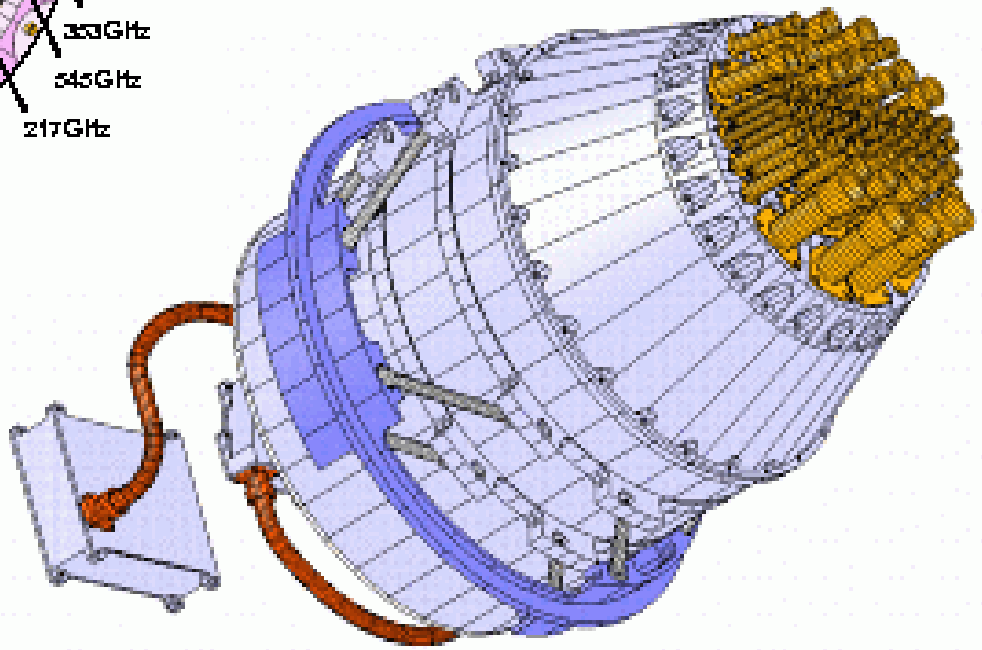

2 instruments
In the focal plane:
LFI (coherent) and
HFI (bolometers)

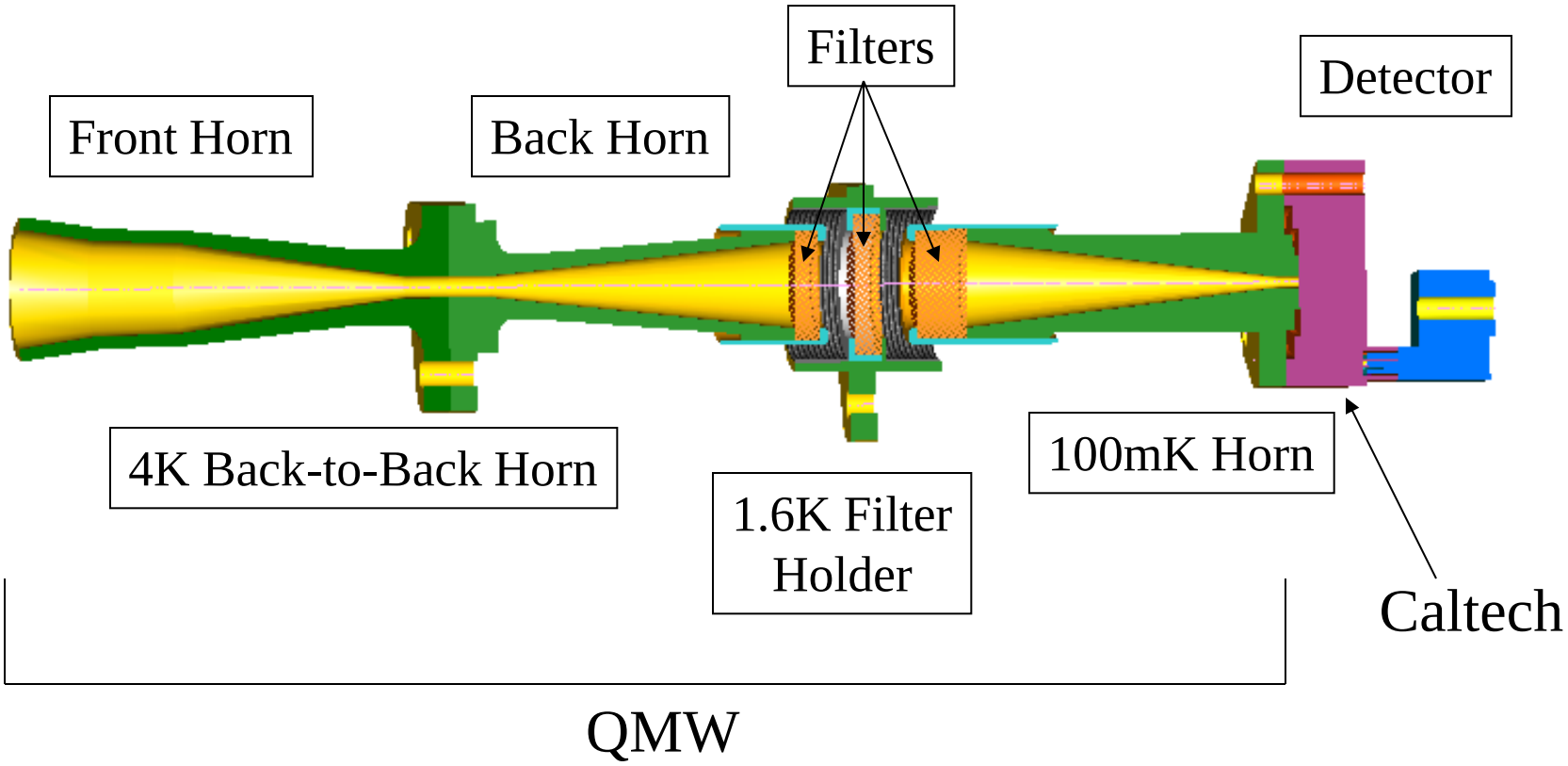
Filters
Detector
Front Horn
Back Horn
4K Back-to-Back Horn
1.6K Filter Holder
100mK Horn
Caltech
QMW

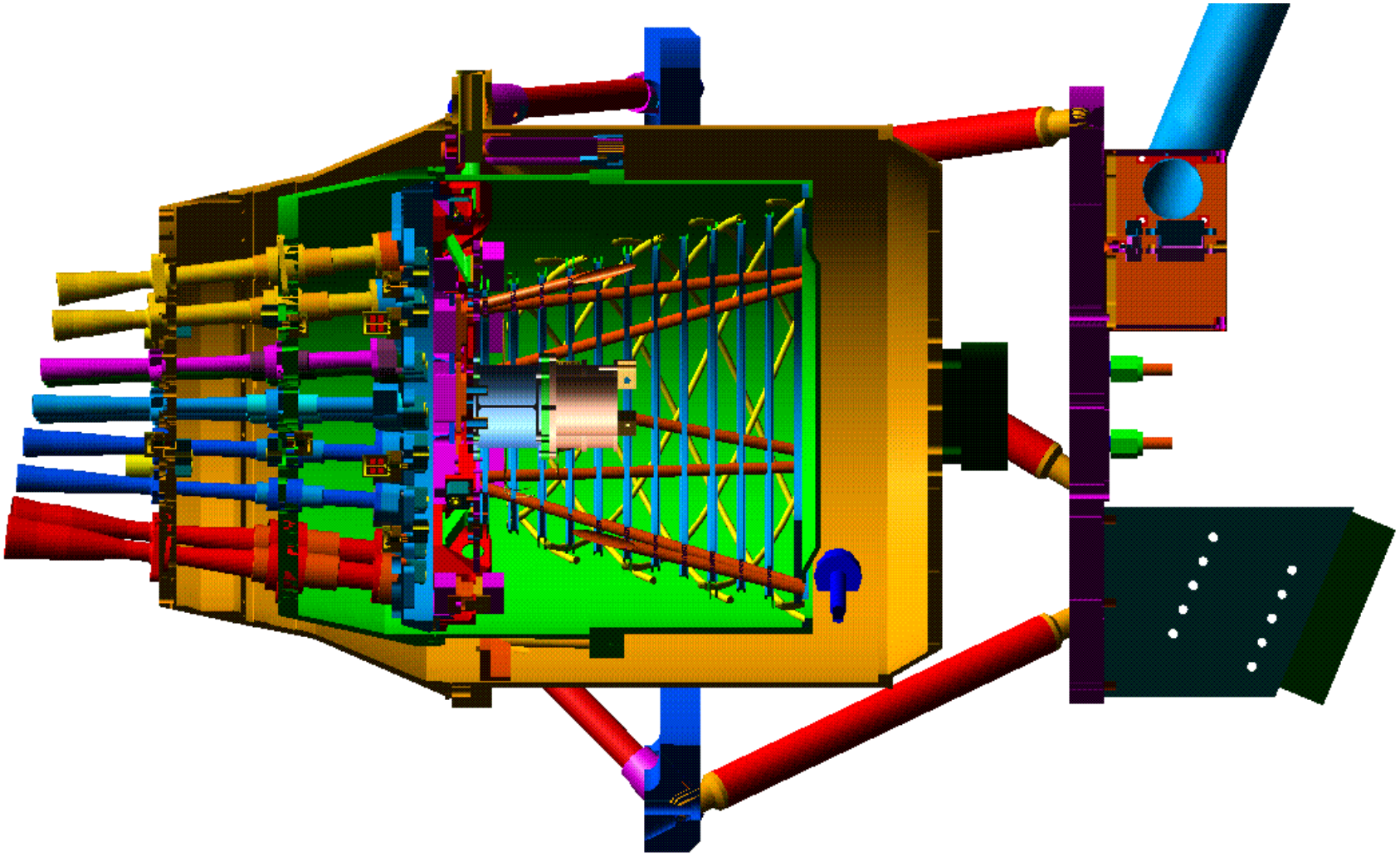

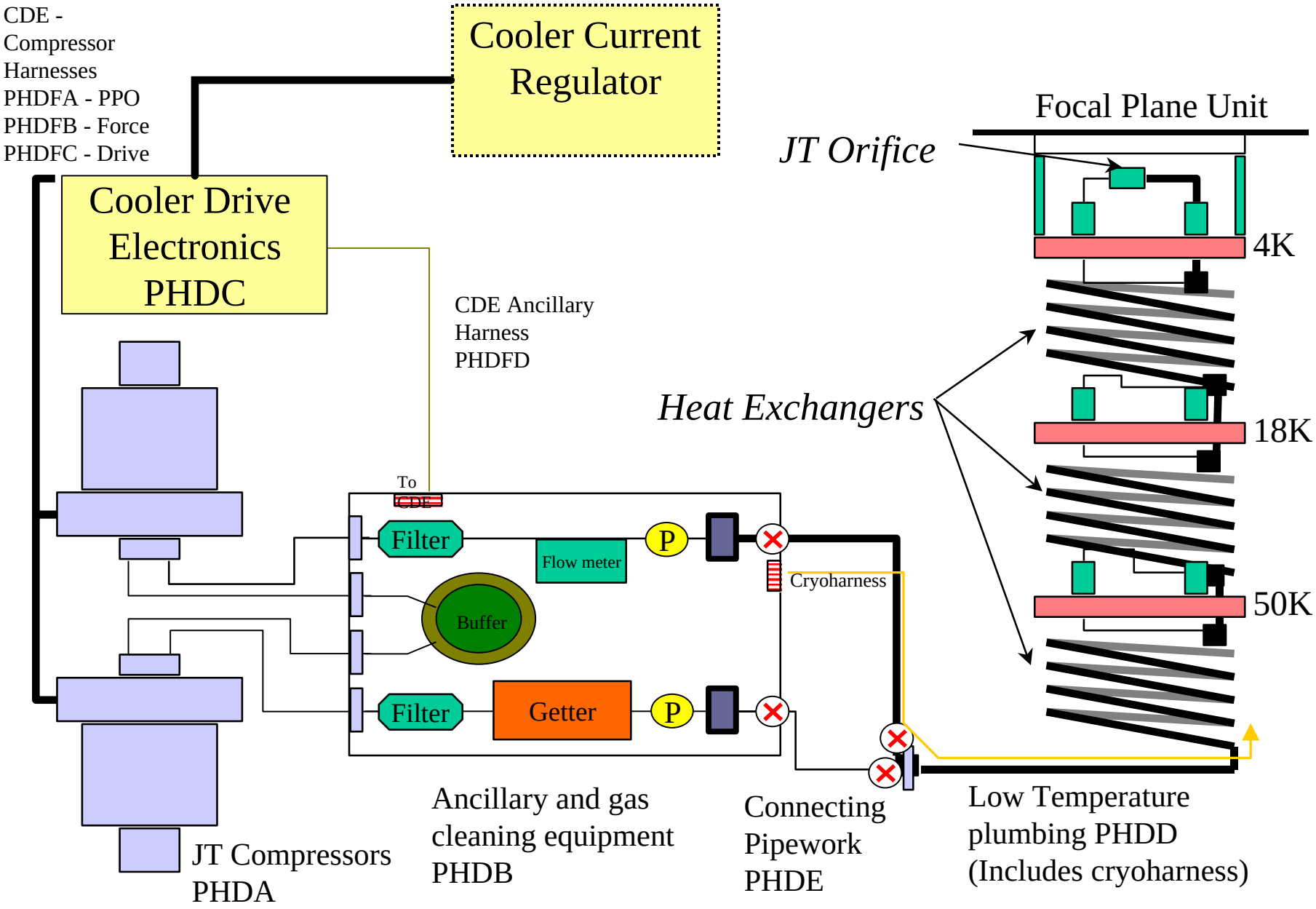
CDE -
Compressor
Harnesses
PHDFA - PPO
PHDFB - Force
PHDFC - Drive
Cooler Current Regulator
Cooler Drive Electronics PHDC
CDE Ancillary Harness PHDFD
Focal Plane Unit
JT Orifice
4K
18K
50K
Heat Exchangers
To CDE
Filter
Flow meter
P
Buffer
Filter
Getter
P
Cryoharness
JT Compressors PHDA
Ancillary and gas cleaning equipment PHDB
Connecting Pipework PHDE
Low Temperature plumbing PHDD (Includes cryoharness)

Galileo Avionica

150K

50K

50K

The JFET BOX: 72 diff. Channels, < 200mW @ 50K, 3nV/sqrt(Hz)

agenzia spaziale italiana

Sensitivity Goals

- Depending on the astronomical application:

Experiment	$NEP_{required}$
Ground-based continuum surveys e.g. BOLOCAM, SCUBA2	10^{-17} W/ √Hz
Space-based CMB e.g. post-PLANCK	10^{-18} W/ √Hz
Ground-based spectrometer e.g. BASS	10^{-20} W/ √Hz
Space-based spectrometer e.g. SPECS	10^{-21} W/ √Hz

Cryogenic Bolometers

- Ge thermistor bolometers have been used in many CMB experiments:
  - COBE-FIRAS, ARGO, MAX, BOOMERanG, MAXIMA, ARCHEOPS
- Ge thermistor bolometers are extremely sensitive, but slow: the typical time constant C/G is of the order of 10 ms @ 300mK
- Transition Edge Superconductor (TES) thermistors can do much better using electro-thermal feedback (100 μs) – Relatively recent development

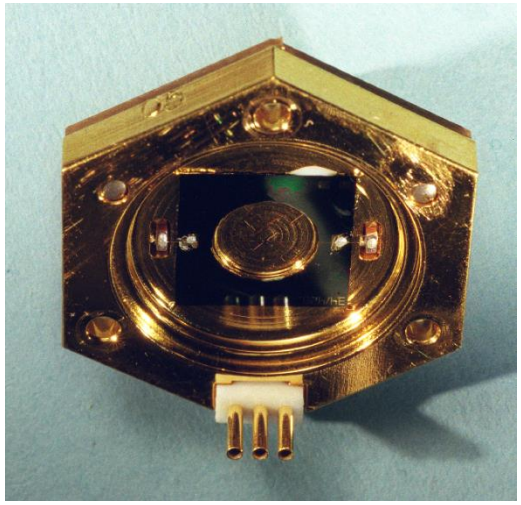

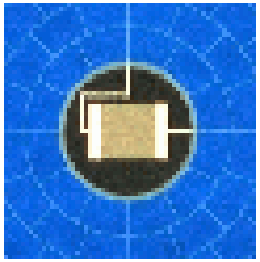

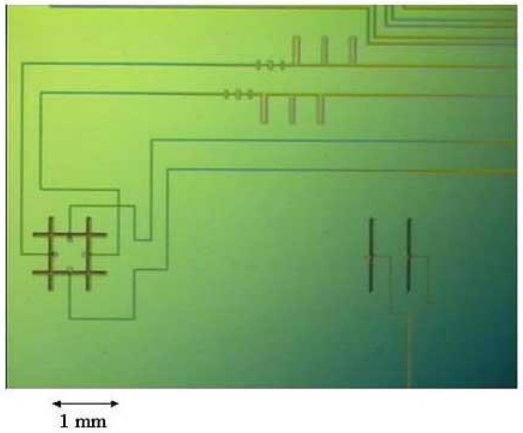

Extreme Electrothermal Feedback

Principle:

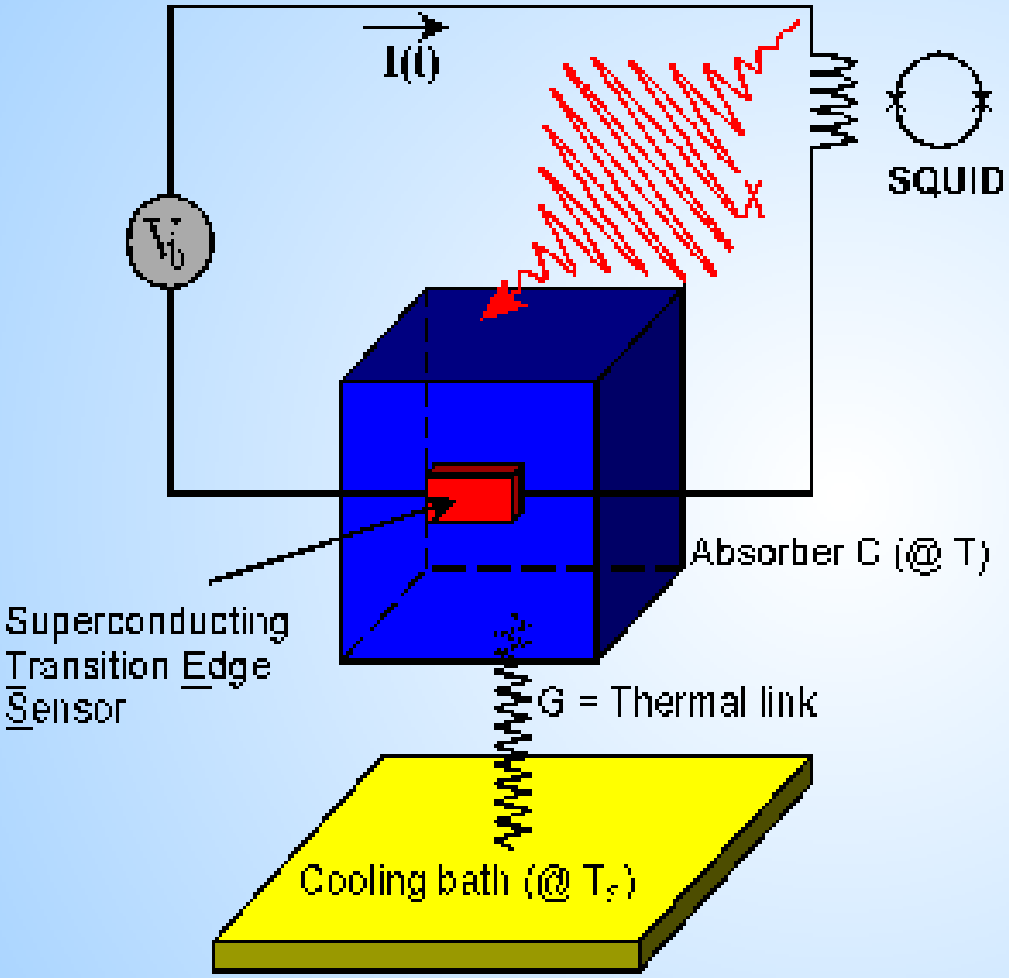

Such a high value for α (which is >0 for TES) induces a large change in the bias power when radiation hits the detector (electrothermal feedback)

This results in a large reduction of the time constant and in stabilization of the responsivity.

Bolometer Arrays

- Once bolometers reach BLIP conditions (CMB BLIP), the mapping speed can only be increased by creating large bolometer arrays.
- BOLOCAM and MAMBO are examples of large arrays with hybrid components (Si wafer + Ge sensors)
- Techniques to build fully litographed arrays for the CMB are being developed.
- TES offer the natural solution.

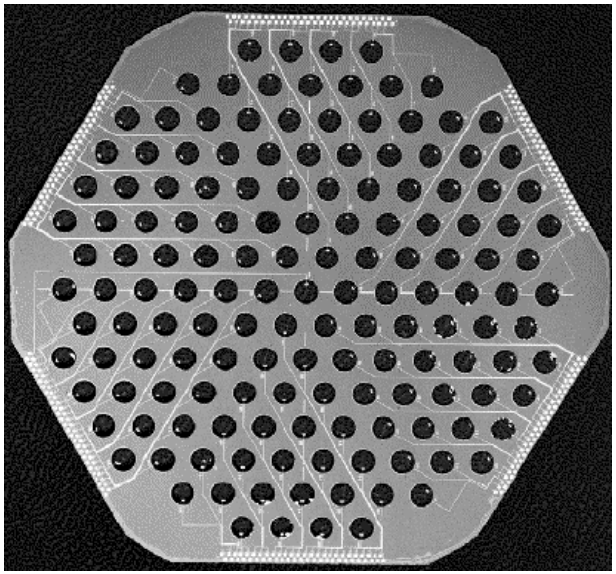

Bolocam Wafer (CSO)

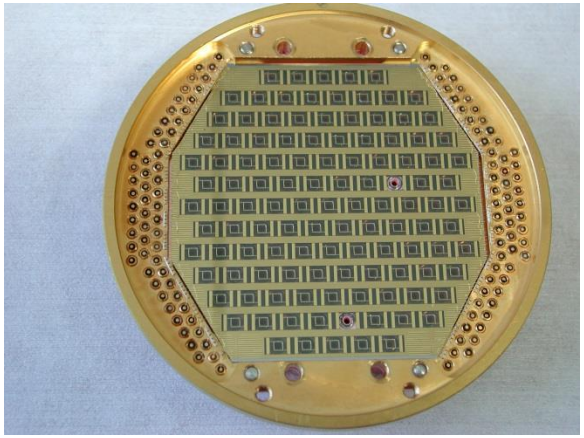

MAMBO (MPIfR for IRAM)

Superconducting transition edge calorimeter

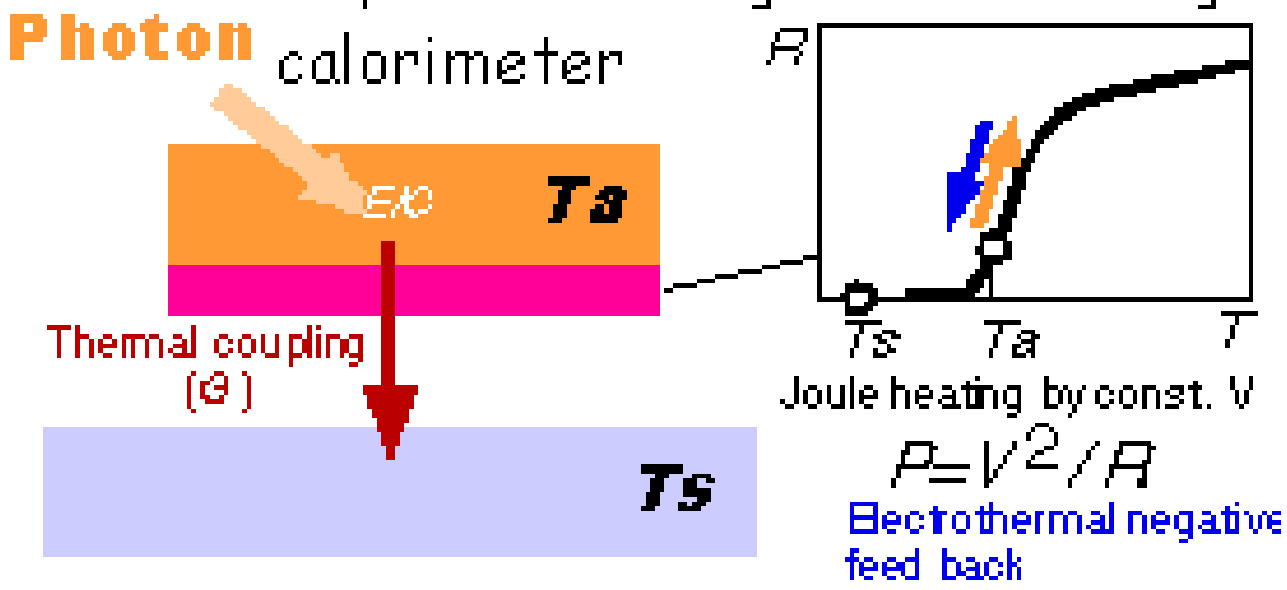

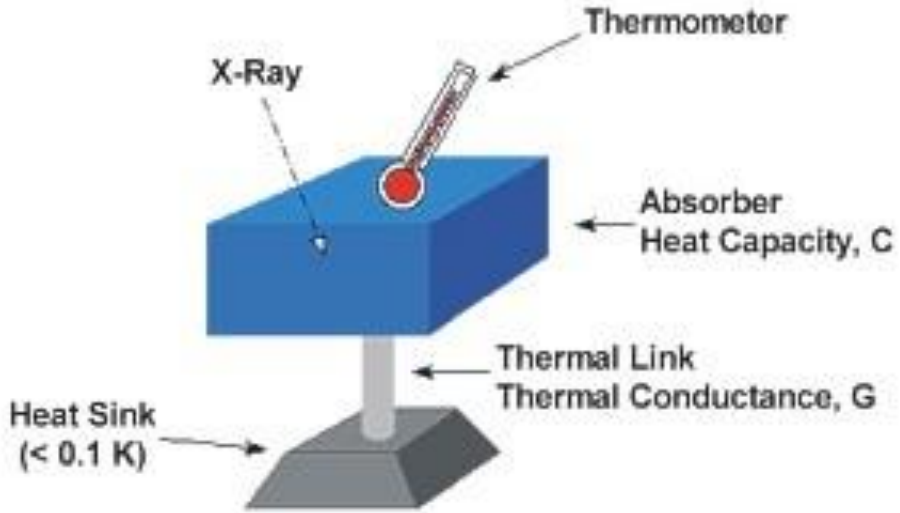

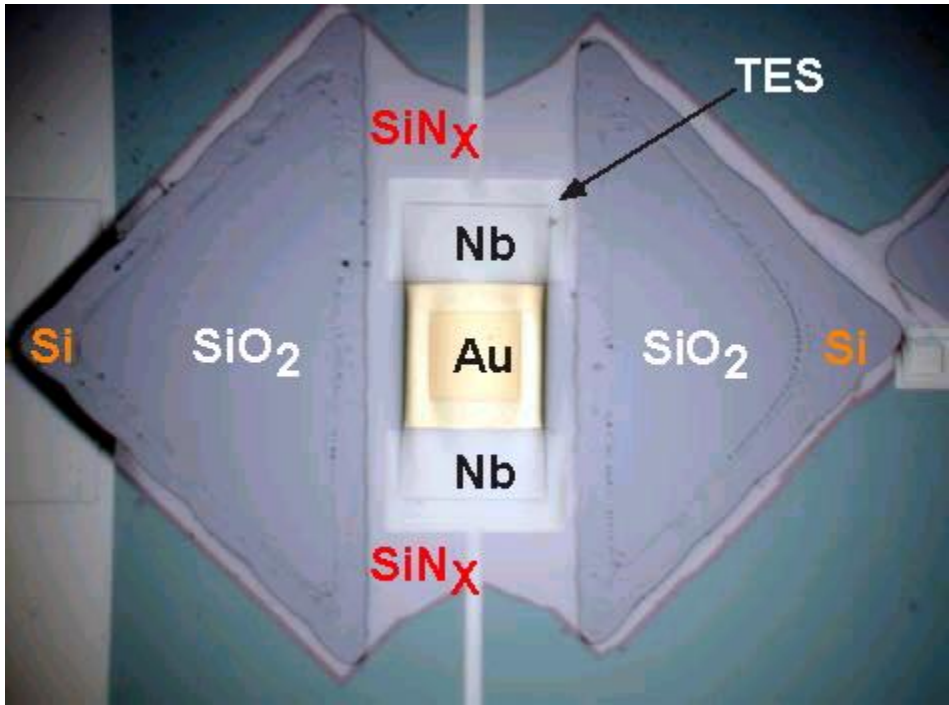

ETF-TES microcalorimeter

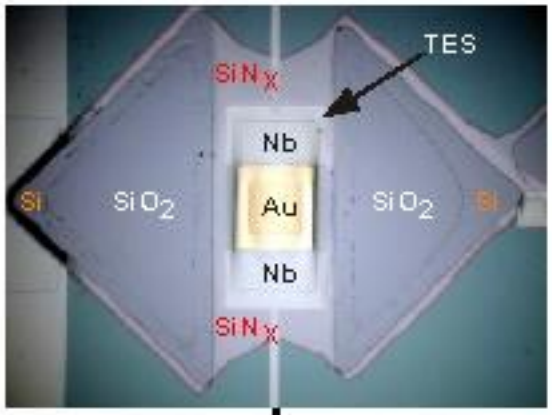

New structure

Conventional structure

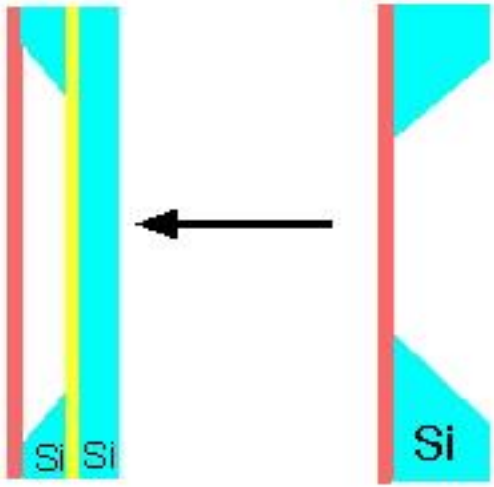

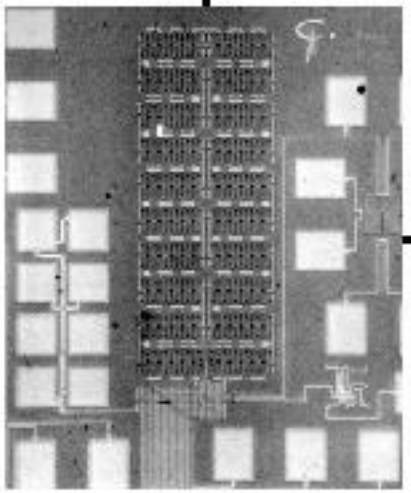

ETL SQUID current amplifier

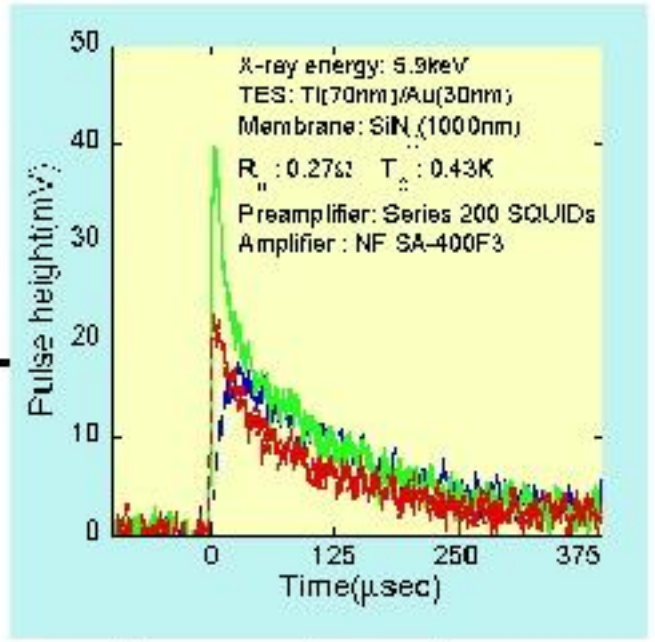

X-ray signals

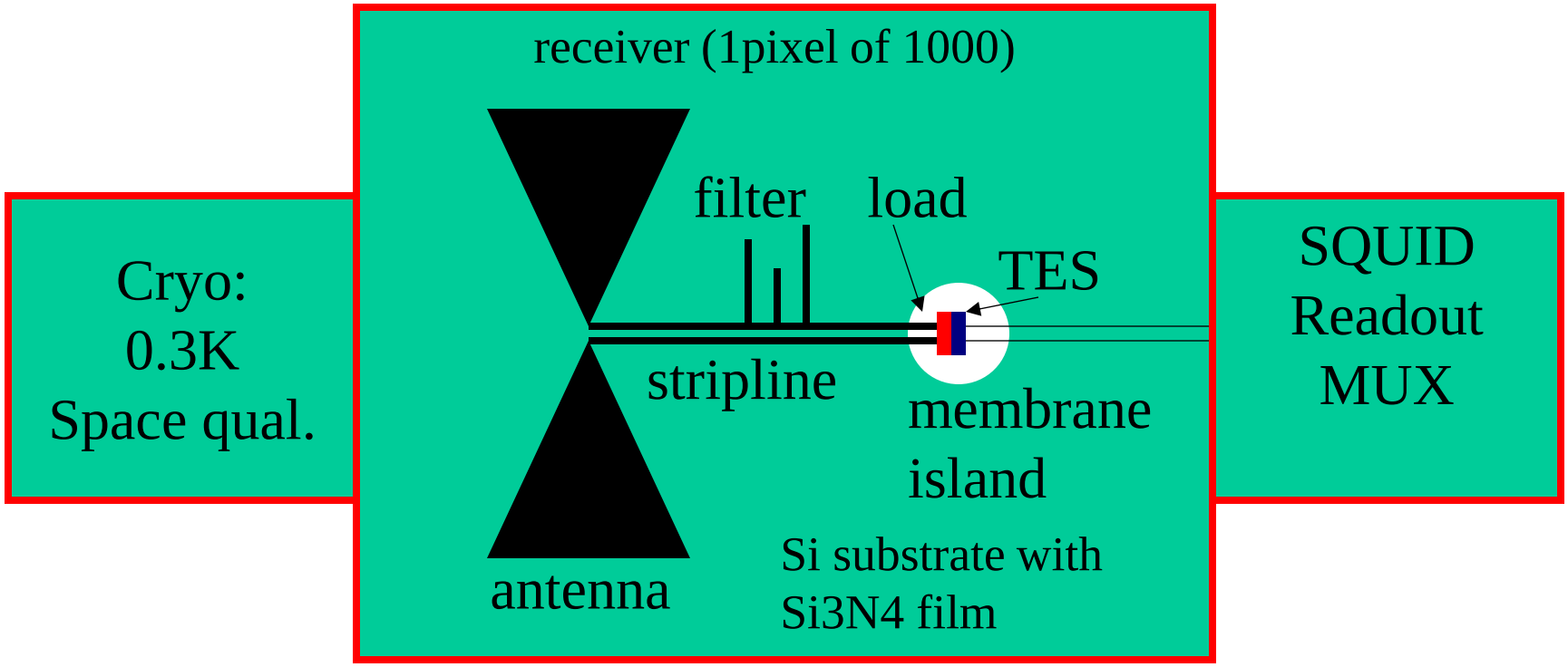

TES for mm waves

(Cardiff, Phil Mauskopf)

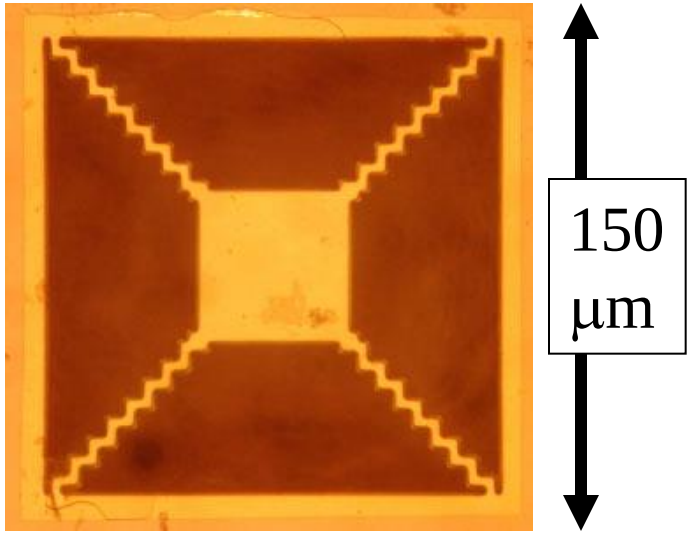

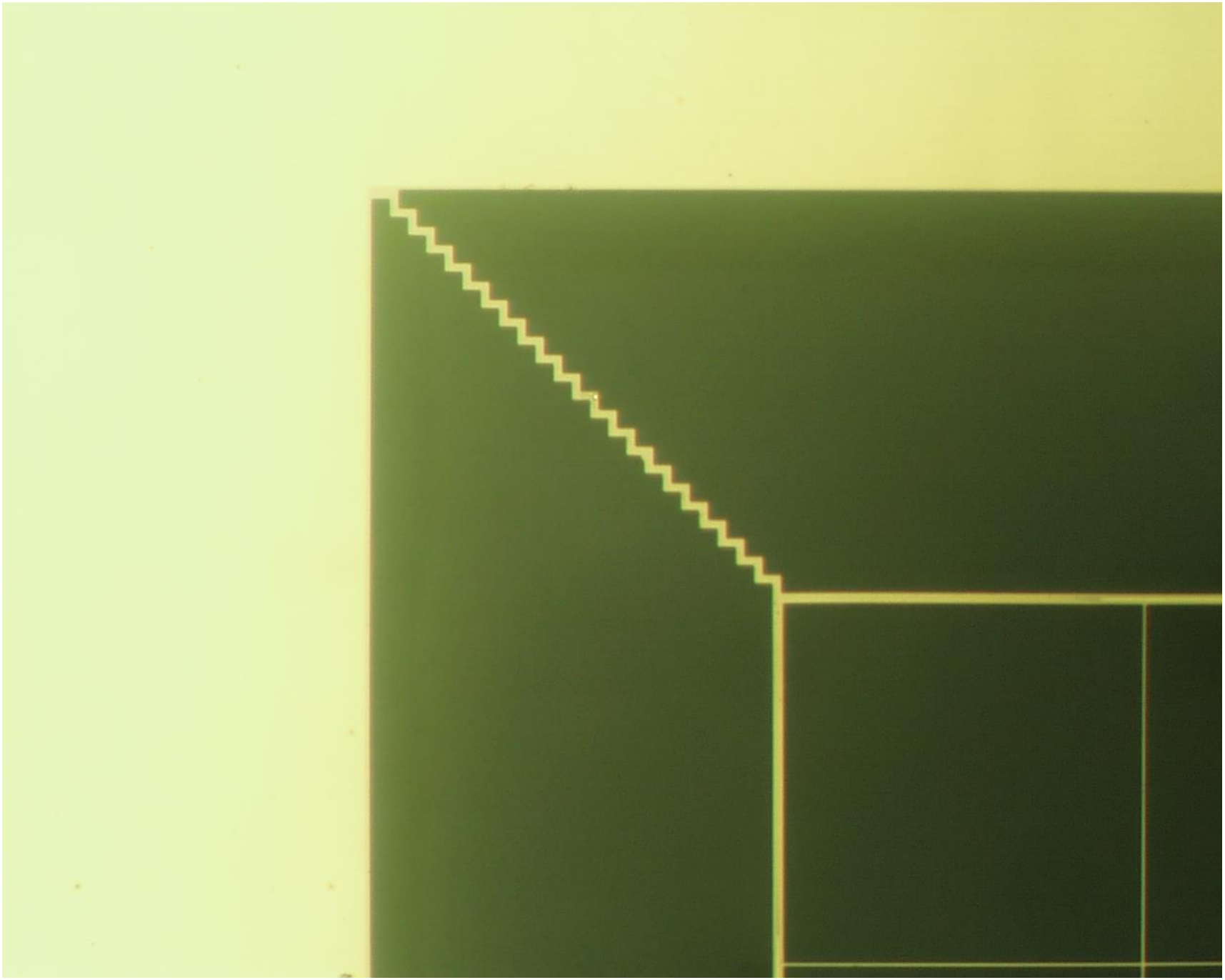

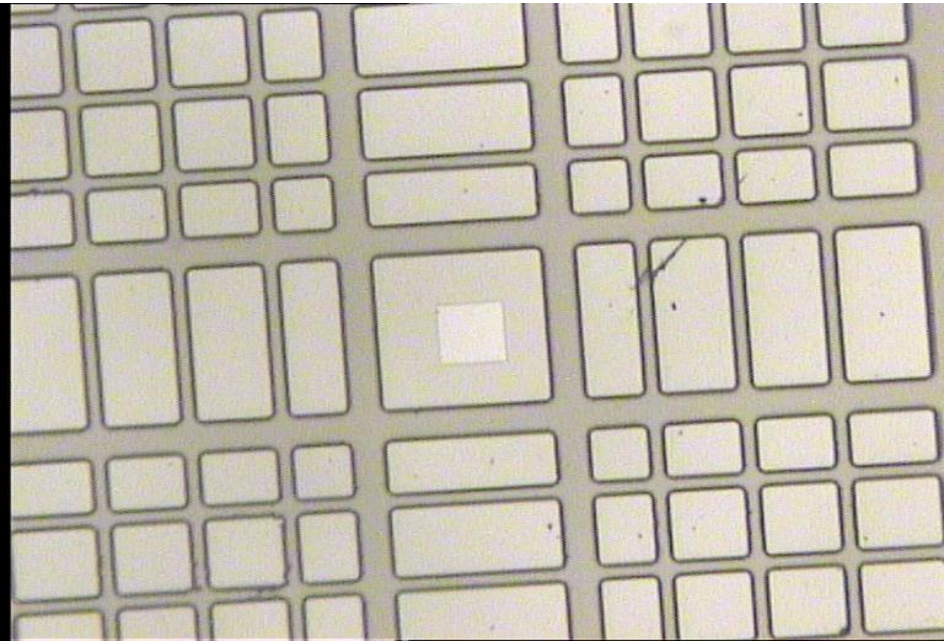

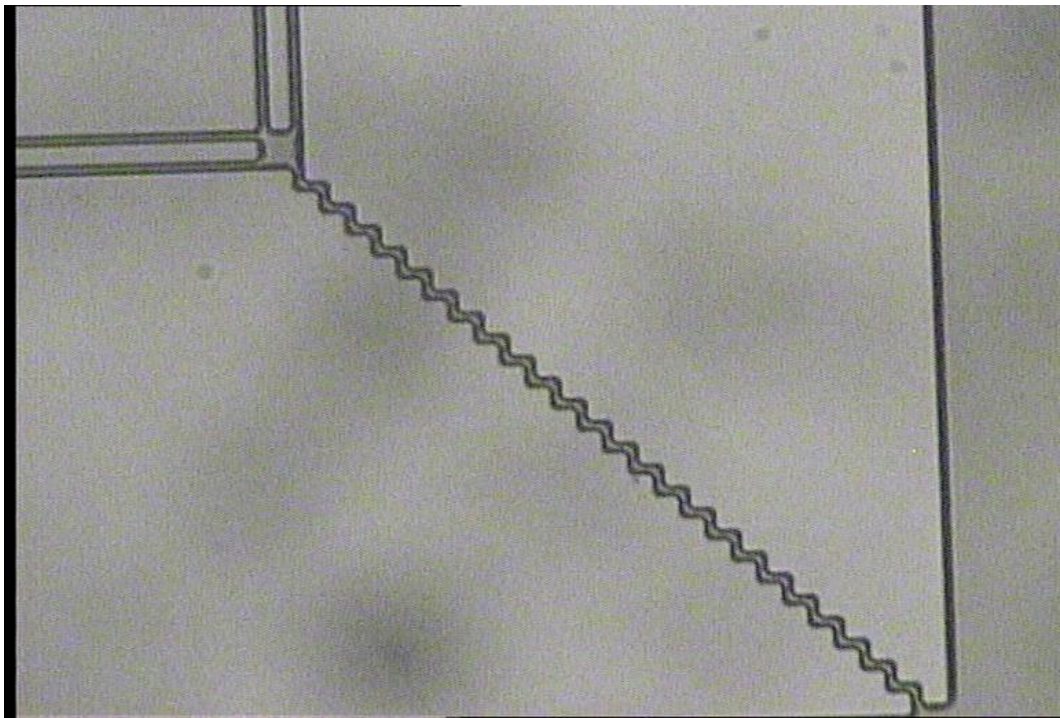

PROTOTYPE SINGLE PIXEL - 150 GHz (Mauskopf)

Schematic:

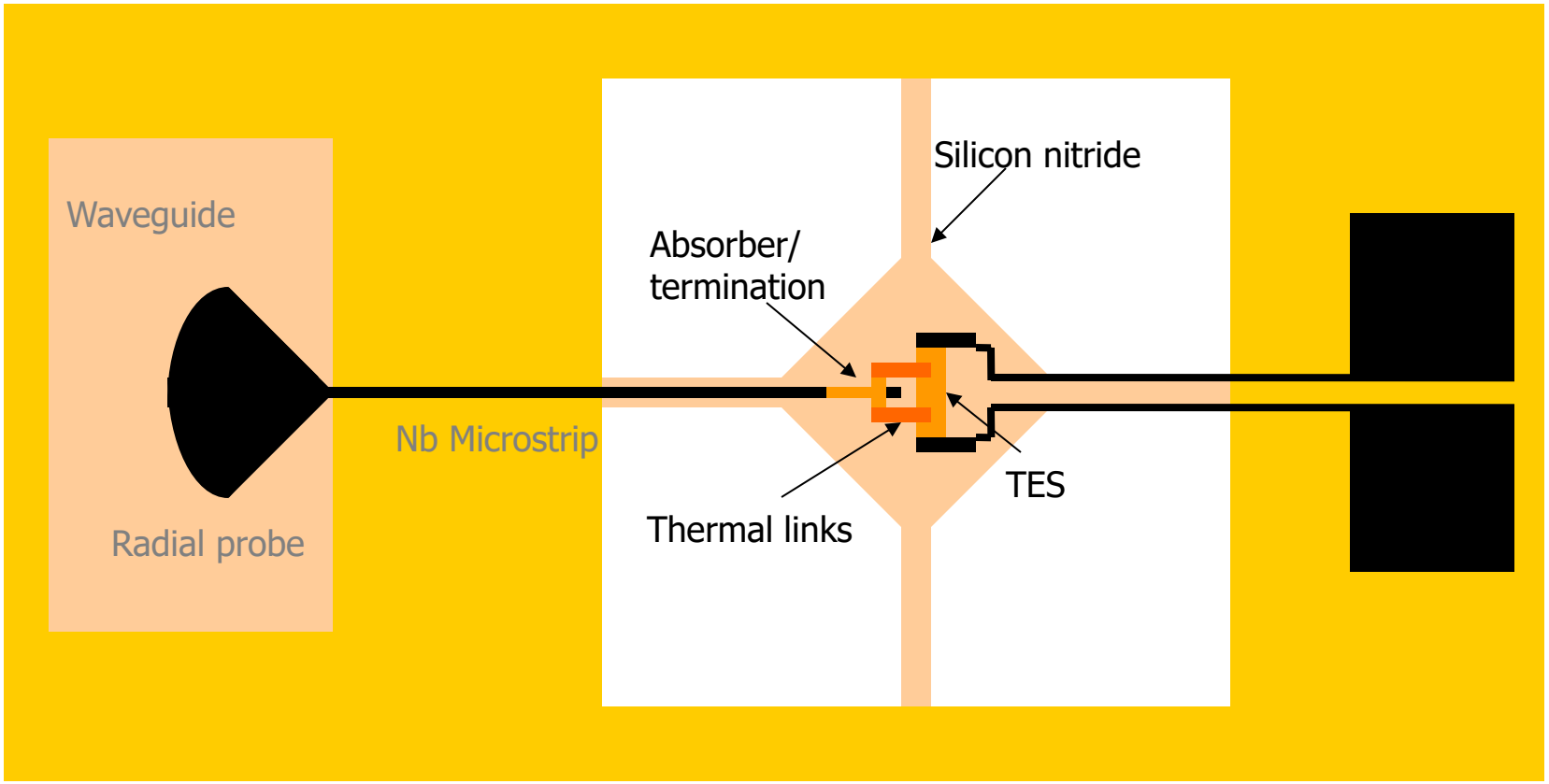

Similar to JPL design, Hunt, et al., 2002 but with waveguide coupled antenna

PROTOTYPE SINGLE PIXEL - 150 GHz (Mauskopf)

Details:

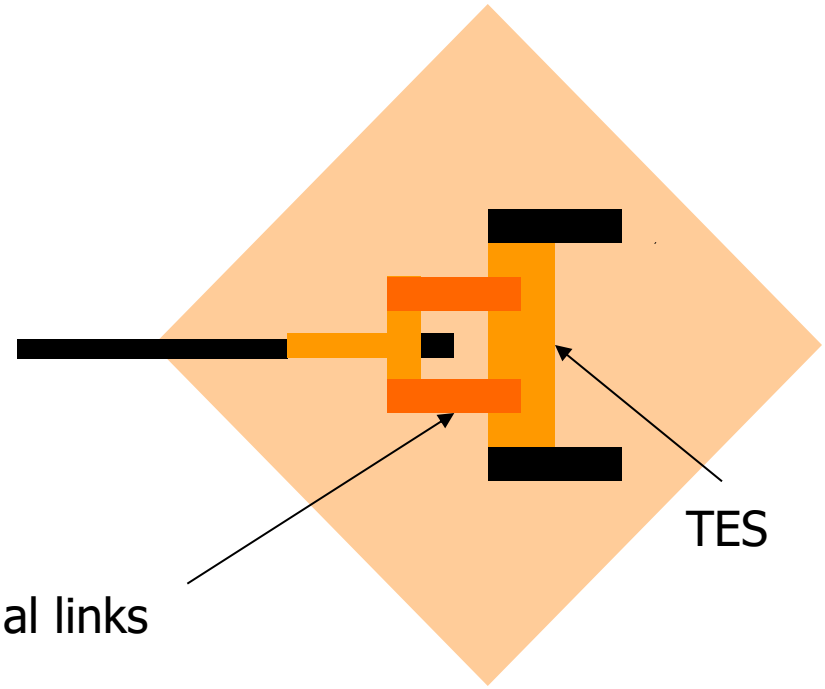

Radial probe

Absorber - Ti/Au: 0.5 Ω/square - t = 20 nm
Need total R = 5-10 Ω
w = 5 μm → d = 50 μm
Microstrip line: h = 0.3 μm, ε = 4.5 → Z ~ 5 Ω

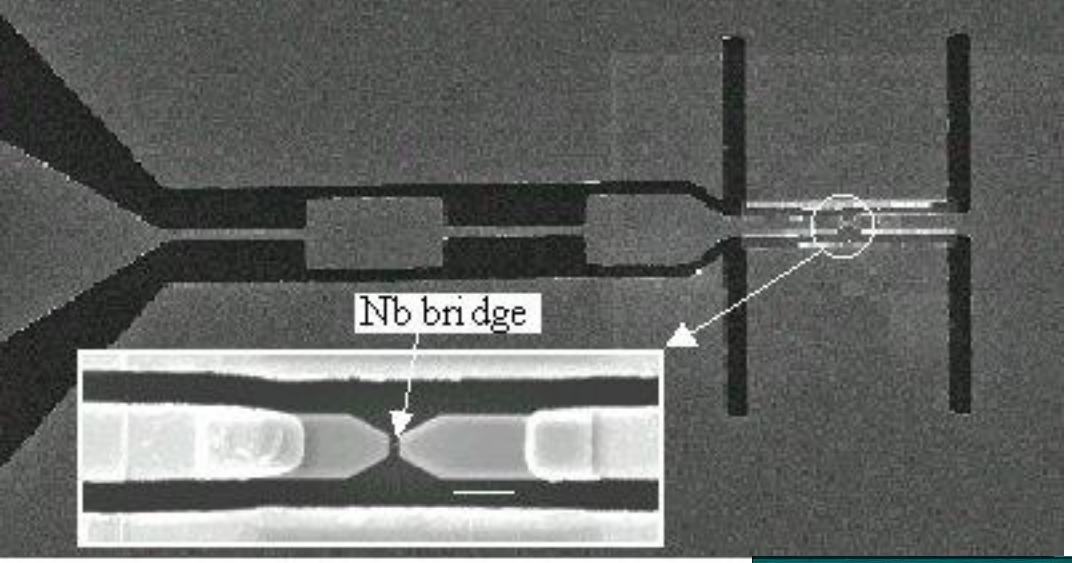

Some HEBs: can detect single photons hitting them. Also really small. Both of these examples use superconductors operating at < -260 C.

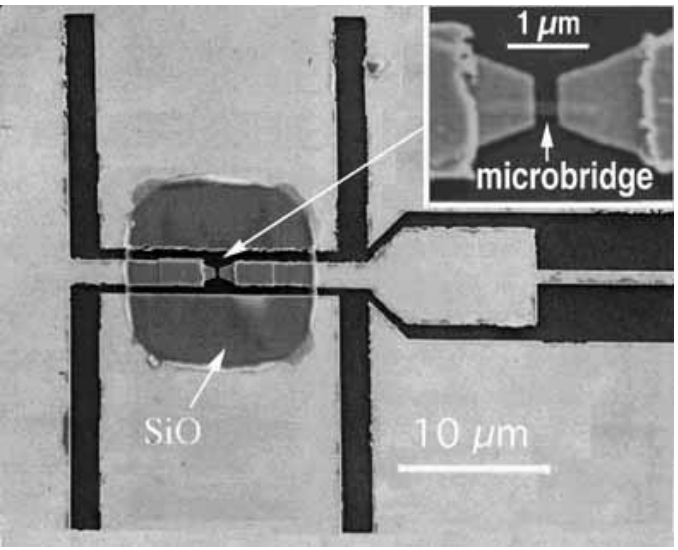

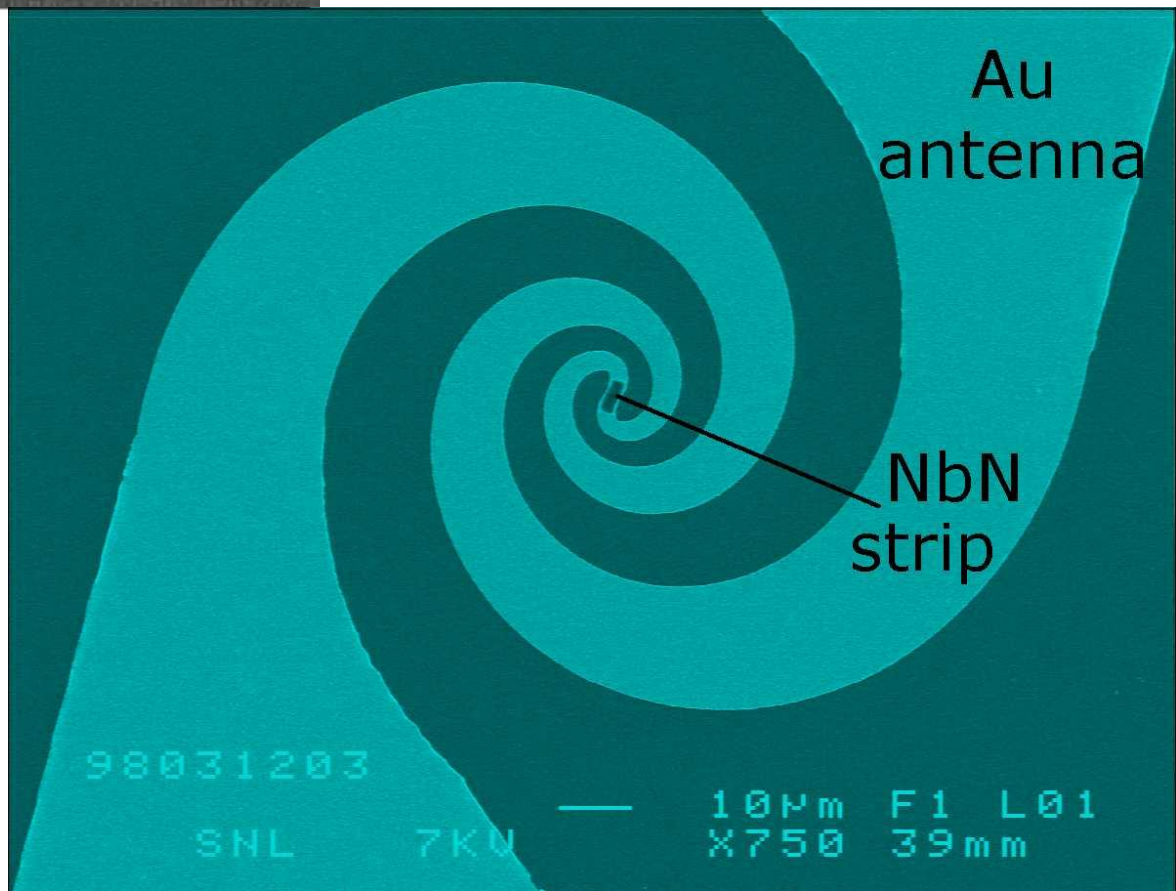

Multiplexing

- Ge and Si thermistors are read out using JFETs at 100K. There is no pratical way to multiplex many sensors on a single amplifier. The number of wires entering the cryostat would be huge for a large format array. Practical limit: the JFET boxes of Planck and Hershel…
- TES sensors have very low impedance (about 1 Ω)
- They can be readout by a SQUID with no power dissipation and large noise margin. Time multiplex and frequency multiplex are being developed (NIST, Berkeley, Helsinki ..)

Time-domain multiplexing

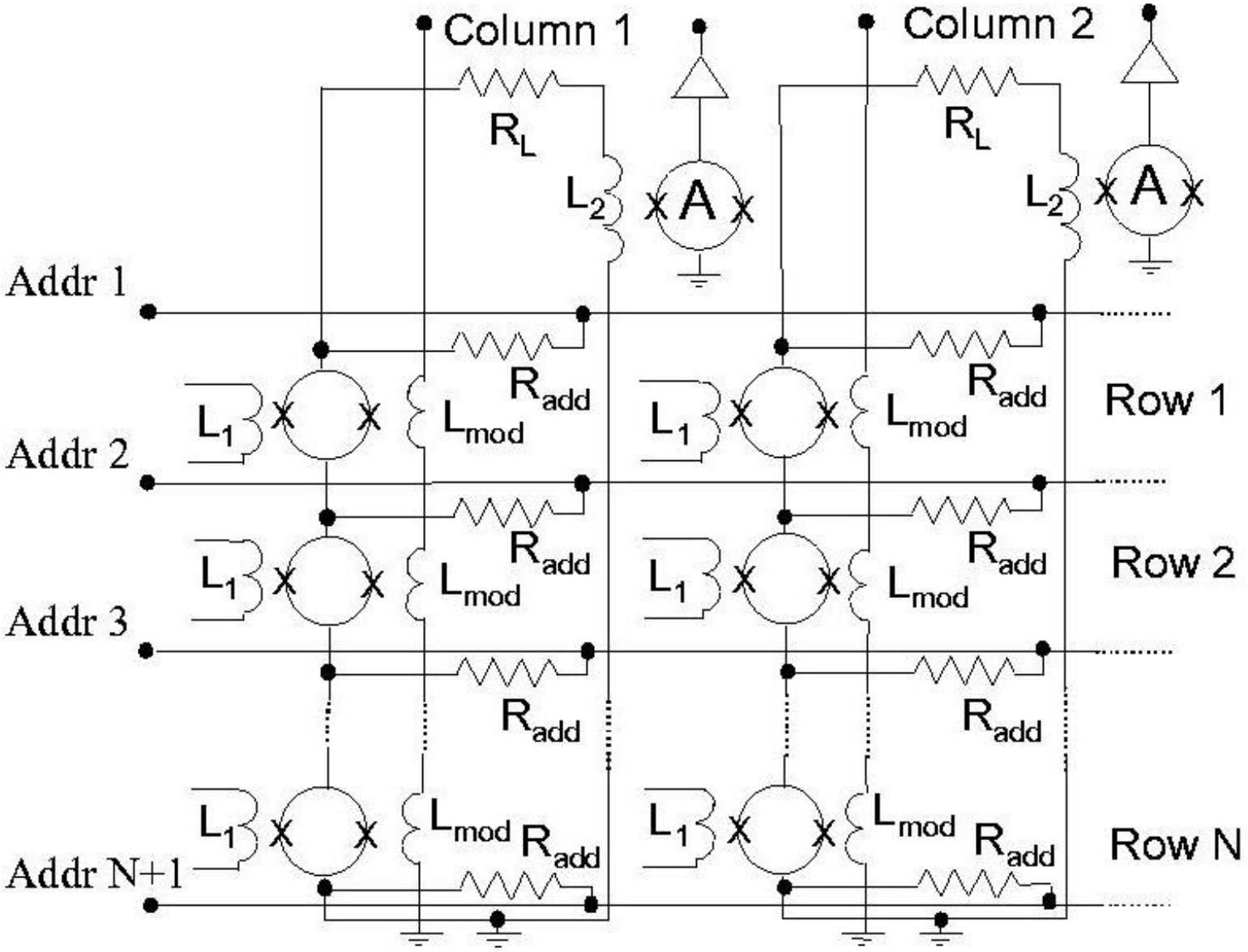

From: Chervenak et al. 99

frequency-domain multiplexing

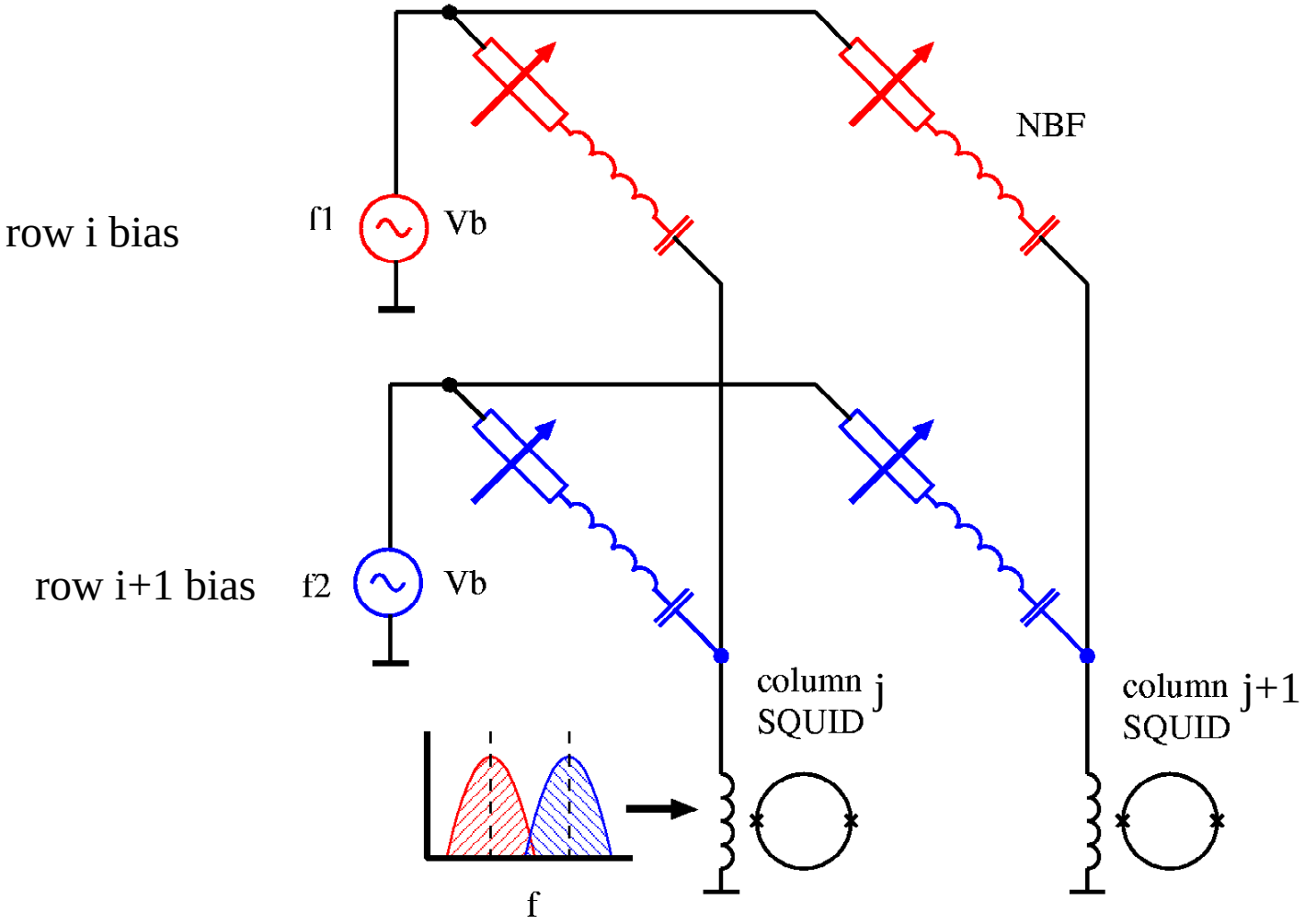

Ref: Berkeley/NIST design

Why TES are good:

1. Durability - TES devices are made and tested for X-ray to last years without degradation
2. Sensitivity - Have achieved few x10^{-18} W/$\sqrt{\text{Hz}}$ at 100 mK good enough for CMB and ground based spectroscopy
3. Speed is theoretically few μs, for optimum bias still less than 1 ms - good enough
4. Ease of fabrication - Only need photolithography, no e-beam, no glue
5. Multiplexing with SQUIDs either TDM or FDM, impedances are well matched to SQUID readout
6. 1/f noise is measured to be low
7. Not so easy to integrate into receiver - SQUIDs are difficult part
8. Coupling to microwaves with antenna and matched heater thermally connected to TES - able to optimize absorption and readout separately

Problems:

- Saturation - for satellite and balloons.
- Excess noise - thermal and phase transition?
- High sensitivity (NEP<10^{-18}) requires temperatures < 100 mK

Solutions:

- Overcome saturation by varying the thermal conductivity of detector - superconducting heat link
- Thermal modelling and optimisation
- Reduce slope of superconducting transition
- Better sensitivity requires reduced G - HEBs?

TES arrays

- Are the future of this field. See recent reviews from Paul Richards, Adrian Lee, Jamie Bock, Harvey Moseley … et al.

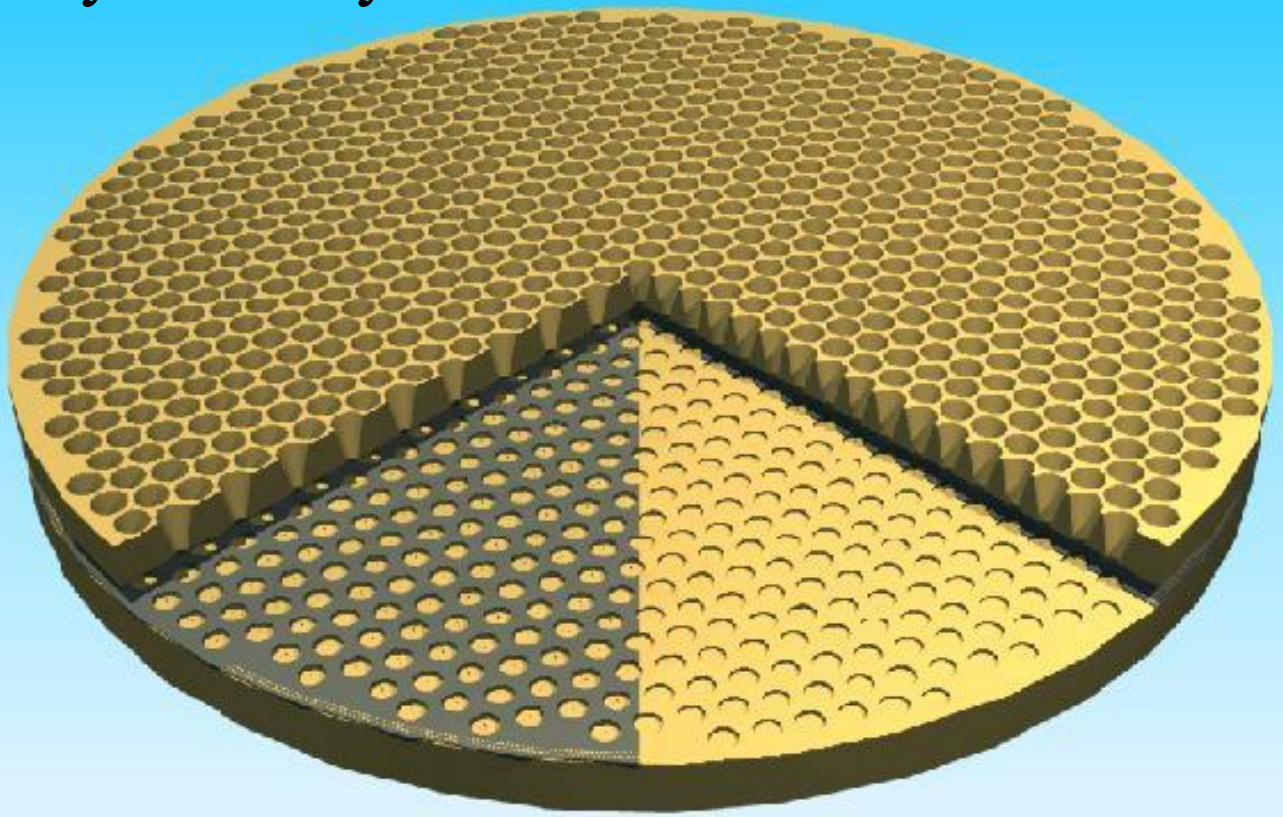

- In Proc. of the Far-IR, sub-mm and mm detector technology workshop, Monterey 2002.

Other ideas:

- Integrating bolometer: the conductivity towards the T reference can be switched on and off (GSFC).
- Superconductor photon detector: low energy photons break Cooper pairs and generate quasiparticles. Problem: detector of quasiparticles, insensitive to Cooper pairs.
  - The inductance of a superconducting strip includes a contribution from the density of quasiparticles. Kinetic Inductance Detectors (Zmuidzinas, Caltech)
  - SIN tunnel junction transmitting quasiparticles but not pairs (YALE/GSFC). Read by a SET.

Applications of Bolometer arrays:

- Study of fundamental physics at very high energy through the accurate study of CMB polarization (post-Planck)
- Study of mm-sub/mm astronomy from space (post Herschel)
- X-ray imaging spectrometers (ASTRO-E2, IMBOSS, XEUS, CONSTELLATION-X)
- X-ray imaging spectrometers X for DNA analysis
- NMR cameras
- Electronic Spin Resonance cameras
- Fast Imaging Spectrometers for nuclear fusion plasma diagnostics
- …